Synaptic mechanisms of noise-induced hearing loss

Dissertation

for the award of the degree

"Doctor of Philosophy"

Division of Mathematics and Natural Sciences

within the doctoral program:

Sensory and Motor Neuroscience

of the Georg-August University School of Science (GAUSS)

submitted by

Mauro Alfonso Malpede

from Lavello, Italy

Göttingen, 2023

Declaration

Herewith I declare that this thesis has been written independently and with no other sources and aids than quoted.

Mauro Alfonso Malpede

Göttingen, March 19, 2023

Dedicato alle persone difficili, che non hanno paura di guardarsi dentro.

A Fadhel,
che non ha mai mancato di motivarmi
Keep pushing

A te,
che mi accompagni
in ogni attimo della mia vita

Contents

Bibliography

Abbreviation List

ABR	Auditory Brainstem Response
DPOAE	Distortion Product Otoacustic Emissions
TTS	Transient Threshold Shift
PTS	Permanent Threshold Shift
D0	Post-exposure Day 0
D1	Post-exposure Day 1
D14	Post-exposure Day 14
ANF	Auditory Nerve Fiber
SGNs	Spiral Ganglion Neuron
IHCs	Inner Hair Cells
OHCs	Outer Hair Cells
MOC	Medial Olivocochlear
LOC	Lateral Olivocochlear
NT-3	Neurotrophin-3
GSDB	Goat Serum Dilution Buffer
ΔCm	Changes in Capacitance of the Membrane
IV	Current-Voltage relationship
PBS	Phosphate Buffer Saline
RRP	Readily Releasable Pool
SRP	Secondarily Releasable Pool
SPL	Sound Pressure Level
LSR	Low Spontaneous Rate
MSR	Medium Spontaneous Rate
HSR	High Spontaneous Rate
SEM	Standard Error Mean
EPSC	Excitatory Post Synaptic Potentials
ACh	AcetilCholin
nAChR	Nicotinic Receptors
AMPA	α-amino-3-hydroxy-5-methyl-4-isoxazolepropionic acid

NMDA	N-methyl-D-aspartate
AZ	Active Zone
BAPTA	1,2- bis (2-aminophenoxy) ethane-N,N,N9,N9-tetraacetate
CaBP	Calcium Binding Protein
CtBP2	C-terminal binding protein 2
MET	Mechano Electrical Transduction
MVR	Multivesicular release
SNARE	soluble N-ethylmaleimide-sensitive factor attachment protein receptors
QCa	Calcium Charge
Vglut	Vesicular Glutamate transporter

List of Figures

General Introduction and M&M

Results

Abstract

Noise-induced hearing loss (NIHL) is a form of acquired hearing impairment, caused by exposure to loud noise, that damages the delicate inner ear structures, possibly including the neural connections between the Inner Hair Cells (IHCs) and Spiral Ganglion Neurons (SGNs). The symptoms of NIHL depend on the nature of exposure and may include difficulty hearing in noise, understanding speech, muffled speech, or tinnitus. In severe cases, the hearing loss can be profound and strongly affect the overall quality of life. Currently, there is no causative treatment and cure for NIHL. The different manifestations of synaptic pathologic changes and the underlying synaptic mechanisms are not yet well understood. Yet, such knowledge could guide development of novel therapies, which was in focus of my thesis.

In my PhD project, I investigated the effects of noise exposure under volatile anesthesia using two levels of noise stimulation. I developed a new mouse model of noise-induced synaptopathy that is mild to moderate and involves partially delayed loss of ribbon synapses that develops in conditions of mild or no immediate loss of hearing sensitivity. Patch-clamp recordings from basal inner hair cells (IHCs) immediately post noise exposure showed a temporary increase in the efficiency of IHC exocytosis upon noise exposure causing a larger temporary hearing threshold shift. Two weeks after exposure, the hearing sensitivity was mildly increased for both noise intensities tested. Despite aprox. 20% loss or ribbon synapses in the IHCs of the basal cochlea, the whole-cell calcium current amplitudes and exocytosis were not affected. These findings indicate that acute noise exposure enhances IHCs exocytosis at the remaining ribbons or possibly extrasynaptically, which should be studied in more detail in the future.

Furthermore, the use of the anesthetic isoflurane, which was previously shown to protect against noise-induced reduced hearing sensitivity, was discovered to provide partial, but not complete protection to ribbon synapses. However, my work further revealed that a moderate loss of ribbon synapses can still occur even in the presence of very mild immediate hearing threshold shift, previously not shown to permanently harm synapses. In conclusion, this study has provided new insights into the manifestations of noise-induced synaptopathy and established a new foundation for future research in this field, which could lead to the development of new therapies to protect auditory systems from damage caused by loud noise.

1. Introduction

1.1 Physical characteristics of the sound

Sound is a form of mechanical energy that is transmitted through longitudinal vibrations of various media, including air, which is the primary means of communication among humans, solids, through which low frequencies are predominantly transmitted, water, where certain species, such as whales, communicate through sound, and more. When this energy is transmitted through air, it creates fast fluctuations in air pressure, which can be recorded by a sound detector. The number of these fluctuations per second is referred to as the "sound frequency." The lower and upper limits of human hearing are typically considered to be around 20 and 20 kHz, respectively, with the greatest sensitivity between 1 and 5 kHz, as demonstrated by the audiogram or frequency curve for human hearing, Fig 1.1 (Geisler 1998).
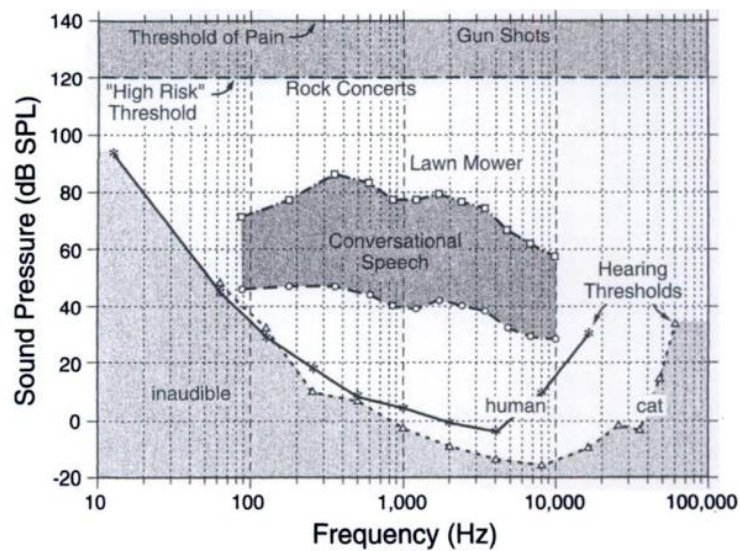
Figure 1.1 Sound pressure and frequency ranges in mice audiograms

In mice, this range goes from 1 to 70 kHz (Taberner and Liberman, 2005). In the audiogram, the left axis represents the loudness of a stimulus, or in terms of physical characteristics, the sound pressure, and it scales from 0 to 120 dB SP, which stands for "decibel sound pressure level". From Geisler 1998.

The formula for SPL is defined as the following:

$$SPL = 20 * \log (pressure/20 \ \mu N/m^2)$$

Right around 120 dB SPL, sounds become painfully loud and highly damaging to human hearing. Gunshots and jet aircraft engines are examples.

In auditory neuroscience, the sound stimulus is represented not only as a function of time but also as a function of sound frequency, the so-called "spectrum" or "frequency domain".

The Fourier Transform equation allows going from one representation to the other.

Here are some very common basic auditory stimuli, Fig. 1.2:

- Pure tone (or sine waves). In the time domain, the stimulus is represented as a sinusoidal waveform, in the frequency domain instead, it shows a unique sound frequency.
- Square wave. This stimulus is equivalent to a *series* of sine waves. Adding up infinite pure tones will result in a perfect square wave.
- Tone burst. It is a brief, single frequency tone that is transmitted for a very short duration, typically less than one second. In the frequency domain, the tone burst is represented as a sharp spike at the frequency of the tone, surrounded by a broader frequency spectrum. The spike in the frequency domain corresponds to the single frequency component of the tone burst in the time domain. The width of the spike depends on the duration of the tone burst, with longer tone bursts having a narrower spike. The surrounding spectrum represents any spectral components introduced by the system, such as noise or distortion. In general, the frequency domain representation of a tone burst is used to evaluate the frequency response of a system and to identify any frequency-dependent effects such as filtering or gain.
- Click. It is a very sharp, impulsive sound that can be infinitesimally short. In this case, it will be a broad-spectrum sound containing all frequencies. The spectrum will be completely flat.
- Noise. It is a broadband sound, like the infinitesimally short clicks, with all frequencies. If all frequencies audible to the human ear have equal power, it is called white noise. Pink noise is

white noise but with reduced high frequencies. Brown noise lowers the higher frequencies even more.

Besides the common basic sounds, there are also some more complex sounds. Music, for example.

When a key on a piano keyboard is struck, it produces a multitude of frequencies that are perceived as a single note. The pressing of a key causes a hammer to strike a string, causing it to vibrate at various harmonically related frequencies. The lowest of these frequencies is known as the "fundamental frequency." Pitch, the attribute of auditory sensation that allows sounds to be ordered on a musical scale, is defined based on frequency. For a pure tone, the pitch is directly proportional to the frequency. However, for complex sounds with multiple harmonics and overtones, the pitch is strongly influenced by the fundamental frequency. In certain instruments, such as the guitar, the fundamental frequency may be weak. Nonetheless, the pitch remains relatively unchanged even if the fundamental frequency is removed, indicating that the ear has the ability to recognize and restore the fundamental frequency.

Besides being important in frequency discrimination, pitch perception is also reported to play a crucial role in the ability to segregate sounds arriving from different locations; pitch discrimination is thus a key index of auditory perception often used in clinics (Oxenham et al., 2008).

Another auditory sensation is the timbre of a sound, defined as the relative volume or amplitude of various overtone partials. The timbre distinguishes different types of sound productions, such as piano or guitar. The second type of complex sound is "speech sounds". We use them when we say a word aloud and, if use them in the right order, they allow us to communicate with other people and understand each other. We can produce speech sounds thanks to complex anatomical structures. The air coming from the lungs goes through the trachea moving the vocal cords (more scientifically called glottis) back and forth, making them hit each other and open up. This movement will periodically interrupt and release the airflow. This opening and closing of the air through the glottis produces a very complicated waveform (Geisler 1998). Our highly efficient

auditory system allows for the rapid association of each speech sound spectrum with a specific vowel or consonant, enabling precise comprehension of complex words.
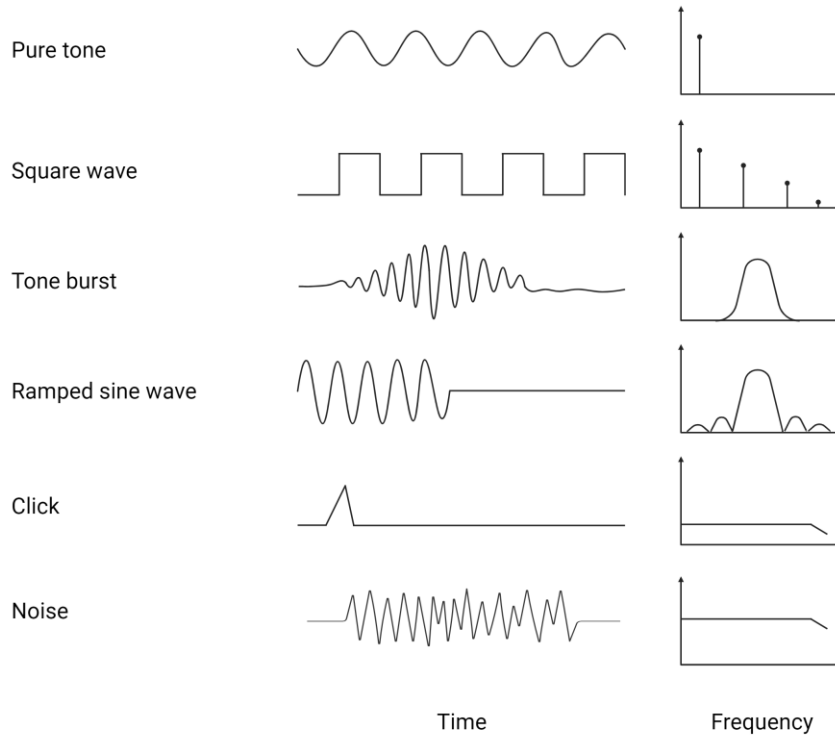
Figure 1.2 Waveforms and Fourier analysis

Some waveforms (left) and their respective Fourier analysis (right). (A) Sine wave. (B) Square wave (infinite time long, with line spectra which components are harmonically related. (C) Ramped sine wave. (D) Gated sine wave. (E) Click. (F) White noise. Adapted from Geisler 1998.

1.2 Sound processing in the inner ear

In order to hear, the ears must first capture sound waves and transmit them to the Organ of Corti, where they are translated into neural impulses and conveyed to the brain. The initial point of contact for sound waves is the outer part of the ear, known as the "pinna," which directs the waves into the auditory canal, also referred to as the "external auditory meatus." From there, the sound wave enters the middle ear, where it strikes the eardrum or "tympanic membrane," causing it to vibrate. This vibration is efficiently transferred to the three small bones known as the "malleus, incus, and stapes," with the stapes moving in a piston-like manner to send the

vibrations to the oval window and, subsequently, to the Cochlea. This is the inner ear, Fig. 1.3 (Purves, 2004).
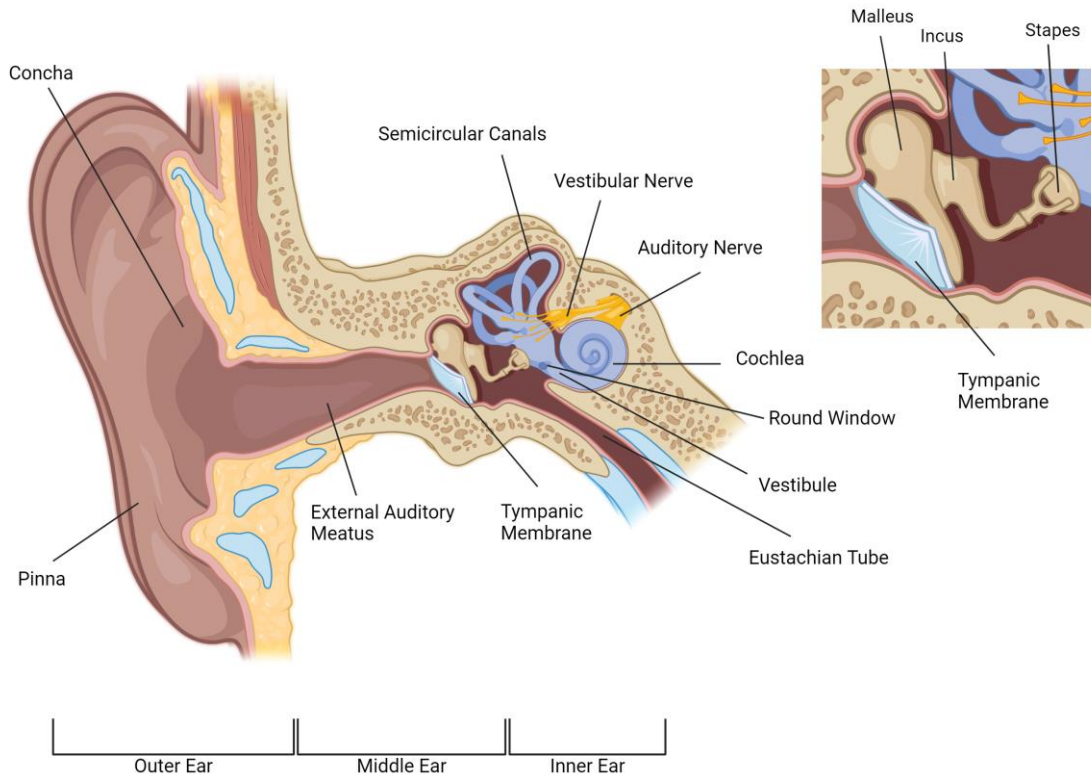
Figure 1.3 The human ear: anatomy and function

The human ear is a complex organ that consists of three main parts: the cochlea, the semicircular canals, and the vestibule. The vestibule and semicircular canals contain sensory epithelia associated with balance while the cochlea contains an organ known as Corti's Organ which is responsible for hearing .. This schematic representation of how these components work together allows us to gain insight into how sound waves are detected by our bodies. Adapted from Purves et al., 2004.

The Cochlea is a spiral three-chambered snail-like structure 10 mm wide within a bony matrix. In a cross-section of the cochlea, the uppermost chamber is called the "scala vestibuli", at the base of which is where the oval window is situated. The lowermost chamber is called the "scala tympani", at the base of which is where the oval window is located. Both the scala vestibuli and the scala tympani contain the perilymph, which is rich in Na+ ions. Between the two scalae is the

"scala media", the house of the organ of Corti, which is referred to as the receptor organ of hearing. The scala media is filled with endolymph, which is unusual in ionic composition by being rich in K+ ions. The membranes separating the two fluid-filled systems are the "Reissner's membrane", on top, and the "basilar membrane", on the bottom, Fig 1.4.
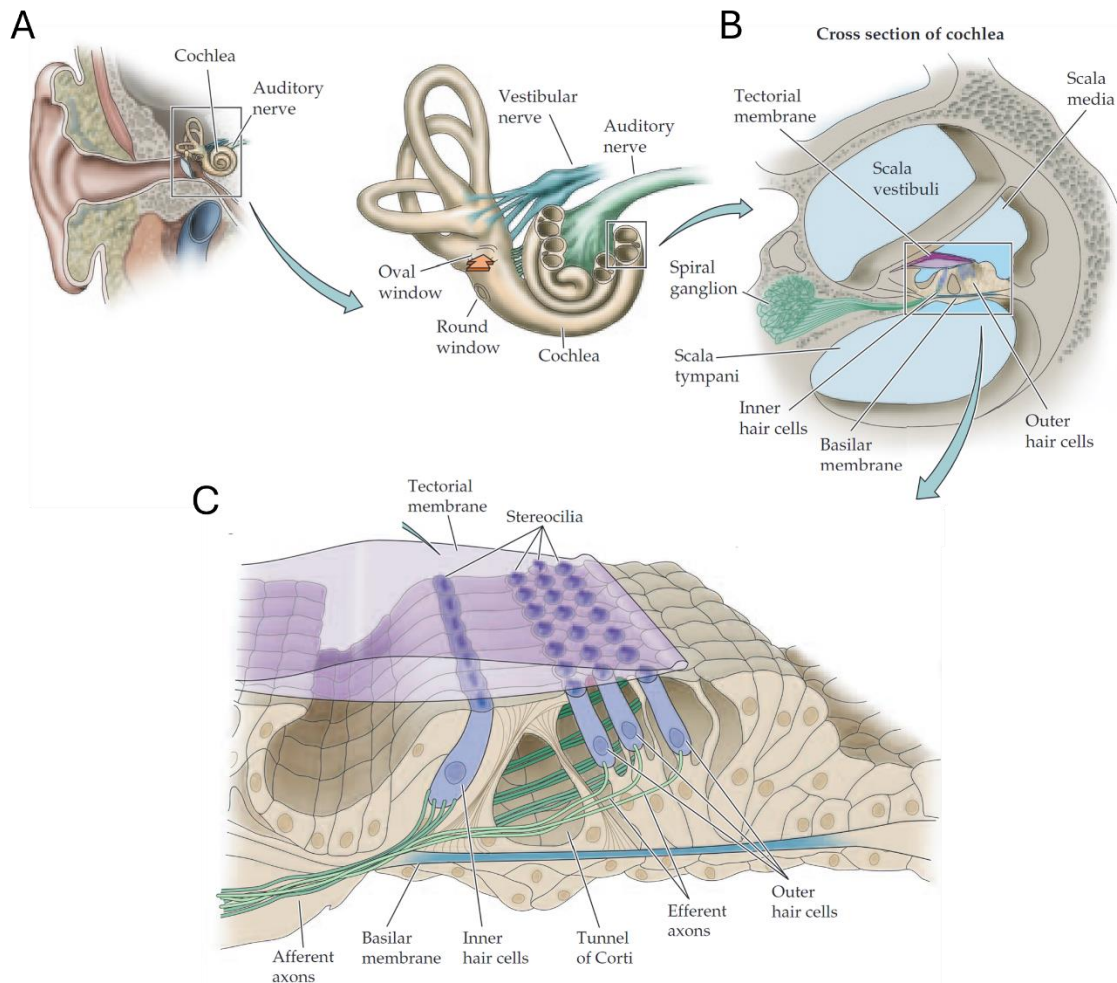
Figure 1.4 Cross-sectional views of the cochlea: anatomy and components

(a) A cross-sectional illustration of the entire cochlea showing the eighth cranial nerve leaving the cochlea and the cochlear ducts, (b) A cross-section of the cochlea that displays the fluid-filled chambers (scala vestibuli, scala media, and scala tympani) and the location of the organ of Corti, (c) The organ of Corti which includes the two types of sensory cells (IHCs and OHCs) and the supportive cells. From Pearson Education Inc., 2006.

The membrane are flexible and move in response to the vibrations traveling up the scala vestibuli. The movements of the membranes are then transferred back down to the scala tympani, reaching eventually the round window. This process keeps happening until the energy of this sound wave eventually causes the fluid to stop moving, and all the energy is dissipated.

On the basilar membrane, in the scala media, is the Organ of Corti. The Organ of Corti, extends from the anterior part of the vestibule and coils for about two and a half turns around a bony pillar called the "modiolus".

As the basilar membrane vibrates, the Organ of Corti is stimulated, and the specialized cells within the Organ of Corti, known as "hair cells," convert the mechanical vibrations into electrical signals. These electrical signals, also referred to as receptor potentials, are then transmitted to the brain via the cochlear nerve. It is important to note that while hair cells generate electrical signals, they do not themselves send nerve impulses. Approximately 16.000 hair cells are within the human cochlea. There are two types of hair cells: the inner hair cells and the outer hair cells. Even though there are roughly three times as many outer hair cells as inner hair cells, it's almost exclusively the inner hair cells that send acoustic information into the central nervous system.

While the outer hair cells (OHCs) are closely covered by a structure called the "tectorial membrane," the stereocilia of the inner hair cells (IHCs) are not embedded in the tectorial membrane but are instead moved by the fluid in the cochlea. As the basilar membrane vibrates, the tiny clusters of hairs, known as stereocilia, situated on the apical portion of the cells are bent against the tectorial membrane, activating the hair cells. The filamentous structures connecting the tips of adjacent stereocilia are known as tip links, which play a crucial role in the mechanoelectrotransduction process. These structures are thought to amplify the forces generated by sound waves in the cochlea, in the area of the molecular sensors located at the top of the hair cell's stereocilia. The tip links are believed to act as gates that open ion channels in response to the mechanical stimuli, leading to the generation of electrical signals that are then transmitted to the auditory nerve fibers.

The basilar membrane exhibits differential vibration along its length. Specific regions are selectively activated by different sound frequencies. Lower frequencies cause vibrations near the
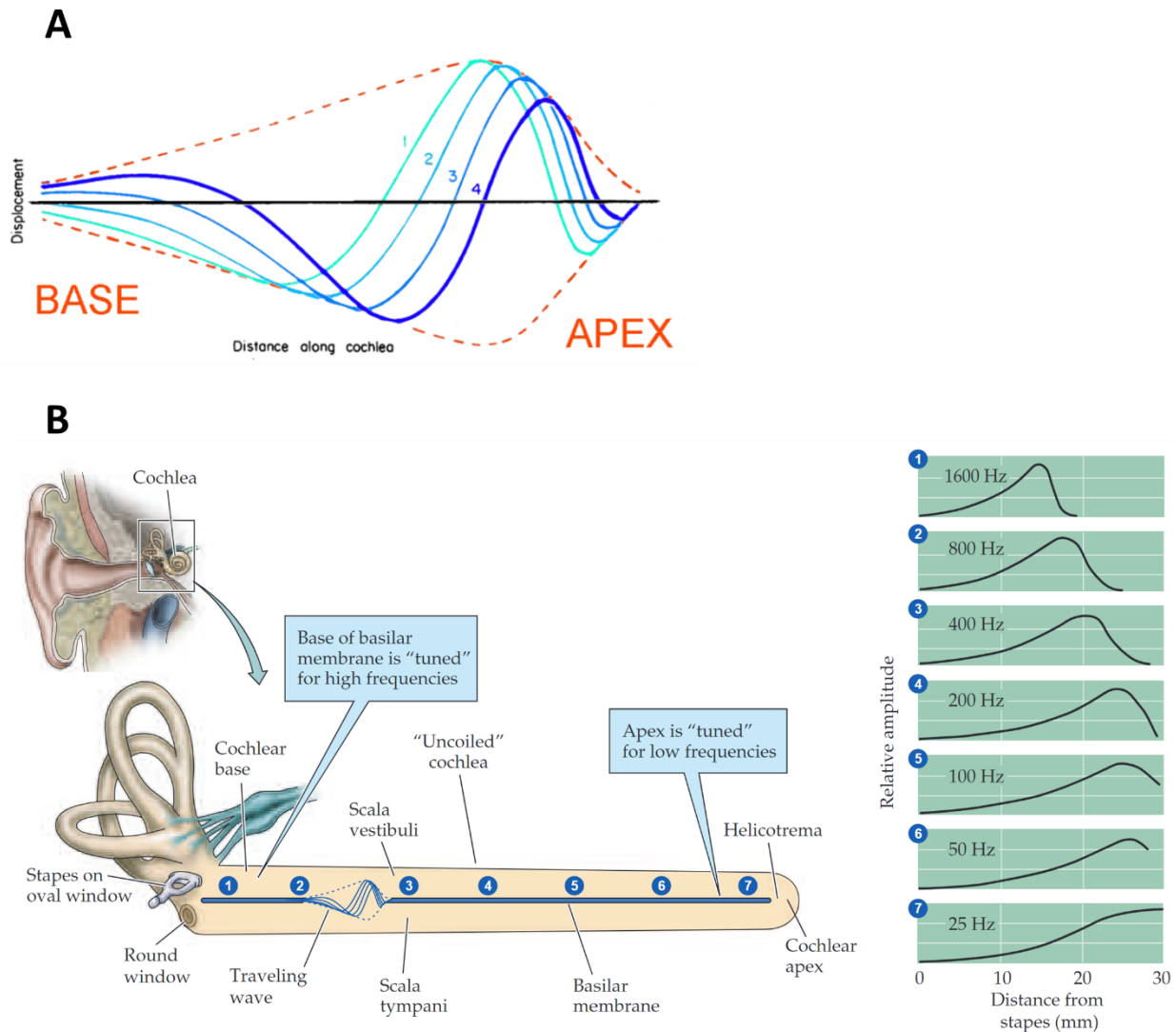
Figure 1.5 Traveling waves in the cochlea: frequency coding and amplitude dependence.

(A) Von Bekesy was the first to demonstrate the presence of traveling waves in the cochlea. The full lines illustrate the pattern of the cochlear portion's deflection at various points in time, as indicated by the numbers. The waves are confined within a static envelope, represented by the dotted lines. The stimulus frequency was 200Hz. From Von Bekesy, 1960. (B) The frequency amplitude of a traveling wave as it progresses along the length of the organ of Corti. The amplitude of the wave increases with the distance it travels through the cochlea and its maximum amplitude is dependent on its frequency. This arrangement plays a crucial role in frequency coding, as adapted from Purves et al., 2004.

apex of the cochlea, while higher frequencies generate vibrations closer to the base. This specific arrangement is referred to as "tonotopic organization." (Fig. 1.5).

The way the basilar membrane vibrates in response to sound is the key to understanding cochlear function. Specifically, the hair cells are located between the tectorial and basilar membranes and are stimulated by the shearing force between the two, caused by the pivot points of the two membranes. When a soundwave travels down the cochlea, the pivot point of the basilar membrane becomes displaced, and the tectorial membrane moves across the tops of the inner hair cells causing the stereocilia to bend.

The ionic environment of the compartments plays a critical role in signal transduction,. The apical portion of the inner hair cells is bathed in high potassium solution and the base of the inner hair cells, instead, is bathed in low potassium solution. In between the stereocilia, there are channels able to respond to mechanical vibrations. When the stereocilia bend in the direction of the highest row of stereocilia, the mechanosensitive channels open allowing cations (mostly potassium) to flow into the cell leading to depolarization, Fig.1.6. This, in turn, opens calcium channels at the basal end of the cell. Ca2+ binds to specific proteins located at the basal part of the inner hair cell determining the fusion of the vesicles with the basolateral membrane. The release of the neurotransmitter glutamate will eventually stimulate the auditory nerve. Glutamate binds to the ionotropic glutamatergic receptors in the peripheral processes of the spiral ganglion neurons (SGNs), which results in the generation of action potentials. These propagate along the auditory pathway towards the brain.

The electrochemical gradient for potassium drives potassium ions out of the hair cells at the basolateral membrane. This establishes that potassium flow through the cell is used for both depolarization (potassium ions flowing in the hair cell through stereocilia at the apex), and repolarization (potassium flowing out at the base of the inner hair cells).

This crucial high potassium solution in the scala media and thus at the apical portion of the inner hair cells is maintained thanks to the stria vascularis, a multilayered epithilium situated at the outer edge of the organ of Corti and composed of cells specialized in secreting potassium in the endolymph, at a constant rate, Fig 1.6 (Rickheit et al., EMBO J, 2008)

The plasma membrane of the OHC lateral wall is tightly packed by the motoprotein prestin (Dallos, J Neurosci, 1992; Zhang et al., 2000; Dallos et al., Neuron, 2008). In response to sound-evoked oscillations in the OHC membrane voltage, this protein undergoes conformational changes which, in turn, shortens and elongates the length of the entire cell. This movement amplifies the vibration of the tectorial membrane, to which the outer hair cells are attached, resulting in an amplification of the signal transmission to the IHCs and finally auditory nerve. Therefore, the outer hair cells are known as the "cochlear amplifiers".
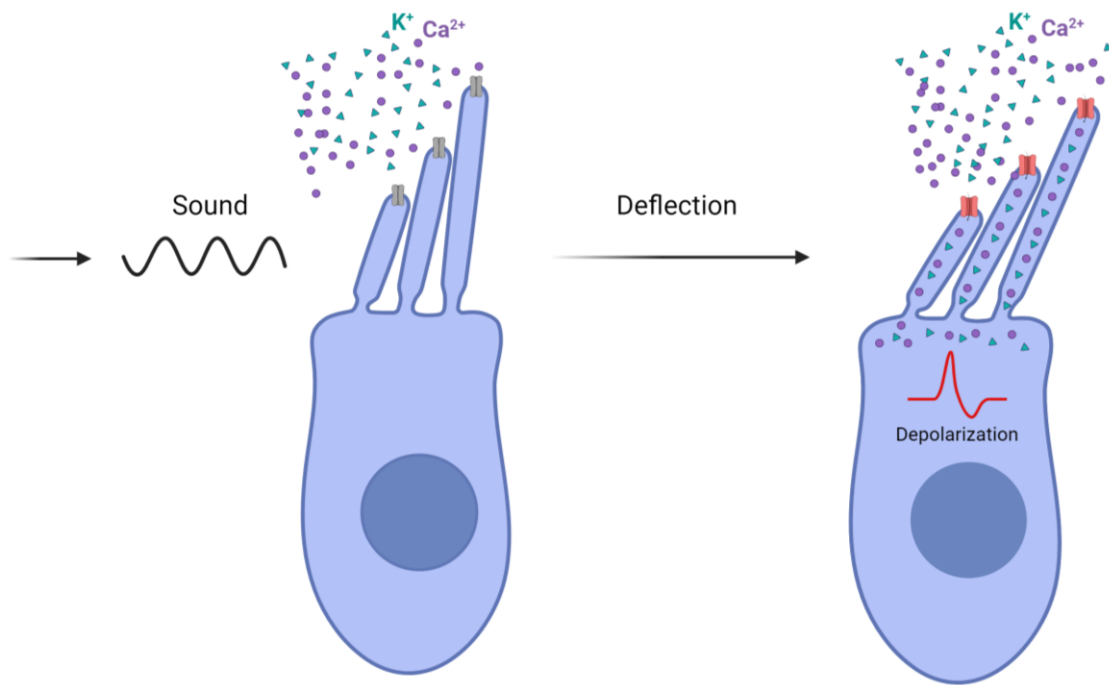
Figure 1.6 Mechanism of hair cell activation in response to sound waves

When sound waves impact a typical hair cell, the stereocilia bend towards the tallest stereocilia and activate the mechanotransduction channels (MET) at their tops. This opens the channels and lets calcium and potassium ions flow into the cell, creating a shift in membrane potential that triggers the opening of L-type voltage gated calcium channels on the cell's basolateral sides. The resulting influx of calcium raises the intracellular calcium levels, causing neurotransmitter release from the ribbon synapse's synaptic vesicles into the synaptic cleft and activating the afferent neurons. Adapted from Koleilat, 2019.

The importance of the protein Prestin comes from the fact that mutations in the gene coding for prestin can cause moderate to profound hearing impairment in humans (Liu et al., Hum Mol Genet, 2003), with the loss of electromotility estimated to account for approximately 45-60 dB threshold shift (Liberman et al., Nature, 2002; Liu et al., 2003), while additional hearing loss may be caused by concomitant loss of hair cells (Liu et al., 2003), Fig.1.7.

Moreover, since the base of the cochlea is very tight, when a high-frequency pitch hits the base of the cochlea, the outer hair cells do not reverberate on the apex as much as they do on the base, and vice versa, when a low-frequency pitch hits the apex of the cochlea, the outer hair cells do not reverberate on the base as much as they do on the apex. In this way, the outer hair cells not only increase the amplitude of the signal but they also increase the frequency resolution.
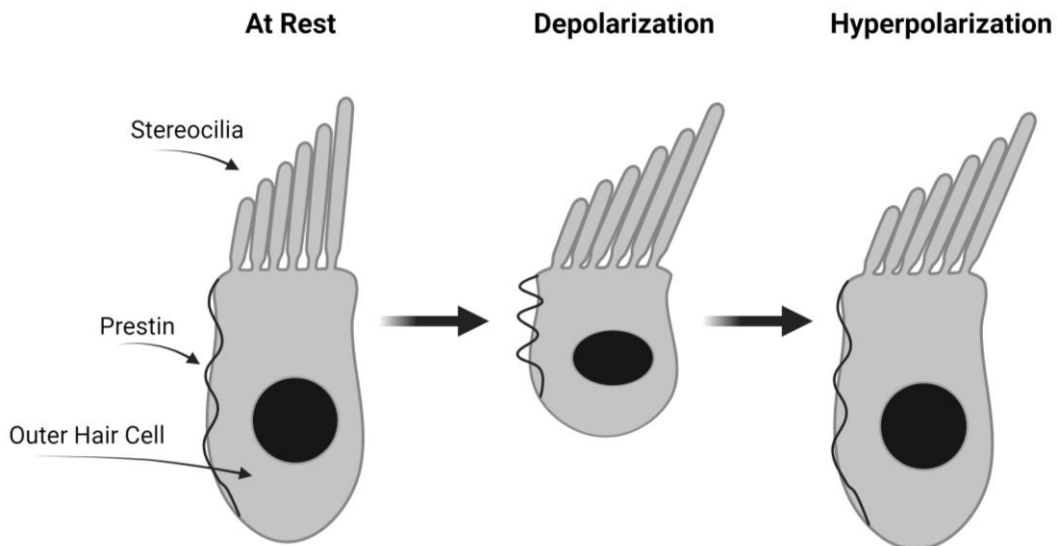
Figure 1.7 Outer hair cell electromotility and hearing sensitivity

A simplified illustration of the outer hair cell (OHC) somatic electromotility and the mechanisms that enable prestin to circulate. Prestin drives the OHCs to contract and elongate in response to transmembrane potential changes, known as somatic electromotility. This electromotility is responsible for acute hearing sensitivity. Adapted from Parker 2022.

The tightness of the cochlear base and the widening of the cochlear spiral towards the apex create a spatial gradient of frequency selectivity. When a high-frequency pitch stimulates the base of the cochlea, the outer hair cells respond with a greater amplitude of movement than they do to the same pitch at the apex. Conversely, a low-frequency pitch that stimulates the apex produces a greater response amplitude in the outer hair cells there than at the base.
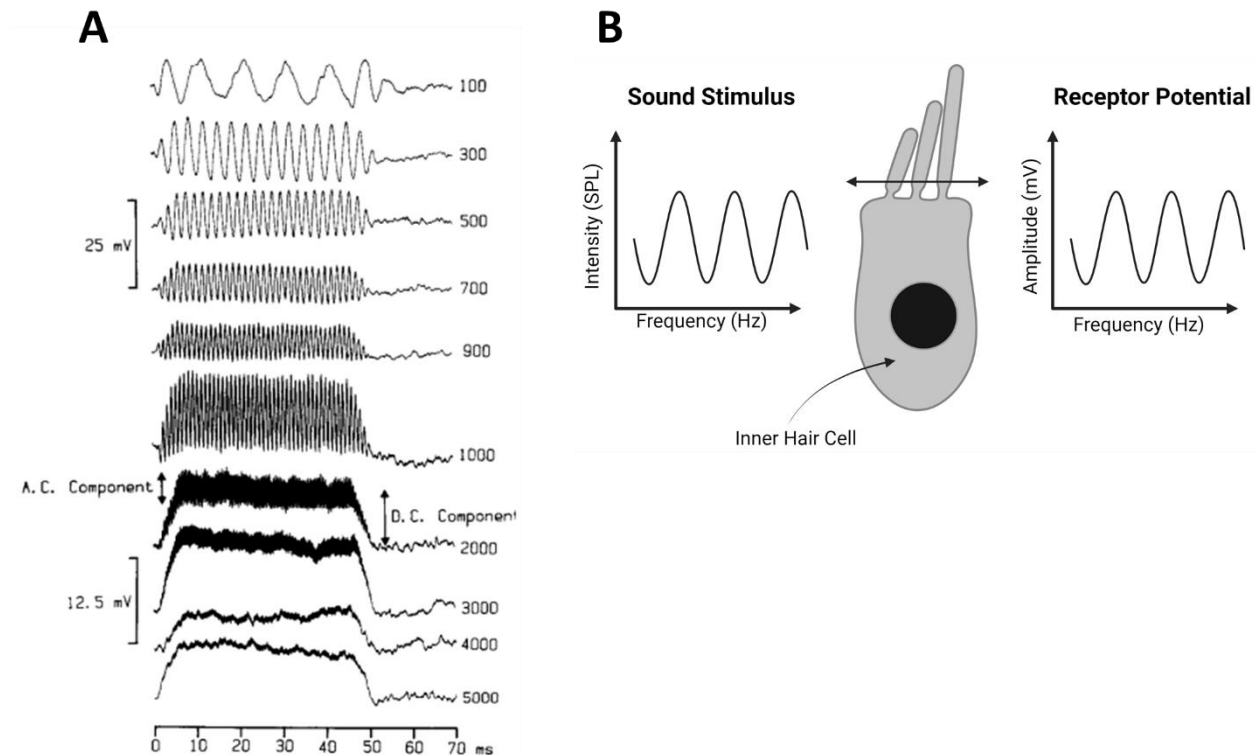
Figure 1.8 Inner hair cell receptor potentials in response to sound stimulation

(A) The intracellular receptor potentials of an inner hair cell were recorded in response to 80 dB SPL tones of different frequencies (indicated in Hz next to each trace). As the frequency increases, the receptor potential's AC component decreases relative to the DC component. Above 1 kHz, the DC component dominates the response. The scale bar at the top is for the frequencies between 100-900 Hz, while the bottom bar is for 1000-5000 Hz. The resting membrane potential of this inner hair cell was -37 mV. From Palmer and Russell, 1986. (B) Illustration of a receptor potential of an IHC during sound stimulation. From Dierich 2020.

This frequency-dependent response of the outer hair cells enhances both the amplitude and the frequency resolution of the cochlear response. This is crucial for the ability to distinguish between sounds of different frequencies, such as 500 and 550 Hz, and ultimately underlies our perception of the auditory world.

1.3 Hair cell and auditory nerve response to sound

The electrical response of hair cells to sound depends on the frequency of the sound. Fig. 1.8 illustrates some noteworthy classic sharp electrode recordings obtained from inner hair cells of mice that were exposed to sound. When the frequency of the sound increases, the voltage change of the hair cells also increases. This demonstrates that at low-frequency sounds, hair cells can follow the sound stimulus with an AC (alternating current) depolarization.

However, when the frequency of the sound increases even further like 1000 Hz, which is still a typical sound frequency for the auditory system to encounter, the hair cells follow this frequency response less faithfully compared to low-frequency sounds. Also, the hair cell potential does not return to baseline. Instead, there is a larger depolarized baseline shift.

In short, above about 650 Hz, the hair cells will still show a sinusoidal voltage response, but they will also have a steady DC (direct current) component, in addition to the AC response, Fig.8.

How does the auditory nerve respond to different sound frequencies? In Fig. 1.9, the responses of a single auditory nerve axon to a 250 Hz tone presented several times are shown. Most of the action potentials occur close to the peak of the sinusoidal sound waveform, t.i. they phase-lock with the sound. At higher-frequency sounds where hair cell voltage response no longer has an AC component, the timing of spiking of the auditory nerve becomes more random.

Clusters of action potentials that occur at the same phase in the sinusoidal response of sound are commonly referred to as "phase locking." This phenomenon can be observed in the auditory system, where every neuron's activity is typically described in terms of its auditory nerve tuning curve. This tuning curve provides a rough explanation of how a neuron responds to different frequencies and intensities of sound (see Fig. 1.10(A)). In general, when exposed to soft sounds, a neuron exhibits heightened sensitivity to a particular frequency.
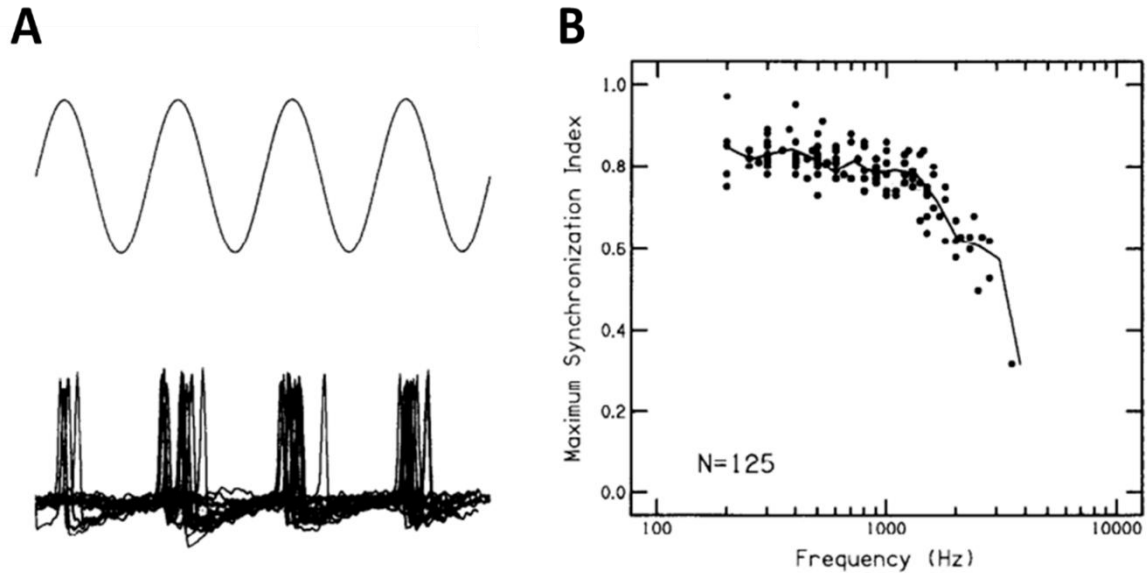
Figure 1.9 Synchronization and phase-locking in auditory nerve fibers

(A) 200 Hz stimulus waveform is displayed at the top and multiple traces of an auditory nerve fiber's response to the tone are overlaid. The spikes tend to cluster in a narrow portion of the waveform cycle, indicating synchronization. (B) This is a graph showing the highest level of phase-locking observed as a function of frequency in cat auditory nerve fibers. From Javel 1988.

However, as the intensity of the sound increases, the neural response becomes less specific and responds to a broader range of frequencies. The auditory nerve tuning curve is typically represented by a V-shaped set of action potentials. Fig. 1.10(B) depicts a range of tuning curves from various neurons with distinct "characteristic frequencies." Each trough in the graph corresponds to the frequency at which the neuron is most sensitive, commonly referred to as its "best frequency." Notably, every neuron in the graph has a specific best frequency.

The characteristic frequency is primarily determined by the location of the neurons and their associated hair cells along the basilar membrane.

1.4 Inner hair cell ribbon synapses

Cochlear hair cells contain specialized presynaptic organelles called the ribbons, Fig. 1.11.

Pre-synaptic ribbon synapses were first observed in retinal bipolar cells using transmission electron microscopy, as an electron-dense structures surrounded by synaptic vesicles (Eccles, 1964; Burns and Augustine, 1995; De Camilli, 1995). Later they were found also in the hair cells in the vestibular system (Matthews and Fuchs, 2010; Moser and Vogl, 2016).
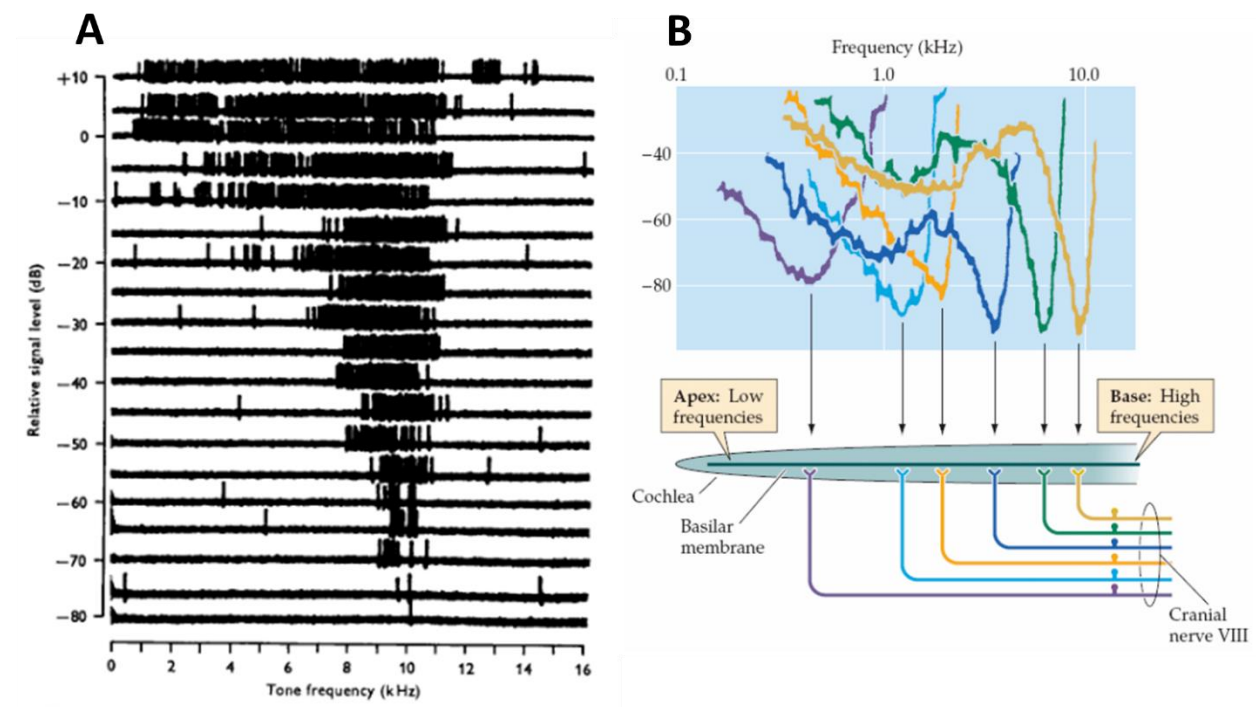
Figure 1.10 Auditory nerve fiber selectivity and frequency tuning curves

(A) A frequency sweep was applied to measure the selectivity and sensitivity of an auditory nerve fiber, where action potentials were recorded as vertical ticks at a specific time point, representing a specific frequency in the sweep. The characteristic frequency (cf) is the frequency that elicits action potentials at the lowest intensity. As the intensity increases, action potentials are triggered by a broader range of frequencies. From Evans 1972. (B) The frequency tuning curves of auditory nerve fibers superimposed and aligned with their approximate relative points of innervations along the basilar membrane. From Salimpour 2006.

Anatomically, the main component of the ribbons is the protein RIBEYE, whose functional role was explored in different studies using knock-out mice for this protein (Becker et al., 2018; Jean

et al., 2018a). These mice do not show the characteristic electron-dense structure, but only ribbonless vesicles that could partially compensate for the loss of the ribbons. Ca^{2+}-dependent exocytosis in the IHCs in these Ribeye-KO mice was reduced for weak depolarizations and the broader spread of Ca2+ signals observed was consistent with the changes in Ca2+-channel clustering detected through super-resolution immunofluorescence microscopy.

Also, activation of Ca2+ channels was shifted to more depolarized potentials, and both the spontaneous and sound-evoked firing rates of SGNs, as well as their compound action potential, were diminished. These findings collectively suggest that there is a disruption in the transmission of signals at the IHC-SGN synapses in the absence of ribbons (Jean et al., 2018a).
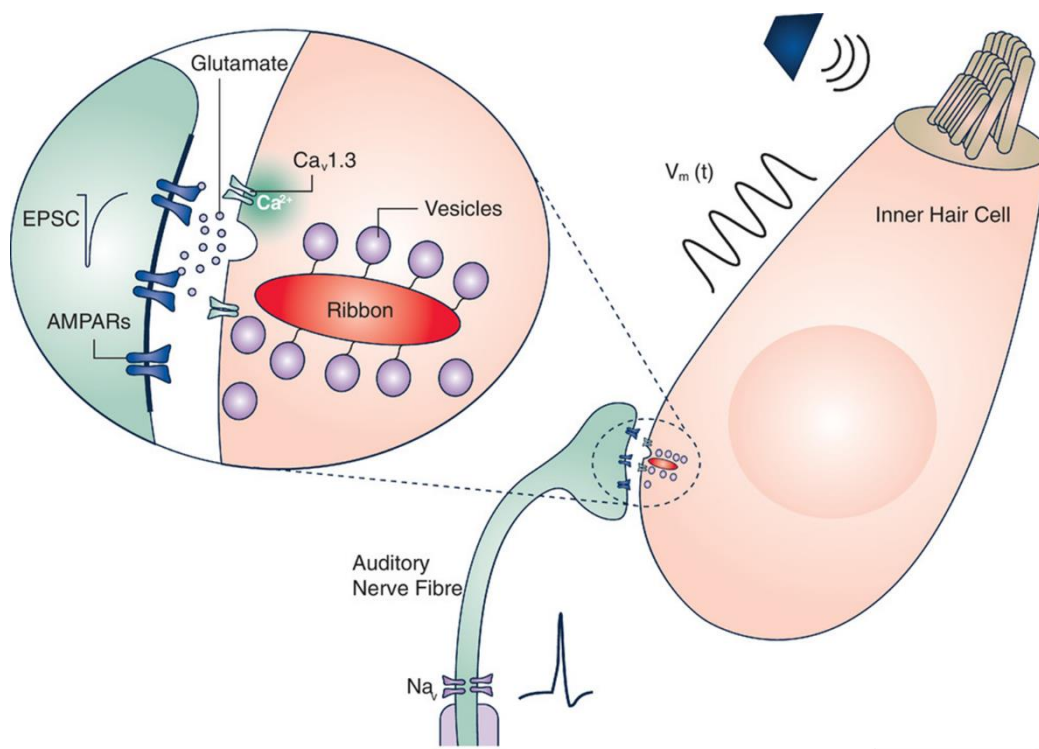
Figure 1.11 Neural activation via IHCs and neurotransmitter release
An illustration depicts an inner hair cell with sound-responsive stereocilia. As previously explained, the influx of positively charged ions leads to depolarization and activation of vesicle release at the pre-synaptic active zones. This release results in the binding of neurotransmitter, usually glutamate, to post-synaptic receptors on spiral ganglion neuron boutons, initiating action potentials. From Rutherford 2021.

Ribbons are anchored to the plasma membrane indirectly via Bassoon (Khimich et al., 2005; Jing et al., 2013). This ubiquitous presynaptic protein is further important in organizing and maintaining Ca2 -channel clusters, and supporting vesicle replenishment (Frank et al., 2010).
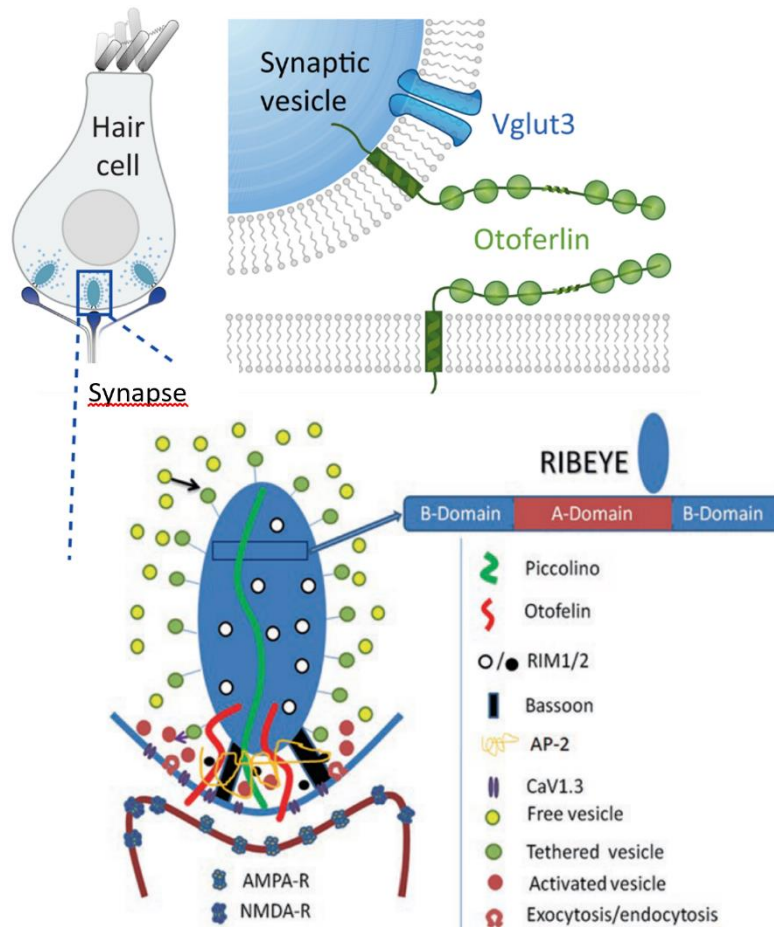
Figure 1.12 Proteins at the IHC ribbon synapse

Schematic Representation of the main proteins at the IHC ribbon synapse. RIBEYE is a key protein in the ribbons of inner ear hair cells, but its absence in mice results in reduced exocytosis and impaired auditory nerve activation. The ribbons also contain specialized proteins such as otoferlin and bassoon, with otoferlin involved in exocytosis and bassoon playing a role in anchoring, organizing and supporting vesicle replenishment. Voltage-gated Ca2+-channel clusters are also present in the hair cells to enable neurotransmitter release, while vGLUT3 is the unique vesicular glutamate transporter responsible for loading glutamate into vesicles (adapted from Pangršič et al., 2012; Chapter 3, Wang 2019).

Synaptic machinery at the IHC ribbon synapse is partially unique (reviewed in Moser et al., 2018). Otoferlin is extremely important for the exocytosis of the vesicles (Roux et al., 2006), likely acting as a calcium sensor to trigger exocytosis (Michalski et al., 2017), Fig 1.12.

It is also believed to be involved in vesicle replenishment, tethering of the vesicles around the ribbons, and clathrin-mediated endocytosis (Roux et al., 2006; Pangrsic et al., 2010; Reisinger et al., 2011; Duncker et al., 2013; Jung et al., 2015a; Vogl et al., 2016; Michalski et al., 2017). IHCs contain an unusual vesicular glutamate transporter, the vGLUT3, which loads glutamate into the synaptic vesicles (Seal et al., 2008). Beneath the ribbon, voltage-gated Ca2+-channels are organized in clusters (Brandt et al., Neef et al., 2018). Interestingly, contrary to most conventional synapses, the release of vesicles in the inner hair cells is independent of the SNARE proteins. (Nouvian et al., 2011).
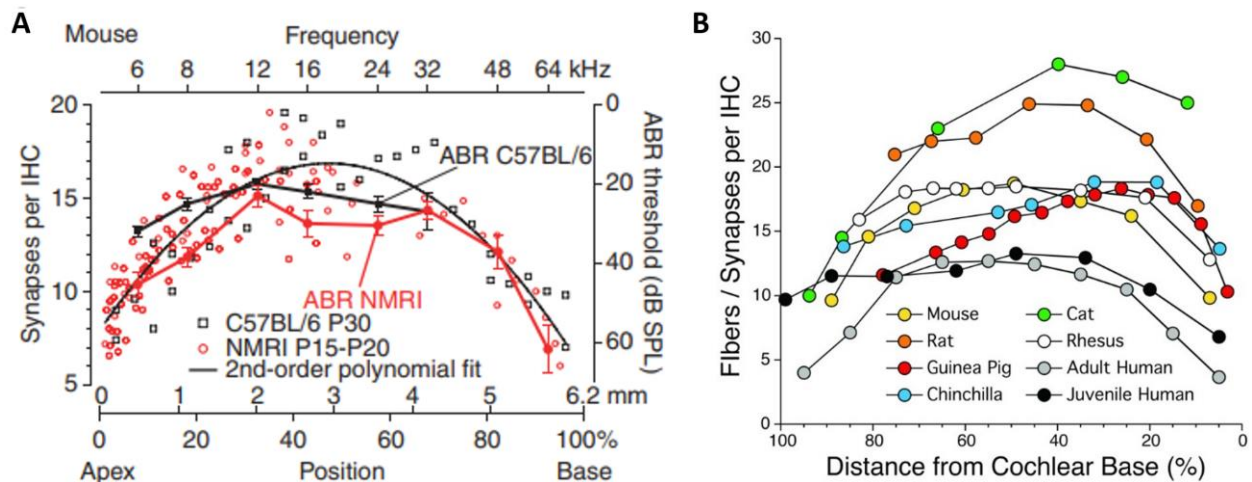
Figure 1.13 IHC ribbon synapses density in different species

(A) The cochlear synaptic connections and tone-burst ABR audiograms of NMRI and C57BL/6 mice have been compared by plotting the distance from the cochlear apex to the tonotopic map of CBA mice (top axis 18). The NMRI mice are represented by red open circles, representing the number of synapses per inner hair cell (26 ears, ages P15-P20), and red filled circles representing the average ABR threshold with s.e.m. (ten ears from six mice). C57BL/6 mice are depicted by black open squares, indicating the number of synapses per inner hair cell (two ears, age P30), and black filled squares linked together, representing

the ABR threshold. The collective data set of both mouse strains is fitted with a continuous black line using a quadratic function. From Meyer et al., 2009. (B) The normal density of auditory nerve fibers in the cochlear spiral is determined by analyzing data from various species including mice, rats, guinea pigs, chinchillas, rhesus monkeys, and adult and juvenile humans. The data for adult humans and other species come from confocal analysis of immunostained synapses in cochlear epithelial whole mounts, while data for cats come from a serial-section ultrastructural study. The difference in the data for low frequencies in the two sets of human data may be due to the presence of ANFs that form two synapses in the apical regions of the cochlea. From Liberman et al., 2017.

The Ca2+-sensor sinaptotagmin1 is also missing at the IHC ribbon synapses. Studies have shown that on average there are approximately 15 different SGNs connecting to each IHC. Fig 1.13 (A) illustrates the ribbon synaptic density per inner hair cell (IHC) in mice, plotted as a function of its position along the basal membrane, as reported in the study conducted by Meyer et al. in 2009. Note that one pre-synaptic ribbon synapse communicates exclusively with one spiral ganglion neuron terminal, without branching (Rutherford et al., 2012; Wichmann and Moser, 2015; Pangrsic and Vogl, 2018). The ribbon synaptic density per IHC is correlated with the position of the cell along the tonotopic axis and can be described with a quadratic function (Meyer 2009). Interestingly, the shape of the synaptic density as a function of the position on the tonotopic axis is overlapping with that of the audiogram, suggesting that cochlear sensitivity correlates with the strength of the IHC innervation. In adult humans, the synaptic density is lower than in mice, on average 12 ribbon synapses per IHC and, instead, the cat seems to have the highest synaptic density among all the animals, on average 28 (Liberman et al., 2017).

1.5 Heterogeneity of SGN fibers

Spiral Ganglion Neurons (SGNs) are bipolar neurons, located in the spiral ganglion. Two types of SGNs have been identified: SGNs type I neurons are myelinated. The "peripheral axon" of a type I SGN forms a synaptic contact with the IHC. Its "central axon" projects to the cochlear nucleus. SGNs type II are pseudounipolar and unmyelinated, and innervate the OHCs. One afferent type-II fiber branches and contacts multiple OHCs, but each OHC is innervated exclusively by one type-II fiber (Liberman, 1982; Spoendlin, 1969, 1972).
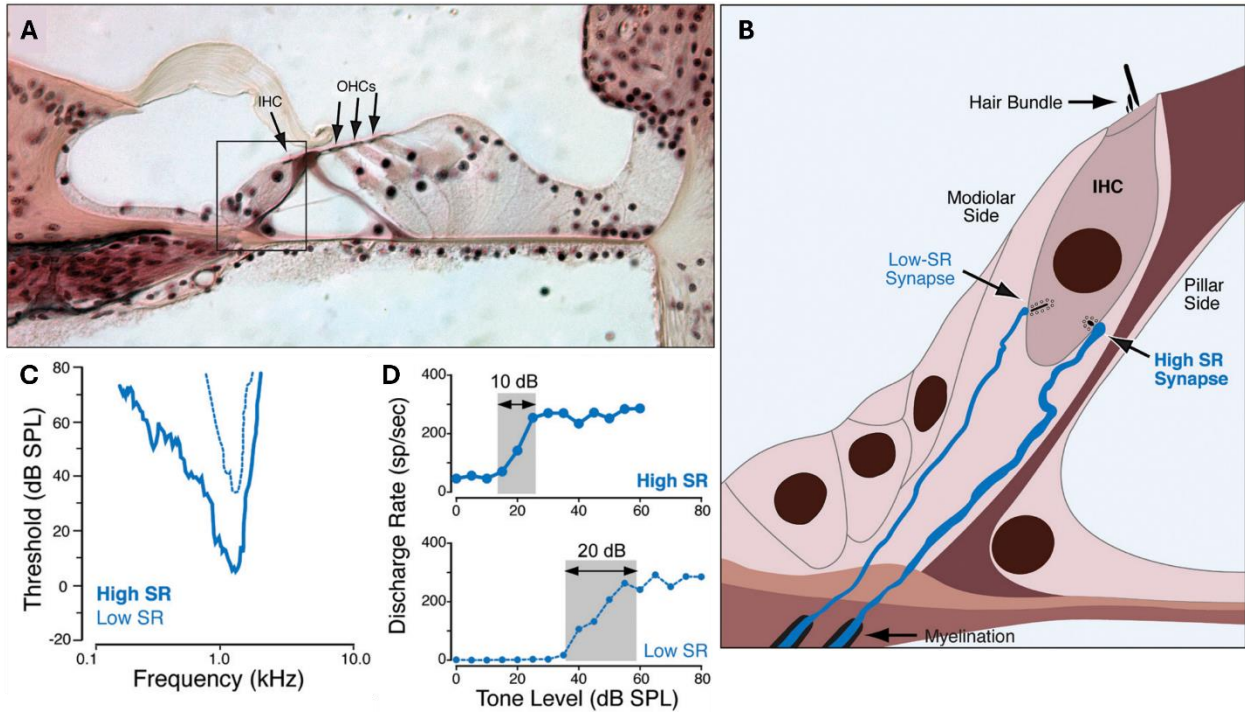
Figure 1.14 Synaptic connections and dynamic range in auditory nerve fibers

These figures display the variance between high and low spontaneous discharge rate auditory nerve fibers and their synaptic placement in regards to the inner hair cell. (A) A light micrograph of the organ of Corti in conventional histological material stained with hematoxylin and eosin is shown, where the peripheral terminals of auditory nerve fibers in the inner hair cell area are not distinguishable. (B) A schematic illustration demonstrates that high and low spontaneous discharge rate fibers make synaptic connections on opposite sides of the inner hair cell. The changes in ribbon synapses in different areas around the IHC can be appreciated. The synapses located on the modiolar side appear to have a wider ribbon, but a smaller postsynaptic terminal. (C) The tuning curves demonstrate that high spontaneous discharge rate fibers have lower thresholds compared to low spontaneous discharge rate fibers. (D) When stimulated with tone bursts at the characteristic frequency, high spontaneous discharge rate fibers have a smaller dynamic range (represented by the grey box) compared to low spontaneous discharge rate fibers. The abbreviation dB SPL stands for decibels sound pressure level and OHC represents the outer hair cell. From Liberman 2017.

The nerve fibers of the type I SGNs are classified as: low-spontaneous rate fibers (LSR fibers), medium- (MSR), and high-spontaneous rate fibers (HSR fibers), (Liberman, 1982; Kiang et al., 1965). In the absence of a stimulus, in the resting state, the first type of nerve fibers fires spikes at low frequency (< 0,5 spikes per second) compared to the third type, which can spike up to 100 spikes per second. These different types of nerve fibers are in the cats well anatomically segregated with respect to where they attach to the IHC.

The LSR and MSR fibers contact the IHCs at the modiolar/neural side (closer to the modiolus) and the HSR fibers at the pillar/abneural side (closer to the OHCs) of the IHC (Liberman, 1980; Merchan-Perez and Liberman, 1996; Tsuji and Liberman, 1997; Pangrsic et al., 2018). Interestingly, immunostaining studies have shown opposing gradients of the sizes of pre-synaptic ribbons and post-synaptic terminals within the same IHC. More specifically, larger ribbons on the modiolar side of the IHC basolateral membrane are associated with small AMPA receptor patches, and small ribbons on the pillar side are associated with large AMPA receptor patches (Liberman et al., 2011; Zhang et al., 2018). Although the same applies to the mouse cochlea, it is not as clear as in the cat cochlea (Ohn et al.).

Electron microscopy studies have also shown that the LSR and MSR fibers innervating the modiolar face contain fewer mitochondria than the thick HSR fibers on the pillar face (Merchan-Perez and Liberman, 1996). Intracellular single SGN labeling after single-unit recording in the cat with horseradish peroxidase, allowed to find out that HSR fibers typically have a larger diameter (1.18 µm on average) than LSR or MSR fibers (0.37 µm on average) (Liberman, 1982).

Besides their anatomical differences, there are also three main functional differences between these nerves. The first difference is that the HSR fibers show a lower threshold for activation, compared to the LSR and MSR fibers. This means that the HSR fibers are more readily activated with responsive sound. The second difference is that the HSR fibers, as shown in Fig. 1.14, have a broader frequency range of activation compared to the LSR and MSR fibers, which respond to a more restricted frequency range. The third difference is that the HSR fibers have a smaller dynamic range compared to the LSR and MSR fibers before they saturate the response, as indicated by the slope of the discharge rate as a function of sound intensity.

Nowadays, it is thought that the differences in cochlear nerve threshold and in the spike rate at resting potentials might be mostly determined by the AMPA receptor expression gradient (Liberman et al., 2011), while the heterogeneity of the EPSC recorded from SGN terminals is mostly determined by the different ribbon size along the IHC basolateral membrane (Niwa et al., 2021). Altogether, these biological properties suggest that the HSR fibers are needed for detecting low intensity sounds with high sensitivity, while the LSR and MSR fibers are well suited to support sound discrimination and hearing in the presence of background noise.
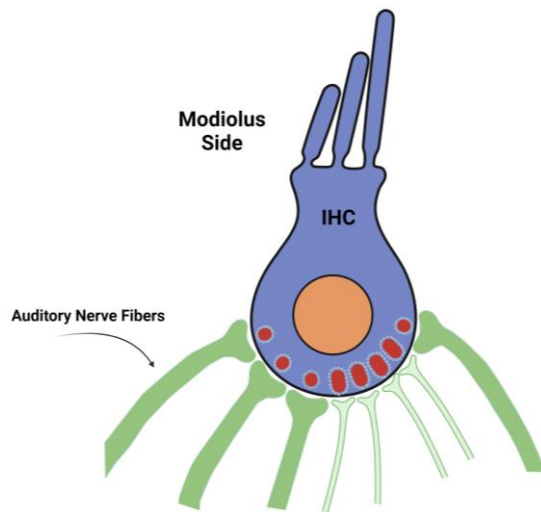
Figure 1.15 Variations in ribbon synapses size around IHC The illustration depicts the changes in ribbon synapses in different areas around the IHC (Inner Hair Cell). The synapses located on the modiolar side appear to have a wider ribbon, but a smaller postsynaptic terminal.

1.6 Ca2+ channel coupling

In the IHCs, synaptic vesicular fusion is triggered by the opening of the voltage-gated L-type $Ca_v1.3$ Ca^{2+}-channels, which are encoded by the *CACNA1D* gene (Platzer et al., 2000). Their short activation time constant (300 µs at 25°C) ensures a fast synaptic transmission and faithful responses to voltage fluctuations of the receptor potential (reviewed in Joiner and Lee, 2015). These channels are further characterized by a low voltage activation, between -65 and -55 mV, and a slow inactivation that, altogether, guarantees reliable responses to small membrane depolarizations, occurring at low-intensity sound, and sustained signaling at long depolarizations (Beutner et al., 2001; Koschak et al., 2001; Platzer et al., 2000; Spassova et al., 2004; Xu and Lipscombe, 2001, Johnson et al., 2008). These biophysical properties make L-type $Ca_v1.3$ channels ideal to meet the IHCs needs.

In mature IHCs, Cav1.3 channels appear clustered in a stripe located under the ribbon of each pre-synaptic active zone (Neef et al., 2018; Wong et al., 2014). These clusters are heterogeneous and as estimated may contain between 20 and 330 Cav1.3 channels (Neef et al., 2018), while in total of 1000 to 3000 channels in the entire basolateral membrane with less than 10% of them located extrasynaptically (Brandt et al., 2005; Graydon et al., 2011; Zampini et al., 2010), but newer estimates suggested that between 20 and 50% of the channels could be present extrasynaptically (Neef et al., 18).

Besides the unique biophysical properties of the Ca2+-channels, also the spatiotemporal diffusion of the Ca2+-current at the level of single active zones in response to membrane depolarization plays a critical role in auditory signal transmission. According to the nanodomain hypothesis of exocytosis, only the Ca2+-channels located in close proximity to the vesicle release site (less than 100 nm) contribute to triggering the vesicle fusion, which typically means one or very few Ca2+-channels (Moser et al., 2006a; Neher, 1998). According to this hypothesis, the exocytosis at a given active zone is linearly dependent on the number of Ca2+-channels contained in that cluster, resulting thus in an apparent cooperativity close to 1. More recently, it has been shown that the distance between Ca2+-channels and synaptic vesicles does not exceed 17 nm (Pangrsic et al., 2015). This tight coupling is thought to play a crucial role in the sensitivity of the synaptic vesicles to the Ca2+ ions and, consequently, to the speed of the synaptic transmission (Eggermann et al., 2012; Jarsky et al., 2010; Matveev et al., 2011). A second hypothesis to explain how IHC synaptic vesicle fusion is controlled by Ca2+ ions comes from the idea that many channels with overlapping Ca2+ domains located at a distance longer than 100 nm from the vesicular Ca2+ sensor are employed in the fusion of a single vesicle. The exocytosis shows thus a non-linear dependence on the Ca2+-channels number, resulting in an apparent cooperativity higher than 4 (Eggermann et al., 2012; Jarsky et al., 2010; Matveev et al., 2011). According to this hypothesis, signal transmission has a reduced signal-to-noise ratio (Matveev et al., 2009, 2011).

1.7 Hearing loss

In the vast majority of cases, the source of the hearing loss originates from the ear itself. Normally, the outer ear gathers sounds from the environment and funnels them through to the

middle ear. But sometimes, sound cannot properly reach the inner ear. This happens when there is a build-up of wax in the ear canal, or of fluid in the middle ear (e.g. caused by an infection and consenquently inflammation of the middle ear as in otitis media). It can also occur as a consequence of damage or malformations of the middle ear ossicles or tympanic membrane, or other ear malformations (e.g. of the outer ear pinna) . This is called "conductive (or mechanical) hearing loss". This type of hearing loss can, depending on the cause and severity, often be fixed with medicine or surgery, e.g. by middle ear prosthetics, tympanostomy tubes to enable fluid drainage etc.

Another kind of hearing loss, and the most frequent, is called "sensorineural hearing loss" because it can include different types of hearing loss:

- **sensory**, which happens when the cochlea does not work well or not at all;
- **neural**, when the auditory nerve or other parts of the brain are affected;
- **sensory and neural**, when a combination of sensory and neural hearing loss is present.

The malfunction of the outer hair cells (OHCs), which amplify the mechanical oscillations of the basilar membrane and sharpen its tuning, can result in reduced hearing sensitivity and frequency discrimination. Complete loss of OHC function in rodent animal models can shift hearing thresholds by 40-60 dB SPL, leading to no or mild to moderate hearing loss. The loss of inner hair cell (IHC) function, on the other hand, can result in no or mild to profound hearing loss. The severity of hearing loss in either case depends on the extent and location of the hair cell dysfunction or loss, which can affect the whole or parts of the cochlea along the tonotopic axis. The treatment or management of sensorineural hearing loss (SNHL) depends on the source of the problem. If it is due to the loss or malfunction of the OHCs, hearing aids are typically used to amplify incoming sounds before they enter the ear canal. In cases of severe to profound hearing loss due to IHC dysfunction or loss, a cochlear implant can be placed in the cochlea to partially restore hearing. For children, auditory verbal therapy is used to aid in language development and communication skills.

SNHL can have genetic, toxic, or age-related causes, among others. Age-related and noise-induced hearing loss are the most common, sharing similar molecular and clinical manifestations. High-frequency hair cells or IHC ribbon synapses in the basal region of the cochlea may die in these cases, resulting in a lack of clarity when listening to sounds or speech comprehension. "Upward spread of masking" may also occur, where background noise drowns out high-frequency components important for speech comprehension.

Unfortunately, there are currently no successful treatments available for age-related and noise-induced hearing loss. However, noise-induced hearing loss can be prevented by wearing earplugs or avoiding acoustic overexposure. Pharmacological treatments are under investigation, and basic research investigating the cellular and molecular dynamics involved in the onset of these diseases can aid in the identification or development of efficient drugs.

Common causes of SNHL can be either genetic factor, tumors on the auditory nerve, head trauma, toxic chemical exposure, and the most common, age-related (ARHL), and noise-induced (NIHL) (reviewed in Wong and Ryan, Front Aging Neurosci, 2015). The last two share several similar molecular and clinical manifestations (Kujawa and Liberman, 2006; Liberman and Kujawa, 2017). Anatomically, either the hair cells or the IHC ribbon synapses in the high-frequency range, which corresponds to the basal region of the cochlea, end up dying. Clinically, this results in a lack of perceived clarity when listening to sounds or other people talking, and this happens because high frequencies encompass clarity in speech, and low frequencies encompass volume in speech instead (Vojtech et al., 2019). A defect in the high-frequency range results also in a phenomenon called "upward spread of masking", which is the condition when the ability to hear the background noise (low frequency) is maintained, but it drowns out all of those high-frequency components important in speech comprehension (Klein et al., 1990; Oxenham and Plack, 1998). For these two types of SNHL, there are no successful treatments available yet. However, noise-induced hearing loss can be prevented by wearing earplugs, for example, or avoiding acoustic overexposure. Pharmacological treatments are under investigation. Identifying or developing most efficient drugs can be importantly helped by basic research investigating the cellular and molecular dynamics involved in the onset of the diseases

1.7.1 Noise-induced hearing loss and the auditory pathway

Traditionally, it was believed that the hair cells (in particular the OHCs) are the primary target of acoustic trauma and that the ribbon synapses and the SGNs degenerate as a consequence of the hair cell's death. In the 1970s, the audiometric thresholds were used in different studies to explore the effects of acoustic exposure to noisy factories with the final aim to determine the limit that noise should not exceed to be considered safe (Wilmot, 1972). At the same time, also the effect of age was explored in adults showing symptoms of hearing loss. Based on the audiograms, both groups of people showed a threshold elevation, often called "notch" at high-frequency range, between 4-8 kHz. In the case of the factory workers, it has been described that the extension of the threshold elevation was positively correlated with the intensity of noise they were exposed to, reaching a profound hearing loss even at low-frequency range (1-2 kHz) in those individuals exposed to noise levels at around 103 dBA (Zare et al., 2016).

An intriguing similarity in the clinical manifestations between noise-induced hearing loss (NIHL) and age-related hearing loss (ARHL) has been observed (Kujawa and Liberman, 2006). In addition to showing threshold elevations in auditory brainstem responses (ABR), patients diagnosed with NIHL and those with ARHL reported similar symptoms, notably the inability to fully comprehend speech in a noisy environment. Histologically, extensive hair cell loss, primarily in high-frequency cochlear regions, was observed in temporal bones obtained from 150 patients across a broad range of ages (Bommakanti et al., 2020).

Together with hair cells loss, degeneration of the auditory nerve fibers has been observed in post-mortem temporal bone materials from adults as well (Makary et al., 2011; Heshmat et al., 2020). Johnsson LG shows that sensorineural degeneration after sound exposure resulted in an initial phase where the basal OHCs and IHCs would die, followed in time by a second phase where neural degeneration of the auditory nerve and its cell bodies in the cochlear nucleus occurred (Johnson, 1974). This cascade of events seemed to be happening also in the ARHL.

An old study published in 1955, demonstrated for the first time that the auditory threshold measured from ABR responses does not sufficiently capture SGN loss, but is rather dependent on the numbers of functional IHCs and OHCs (Mackenzie and Wolfenden, 1955). The authors used cats as animal models. They performed craniotomy in these animals and selectively cut

parts of the auditory nerve to remove certain populations of SGNs, while maintaining the hair cell population intact.
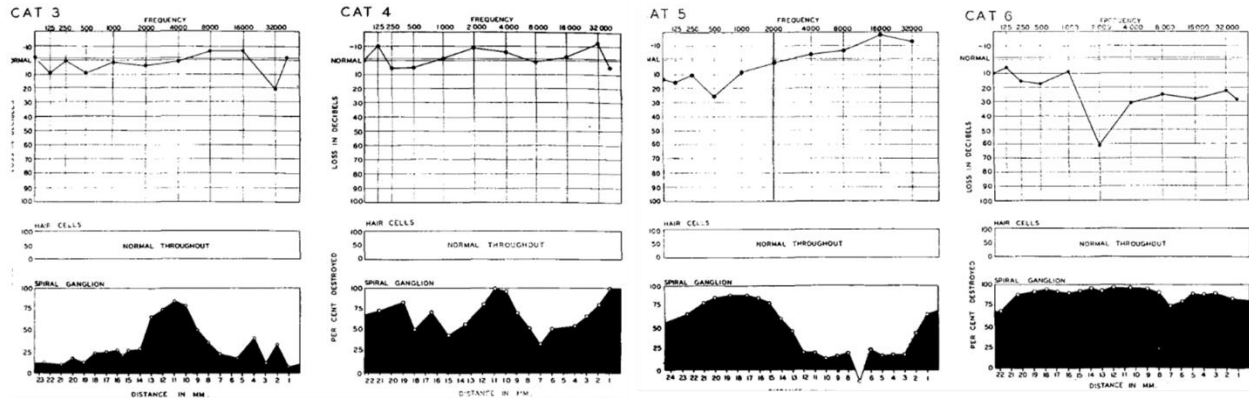
Figure 1.16 Impact of spiral ganglion neuron loss on auditory function in cats

This figure explains the impact of spiral ganglion neuron loss on auditory function in cats after a craniotomy study. The researchers utilized cats as their test subjects for their study. They performed a surgical procedure known as craniotomy and selectively removed certain portions of the auditory nerve in order to eliminate specific populations of spiral ganglion neurons (SGNs). The hair cell population was kept intact during the procedure. The findings showed that as long as the hair cell number was preserved, the audiometric thresholds remained unchanged, regardless of the SGN loss. However, when the SGN loss reached 80-90% of the total neuronal population, the auditory brainstem response (ABR) thresholds began to shift towards higher-intensity sounds. The black area in the graphs represents the amount of SGN loss. From Mackenzie and Wolfenden, 1955.

The result was that as long as the hair cell number is maintained, the audiometric thresholds are maintained as well, irrespective from the SGN loss. However, when the SGN loss reached 80 to 90% of the entire neuronal population, the ABR thresholds started shifting to higher intensities. In the Fig. 1.16, the amount of SGN loss is indicated by the black area.

The theory, which regards the hair cells as the primary target for acoustic trauma and neural degeneration as a secondary event, had been reinforced in several studies published in the early 2000 where animals were exposed to loud noise (for example 116 dB SPL, "decibels Sound

28

Pressure Level", at 4 kHz in Bohne and Harding, 2000; or from 94 dB to 116 dB SPL in Wang et al. 2002) for several days. In response to that, as expected, a "primary damage" corresponding to small focal losses of both OHCs and IHCs in the high-frequency region (4-8 kHz) was observed, Fig. 1.17 and 1.18.
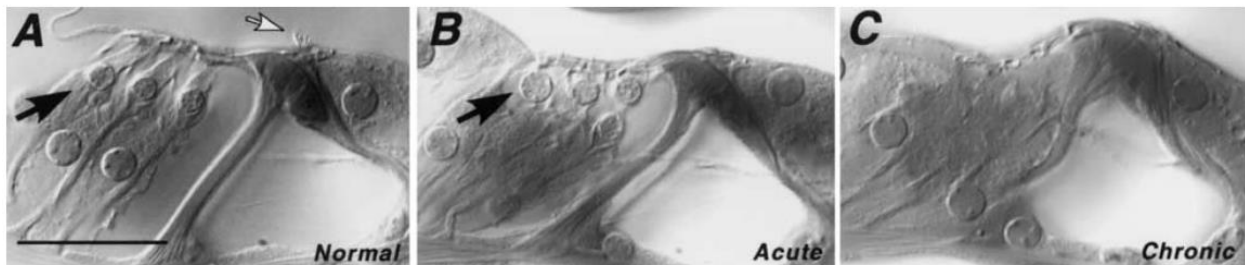
Figure 1.17 Hair cells loss: primary event

24 hours after being exposed to a noise band at 116dB in the midbasal turn region around 22 kHz, there is a noticeable increase in swelling in the OHC nuclei (as indicated by the arrow in image B). This region in all chronic ears displays a total loss of OHCs (C). For comparison, a normal control cochlea in the same cochlear region (A) is also shown. The normal bundle of stereocilia can be seen in the control section (open arrow). The scale bar represents 25 μm. From Wang et al. 2002.
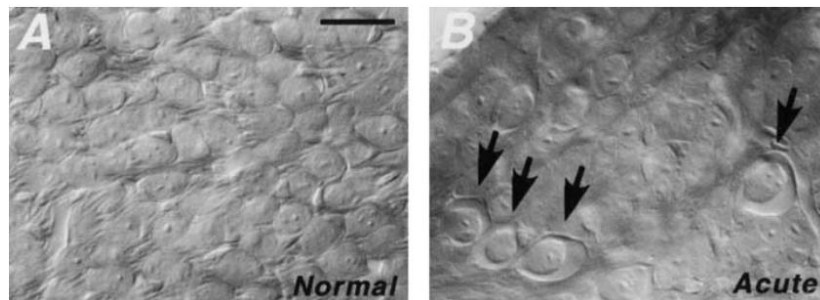
Figure 1.18 Spiral Ganglion cell loss: secondary event

A noticeable swelling of cells in the spiral ganglion (arrows in image B) was observed 24 hours after being subjected to a 112 dB sound exposure. Image A shows the typical appearance of the spiral ganglion in control ears for comparison. Both micrographs were taken from the upper basal turn. From Wang et al. 2002.

The animals exposed for longer periods instead, showed a more diffuse cellular loss involving also lower-frequency regions, along with degeneration of adjacent myelinated fibers.

After the introduction of a new approach of single-unit labeling technique to study the functional properties of the auditory nerve using horseradish peroxidase after measuring the tuning curve and spontaneous discharge, it became clear that noise can trigger the SGN type I terminals to swell within 24 hours post-exposure (Liberman 1982).

The involvement of the SGN terminals acquired more attention when it has been shown that in the case of a temporary threshold shift (TTS) of the ABR, which means that after an initial threshold elevation following noise, they can recover to the original values showed before the exposure, the SGNs terminals showed a recovery of their shape after an initial swelling post-noise, in absence of any hair cell damage. This study introduced for the first time a new player in the well-established noise-induced cascade of events: the IHCs-SGNs synapses (Kujawa and Liberman 2009). Apparently, the auditory nerve terminals could be affected, although temporarily, independently from the IHCs.

To fully understand how the IHCs-SGNs synapses behave after noise exposure, analyzing them using serial-section ultrastructural analysis was the path forward. However, this is extremely labor-intensive and time expensive. For this reason, unfortunately, the question of whether or not noise destroys IHCs-SGNs synapses on surviving IHCs has been set aside for a long time. In the study of Kujawa and Liberman (2009), the mice were exposed to 100 dB SPL noise for two hours (8-16 kHz) and both the cochlear functionality and the synapses between IHCs and SGNs were explored at different time points after the insult by the use of immunohistochemistry and confocal microscopy. The ABR thresholds appeared to shift immediately after the noise trauma, resulting in hearing loss. However, over the next eight weeks, ABR thresholds recovered completely. DPOAEs (Distortion Product of Oto-Acoustic Emissions) and CAPs (Compound Action Potentials), two audiometric recordings that measure the functionality of the OHCs and the auditory nerve fibers, respectively, also showed a transient shift, which recovered completely already two weeks after the noise trauma. At the synaptic level, one day after the noise exposure, a dramatic drop off of the ribbon synapses and their post-synaptic partners was observed (~50%), particularly at high cochlear regions, in line with the previous reports on both humans and animal

models (Kujawa and Liberman, 2009; Sebe et al., 2019; Kim et al., 2019; Liu et al., 2019; Valenzuela et al., 2020). Moreover, two weeks after the exposure, a slight loss of SGNs in the cochlear nucleus started appearing, which became even more evident after one year (Kujawa and Liberman, 2009; Liberman et al. 2015; Fernandez et al. 2015). This loss of auditory nerve synapses was seen also in other animal models, like monkeys, rats, chinchillas, and guinea pigs (Hu et al., 2000; Furman et al., 2013; Hickman et al., 2020). In the latter, however, a partial post-exposure recovery of the synaptic immuno-signal was observed, which may represent, as reported by the authors, "transient down- and up-regulation of ribbon or receptor proteins rather than degeneration and regeneration of synaptic contacts" (reviewed by Hickox et al. 2017).

Other animal models of sensorineural hearing loss also show synaptopathy. Aging mice (2 years old) show ~50% of synaptic loss in the basal region of the cochlea preceding hair cell loss (Ruan et al. 2014; Liberman et al. 2015). A significant drop of synapses also appears after treatment with low doses of ototoxic drugs, with no audiometric threshold elevation or hair cell loss (Ruan et al. 2014).

Since the synaptic loss does not affect the audiometric threshold until it exceeds ~80% (Schuknecht and Woellner 1955; Lobarinas et al. 2013), and since it in the past could not be easily seen by traditional cochlear histology, this permanent synaptopathy was termed "hidden hearing loss" (Schaette and McAlpine 2011).

To understand if synaptopathy is also present in humans, temporal bones from aging adults were harvested 40 hours post-mortem, fixed, the cochleae dissected out and stained for SGN type I fibers, pre-synaptic ribbons, and IHCs (Viana et al 2015). As a result, the overall IHCs counts are preserved throughout the individuals examined except for the basal region, which shows a dramatic difference with the apical region. This is also the case for the SGN type I fibers and the pre-synaptic ribbons, which showed a significant decrease in density per IHC with a preference for the high-frequency region, in Fig. 1.19 (Viana et al 2015).

The synaptic count's drop-off was rather strictly correlated with age. The older the individual, the bigger the synaptic loss. This study demonstrates that:

•IHCs in the basal regions are more vulnerable to age than those in the apical region;

- IHC synapses are more vulnerable than the IHC per se;

- IHC synaptic loss is positively correlated with age;

- Synaptopathy of IHCs-SGNs occurs in animals as well as in humans.

The finding that the IHCs-SGNs synapses can degenerate much earlier in time compared to hair cells, gave rise to the hypothesis that synaptopathy might play an important role as an early indicator of auditory functional decline. This question was addressed by (Sergeyenko et al. 2013).
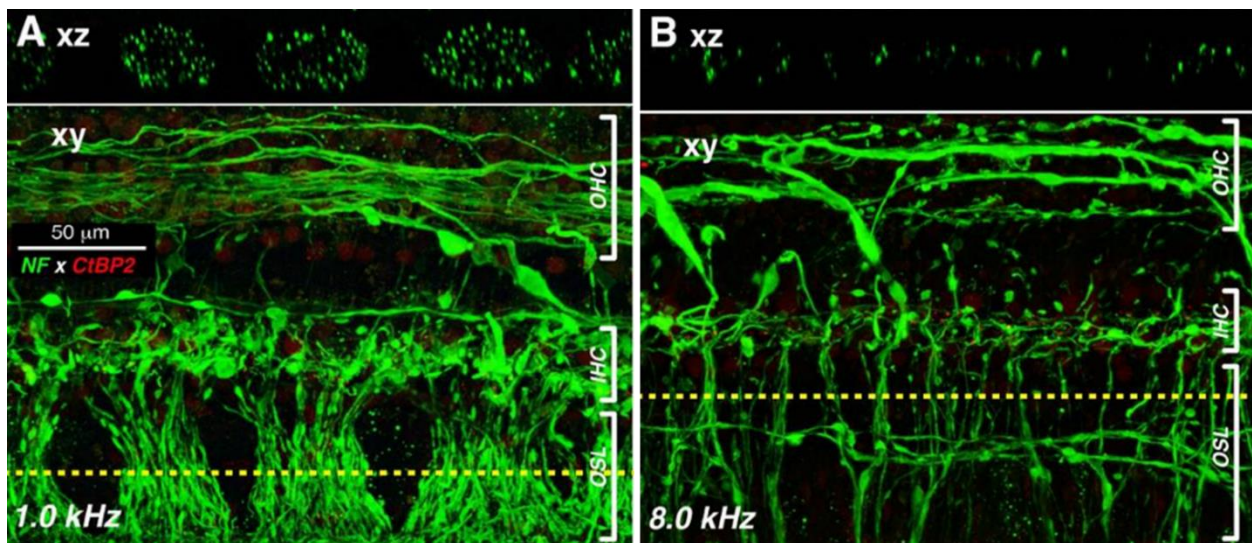
Figure 1.19 Degeneration of peripheral axons in the cochlea

The figure shows the degeneration of peripheral axons in the basal turn of the cochlear nerve, as seen through confocal image stacks of the osseous spiral lamina and organ of Corti in a 67-year-old female at 1 and 8 kHz regions. A and B show pairs of images from different locations in the cochlea, with the maximum projection (xy) of the confocal z-stack stained for neurofilament (green) and an orthogonal slice (xz plane) through the image stack, indicated by a yellow dashed line (from Viana et al., 2015) .

In that study, the authors exposed mice as young adults to moderate-intensity noise, producing either a slight but permanent threshold elevation in the ABR (PTS) or a temporary threshold shift (TTS), and then let them age for 2 years, to explore if the noise exposure could worsen the cellular

and synaptic loss observed frequently in aging mice. The result was that the noise-exposed mice showed ~50% loss of SGN terminals in the basal cochlea versus less than 5% in age-matched controls despite limited hair cell loss. These results confirmed that the synaptic count can be used as an early indicator of auditory functional decline. Single-unit recordings from auditory nerve fibers in 3-year-old gerbils revealed that the percentage of low spontaneous rate (LSR) fibers in the high-frequency region decreased by approximately 30%, while high spontaneous rate (HSR) fibers were unaffected (Heeringa et al., 2020). The loss of LSR fibers was also observed in animals exposed to noise or injected with ouabain, which selectively destroys auditory nerve fibers (Furman et al., 2013; Bourien et al., 2014; Kujawa and Liberman, 2019.

Exposure to loud noise for two hours resulted in a 50% loss of pre-synaptic inner hair cell (IHC) ribbons and postsynaptic terminals in the basal region of the cochlea, with a preferential loss of synapses on the modiolar side, where LSR and medium spontaneous rate (MSR) fibers preferentially innervate IHCs (Kujawa and Liberman, 2015). These findings suggest that noise exposure may mostly damage LSR fibers (Lin et al., 2011; Furman et al., 2013). The functional consequences of auditory synaptopathy are multiple. Studies have shown that the ribbon survival is negatively correlated with the wave I amplitude of the ABR (Kujawa and Liberman, 2009; Lin et al., 2011). So the bigger the synaptic loss is, the lower the wave I amplitude will be. The auditory nerve fibers play a crucial role in encoding sound intensity or changes in sound intensity through two distinct strategies, namely rate coding and population coding. In rate coding, the higher the intensity of sound, the higher the rate of spiking in an individual auditory nerve fiber (ANF). In population coding, sounds with higher intensity recruit more ANFs. Clinically, the loss of some SGN fibers can result in difficulty with sound perception as the auditory nerve fibers are involved in intensity coding (Bharadwaj et al. 2014; Plack et al. 2014; Kujawa and Liberman 2015; Lesica 2018). Synaptopathy also affects the temporal coding, which is the ability of the SGN fibers to follow quick changes of acoustic signals (Lopez-Poveda 2013; Bharadwaj et al. 2014). The activity of individual auditory nerve fibers from noise-exposed guinea pigs showed a bigger latency of the ABR wave I peak (reporting the synchronized activity of the ANFs) compared to fibers from non-exposed animals, without recovery (Mehraei et al., 2016). Clinically, the effect of temporal coding defects results in difficulty with sound localization (Song et al 2016). As described above (section

1.5), the LSR fibers are believed to play a critical role in hearing in the presence of masking noise by virtue of their larger dynamic range. A loss of LSR fibers, particularly at high-frequency range, may cause a difficulty in speech discrimination, especially in noisy environments.

1.7.2 Cellular mechanisms of noise-induced synaptopathy

Studies have shown that infusing the cochlea with a glutamate agonist AMPA results in morphological changes in the SGN terminals, including the swelling, Fig. 1.20 (Ruel et al. 2007). The swelling of the SGN terminals was also observed upon exposure to loud noise (Puel et al., 1998). It was suggested that noise exposure causes an excessive activation of hair cells, inducing a massive presynaptic release of glutamate that, in turn, over-activates post-synaptic AMPA receptors. This then leads to Ca^{2+} excitotoxicity and SGN terminals swelling (Pujol et al., 1985; Puel et al., 1998; Pujol et al., 1999; Ruel at al, 2005; Ruel et al. 2007).

This hypothesis was supported by the study demonstrating that infusion of the inhibitors of glutamate release (Ruel et al., 2005) reduced or prevented noise-induced loss of ribbon synapses, and preserved the auditory metrics (ABR and CAP amplitudes). More recently, new studies came in support of the critical role of glutamate in noise-induced cochlear synaptopathy. For instance, it has been shown that mice deficient in the glutamate transporter expressed in the cochlea (GLAST-deficient mice) exhibit an exacerbation of the functional, cellular and synaptic alterations induced by acoustic overexposure, due to the increased accumulation of glutamate in the perilymph (Hakuba et al., 2000). Furthermore, mice deficient in the vesicular glutamate transporter (vglut3KO mice), thus unable to release glutamate and activate the SGN terminals, show no synaptic loss when exposed to noise (Kim et al., 2019), and finally, blocking post-synaptic Ca^{2+} permeable AMPA receptors, result in complete protection from noise-induced synaptic loss (Hu et al., 2020). All these results confirm the glutamate excitotoxicity as the underlying mechanism of noise-induced cochlear synaptopathy.

Studies have shown that infusing the cochlea with a glutamate agonist AMPA results in morphological changes in the SGN terminals, including the swelling (Ruel et al. 2007). The swelling of the SGN terminals was also observed upon exposure to loud noise (Puel et al., 1998).

It was suggested that noise exposure causes an excessive activation of hair cells, inducing a massive presynaptic release of glutamate that, in turn, over-activates post-synaptic AMPA receptors. This then leads to Ca2+ excitotoxicity and SGN terminals swelling (Pujol et al., 1985; Puel et al., 1998; Pujol et al., 1999; Ruel at al, 2005; Ruel et al. 2007).

The mechanism by which glutamate excitotoxicity induces nerve terminal degeneration has been studied extensively. Studies have shown that excess glutamate leads to a sharp decline in adenosine triphosphate (ATP), resulting in a cascade of events that activates AMP-kinase, which mediates various reactions ultimately leading to apoptosis (Weisova´ et al., 2011).
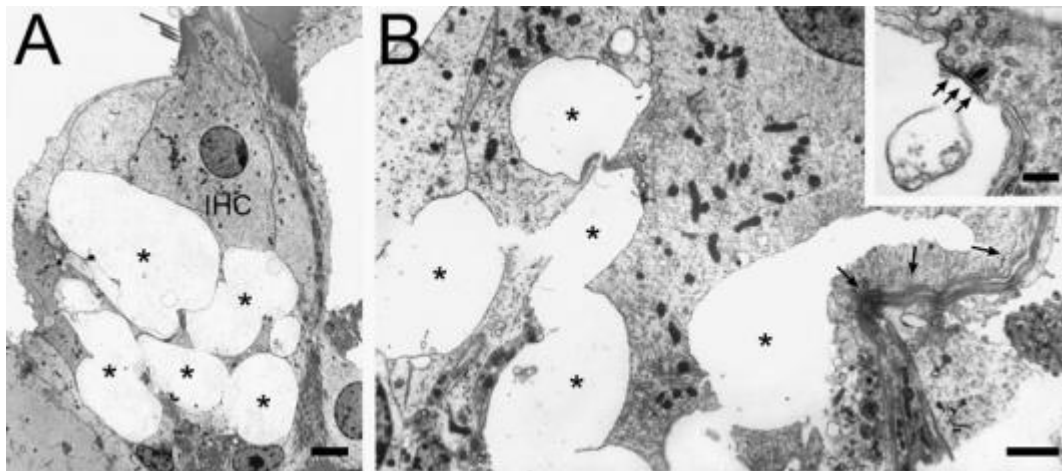
Figure 1.20 Micrographs of guinea pig cochlea after excitotoxic injury

The following are micrographs taken from the cochlea of guinea pigs immediately after experiencing an excitotoxic injury, either from 200 microliters of AMPA or acoustic trauma, and they show the inner hair cell synaptic complex through transmission electron microscopy. In the images (A, B, and inset B), a significant swelling of all the afferent endings at the basal pole of the inner hair cell (IHC) can be seen (indicated by asterisks). This swelling causes mechanical distortions in the basal membrane of the IHC and sometimes in the nearby inner pillar (indicated by arrows in image B). When viewed at high magnification (inset B), the IHC-auditory nerve synapse appears as a normal presynaptic body surrounded by synaptic vesicles (indicated by arrowhead) facing a remaining portion of the postsynaptic membrane (indicated by small arrows). From Ruel et al., 2007.

This mechanism is also proposed to underlie inner hair cell (IHC) degeneration after exposure to loud noise. Traumatic noise induces transient cellular ATP depletion, activating p-AMP-kinase, which then activates Rho-family GTPase, ultimately leading to cellular apoptosis (Chen et al., 2012).

More recently, new studies came in support of the critical role of glutamate in noise-induced cochlear synaptopathy. Furthermore, mice deficient in the vesicular glutamate transporter (vglut3KO mice), thus unable to release glutamate and activate the SGN terminals, show no synaptic loss when exposed to noise (Kim et al., 2019), and finally, blocking post-synaptic $Ca2+$-permeable AMPA receptors, result in complete protection from noise-induced synaptic loss (Hu et al., 2020). All these results confirm the glutamate excitotoxicity as the underlying mechanism of noise-induced cochlear synaptopathy.

How can the glutamate excitotoxicity induce degeneration of the nerve terminals to degenerate? Studies have shown that excess glutamate leads to a sharp decline in ATP (adenosin-3-phospahate), causing a cascade of events that activate AMP-Kinase and ultimately cause the cell to undergo apoptosis (Weisova´ et al., 2011). A similar mechanism was proposed as the underlying basis of IHC degeneration upon exposure to loud noise (Hill et al., 2016). Traumatic noise induces a transient cellular ATP depletion which activates p-AMP-Kinase, which in turn activates Rho-family GTPase that ultimately causes cellular apoptosis (Chen et al., 2012). After the finding of found a permanent increase in reactive oxygen species (ROS) and toxic free radicals like superoxide ($O2.-$), hydroxyl radical ($OH.$), or the peroxynitrite radical ($ONOO .1-$) in both the stria vascularis and outer hair cells (OHCs) (Yamane et al., 1995; Ohlemiller et al., 1999; Ohinata et al., 2000a; Nicotera et al., 1999; Nicotera et al., 2003; Sha and Schacht, 2017; Wu at al., 2020) following noise trauma, a number of studies emerged with the attempt to study in more detail the exact mechanisms of ROS leading to cell/synaptic loss. However, the lack of an in-vitro model for noise-induced hearing loss made it difficult to address this question. It is also et al., 2020). Despite these findings, it is not yet understood if the ROS are produced as a direct consequence of noise trauma or from damaged/dying cells. The development of an in-vitro model for noise-induced hearing loss may allow to better address this question and further unravel could aid in unraveling the molecular pre- and post-synaptic mechanisms leading to the loss of the ribbons

and ribbon synapses and the possible involvement of actin filaments, molecular motors, proteasomes and autophagosomes in the processes of removal and degradation of synaptic elements.

Nowadays, various techniques such as cell culture, proteomic analysis, optogenetics, and pharmacology are being used to study the cellular and molecular effects of acoustic overstimulation on the cochlea of various animal models, with the aim of developing methods for treatment or prevention. More recently, patch-clamp of single IHCs has been employed in a few studies to characterize the functional alterations of the IHC ribbon synapses following noise exposure. However, a major limitation of these studies is that patch-clamp was performed on apical IHCs, which are much more resistant to noise than basal IHCs. Performing single-cell electrophysiology recordings of basal IHCs would significantly contribute to adding new valuable information on the mystery of hidden hearing loss.

1.7.3 Mouse models for the noise-induced loss of IHC ribbon synapses

It is common knowledge that exposure to loud noises can cause permanent hearing loss. Research has shown that noise exposure can damage several structures in the middle and inner ear. Extremely high sound pressure levels, like those from explosions, can cause severe ear damage, including eardrum perforation and disruption of the inner ear's sensory cells. This trauma can detach the cells from their base, leading to their suspension within the inner ear fluids and immediate, permanent deafness (Kerr and Byrne, 1975; Hamernik et al. 1984). Hamernik et al. conducted a pioneering study to determine the anatomical correlates of damage in the cochlea caused by impulse noise stimuli of various intensities to simulate the effects of a gunshot or an explosion.

Besides demonstrating that impulse noise exposure led to immediate and severe damage to the cochlea, such as the complete separation of the basilar membrane from the organ of Corti, the study revealed that the extent of the damage was associated with both the intensity and duration of the noise exposure. For example, exposure to high-intensity noise (170 dB peak SPL) resulted in more extensive damage to the cochlea than exposure to low-intensity noise (144 dB peak SPL). Several other anatomical correlates of noise-induced cochlear damage were identified, including

damage to the tectorial membrane and the stereocilia of the hair cells. The authors noted that the degree of hair cell damage was related to the intensity of the noise exposure, with higher intensity exposures resulting in more extensive damage to the stereocilia.

At more moderate sound pressure levels and longer durations, such as those from a noisy factory (>85 dB SPL), a gradual degeneration of the IHCs, OHCs and SGNs, can occur. This degeneration causes permanent and progressive hearing loss with increasing exposure time because these sensory cells and neurons never regenerate (Clark et al. 1987).

Aside from the anatomical and structural changes that occur in the cochlea following exposure to noise, functional changes can also be measured using techniques such as the Auditory Brainstem Response (ABR) and Distortion Product Otoacoustic Emissions (DPOAE). The ABR was first described in the early 1970s (Teas and Kiang, 1964), and became more widespread in the 1980s with the development of better instrumentation and signal processing techniques. This technique has since been used to study a wide range of topics related to auditory function, including the effects of noise exposure, aging, and auditory neuropathy, among others. To measure ABR, subcutaneous needle electrodes are placed on the scalp. In an anesthetized animal, short tone bursts at varying frequencies are presented, and the resulting signals are averaged over several minutes. This allows the recording of the summed activity of the cochlear nerve fibers. The "threshold" is determined as the lowest sound pressure that produces an electrical response of a specified magnitude. While tone bursts are commonly used as sound stimuli to elicit ABR, other types of sound stimuli may also be used depending on the research question being addressed. For example, clicks, chirps, and pure tones may be used instead of or in addition to tone bursts to assess different aspects of hearing function or to evaluate the effects of different interventions on auditory processing. The choice of sound stimulus used in ABR testing depends on the research question being addressed, the animal species being studied, and the available resources.

Otoacoustic emissions (OAEs) can be used to measure cochlear thresholds. OAEs are mechanical vibrations that are generated by the motion of hair cells in the cochlea in response to sound. These vibrations travel back to the ear canal and can be detected with a sensitive microphone. When two tones of different frequencies are simultaneously presented to the ear, they create a

third, distorted tone that can also be measured using a microphone in the ear canal (DPOAE). DPOAEs are a specific type of OAE, particularly useful in assessing hearing function, such as detecting small changes in hearing sensitivity over time or evaluating specific regions of the cochlea.

Measuring both DPOAEs and ABRs allows a differential diagnosis at the site of an inner ear lesion. When the hair cells are damaged, both DPOAEs and ABRs are attenuated; if only the ABRs are attenuated, it suggests that there might be an issue with the auditory nerve or the IHCs responsible for transmitting sound information from the cochlea to the brainstem. The minimum sound pressure that is required to produce an electrical response of a certain magnitude can be considered as the "threshold".

Before the introduction and widespread use of minimally invasive techniques for ABR recording, evoked responses to acoustic stimuli were often measured by recording the function of single auditory nerve fibers. This technique involves inserting a glass micropipette filled with a conductive solution into the cochlea of an anesthetized animal, such as a cat. The micropipette is positioned near a single auditory nerve fiber, and the electrical activity generated by the fiber in response to acoustic stimuli is recorded using an extracellular amplifier.

The recording of single auditory nerve fiber function provides a detailed and precise measure of the physiological response to acoustic stimuli at the level of the individual nerve fiber. This technique has been used extensively in auditory neuroscience research to investigate the tuning properties and temporal processing abilities of auditory nerve fibers, as well as to study the effects of noise exposure, aging, and other factors on auditory function.

Exposure to an intense noise stimulus can result in threshold elevation of the Auditory Nerve Fibers at their Characteristic Frequency (CF), which may persist for several weeks (Liberman and Beil, 1979; Liberman and Dodds, 1984b;). Any residual threshold shift is considered permanent. This condition is known as permanent threshold shift (PTS). As said, PTS occurs when the hair cells in the inner ear are damaged beyond repair. These sensory cells and neurons never regenerate, at least in the mammalian inner ear, and the hearing deficits that this degeneration causes are permanent and progressive with increasing exposure time. Numerous studies

conducted over several decades have consistently shown that PTS is closely related to the pattern of hair cell damage or loss in different regions of the cochlea.

In their 1979 study, Liberman and Beil further investigated the relationship between hair cell condition and auditory nerve response in normal and noise-damaged cochleas. They found that noise exposure caused a reduction in the number of hair cells and a loss of synapses between hair cells and auditory nerve fibers. This loss of synapses was accompanied by a reduction in the amplitude of the compound action potential (CAP) of the auditory nerve. These findings suggested that noise-induced damage to the cochlea can result in a loss of synaptic connections between hair cells and auditory nerve fibers, leading to a reduction in the amplitude of the CAP.

Few years later, Liberman and Dodds used single-neuron labeling techniques to investigate the effects of chronic cochlear pathology on the physiology of auditory nerve fibers in cats. These studies built upon the earlier work by Liberman and Kiang (Liberman and Kiang, 1978) and provided further physiological insights into the mechanisms underlying noise-induced hearing loss. Specifically, in their 1984a study, Liberman and Dodds labeled single auditory nerve fibers in cats that had been exposed to high-intensity noise and measured their spontaneous discharge rates (SDRs) over time. They found that noise exposure caused a reduction in SDRs, which persisted for several weeks after the noise exposure had ended. This reduction was most pronounced in fibers that were tuned to the frequency of the noise exposure.

Similarly, in their 1984b study, Liberman and Dodds labeled single auditory nerve fibers in cats that had been exposed to high-intensity noise and measured their tuning properties over time. They found that noise exposure caused a shift in the tuning properties of auditory nerve fibers, with a reduction in tuning sharpness and an increase in tuning bandwidth. These changes were observed in both Type I and Type II auditory nerve fibers and were most pronounced in fibers that were tuned to the frequency of the noise exposure. The authors hypothesized that noise-induced changes in tuning properties and spontaneous discharge rates of auditory nerve fibers could be attributed to damage to the stereocilia of the sensory hair cells and associated alterations in the mechanical properties of the cochlea, including the loss of synaptic connections between hair cells and auditory nerve fibers.

The research by Liberman and Dodds in 1984a and 1984b showed that the hair cell loss was mainly concentrated in the basal turn of the cochlea, responsible for processing high-frequency sounds, and that the severity of the damage was directly related to the intensity and duration of the noise exposure. The hair cell loss was observed at sound levels above 100 dB SPL, with the greatest damage occurring at higher sound levels and longer exposure durations. The authors explain the higher vulnerability of the hair cells in the basal turn of the cochlea to noise-induced damage because they experience greater mechanical stresses compared to hair cells in other regions of the cochlea. This is because the basilar membrane, which supports the hair cells, is narrower and stiffer in the basal turn, causing it to vibrate more strongly in response to high-frequency sounds. Additionally, the hair cells in the basal turn have a higher metabolic demand and are therefore more susceptible to damage from metabolic disturbances caused by noise exposure.

The loss of outer hair cells, which are responsible for amplifying the sound-induced vibration of the sensory epithelium, can lead to threshold shifts of up to 50 dB, while the damage to stereocilia, which are crucial for the hair cell's mechanoelectric transduction, is a common result of noise exposure and can cause significant and sometimes profound permanent threshold shifts (Dallos and Harris 1978; Robertson et al. 1980; Liberman and Dodds 1984).

Additional irreversible damage resulting from PTS has been reported to occur at the level of type IV fibrocytes of the lateral wall in the basal half of the cochlea and the stria vascularis. Although this damage has been observed in other animal models of acoustic injury, it seems to occur only at exposure levels higher than those causing significant hair cell damage in the cat ear (Liberman and Kiang 1978). Wang et al. (2002) found significant strial shrinkage in midcochlear regions following all exposures, which worsened monotonically with exposure level. Ultrastructural analysis of the same cases revealed extensive degeneration of intermediate cells associated with this shrinkage and decreased staining intensity visible at the light microscopic level. This suggests that there may be some diminution in the endolymphatic potential. Acute and chronic changes in the endolymphatic potential have been documented after acoustic overexposure. If true, this chronic strial pathology is expected to contribute to threshold shift, given the consistent

correlation between reduction in endolymphatic potential and threshold elevation. Thus, some diminution in the endolymphatic potential would be anticipated (Syka et al., 1981; Sewell 1984). It has been well-documented that the degree of hearing threshold elevation following noise exposure can vary widely and, in some cases, may be completely reversible, with a return to pre-exposure levels observed within a few days post-exposure (Miller et al. 1963). For example, acute threshold elevation of up to 50-60 dB measured immediately post-exposure has been shown to recover within 3-7 days. Despite the apparent severity of this temporary threshold shift (TTS), histological analysis has revealed no significant hair cell loss or stereocilia damage even at peak threshold shift, lending further support to the notion of a reversible effect. The nature of the most functionally important structural changes underlying temporary threshold shifts remains poorly understood, despite histological evidence indicating that hair cell loss and obvious stereocilia damage are not typically observed even at peak threshold shift, and that there may be only a reversible collapse of some of the supporting cells of the sensory epithelium or subtle submicroscopic damage to the rootlets anchoring the hair bundles into the tops of the hair cells. In Wang et al., 2002, the relevance of the 94 dB exposure level in the context of temporary/reversible threshold shift is discussed. The study found that this level of exposure led to a severe form of TTS, just at the border of full reversibility, with a 50 dB peak threshold shift at 24 hours post-exposure, recorded from ABRs, which recovered almost completely by two weeks post-exposure. This finding suggests that the severity of exposure is a critical factor in determining the extent of TTS.

The study also identified several types of structural changes in the cochlea that contribute to the reversible components of noise-induced hearing loss, including collapse of the supporting cells in the organ of Corti, excitotoxic effects on neural elements, and strial edema. The severity of the exposure and the species involved play a crucial role in determining the type of damage observed. Among all these cellular and structural alterations, the collapse of the outer space of Nuel, associated with buckling of the arching portion of the Hensen cells and a decrease in the height of the organ of Corti, contributes significantly to temporary threshold shifts. The collapse of Nuel space and the height of the Hensen cells recover completely by 2 weeks only for the 94 dB exposure (Wang et al., 2002). These changes in supporting cell architecture would be expected

to change cochlear micro-mechanics and thus cochlear sensitivity (Wang et al., 2002). The collapse of supporting cells in the organ of Corti is a critical contributor to reversible threshold shift, which has been observed in several animal models of noise-induced hearing loss (Nordmann et al. 2000; Flock et al. 1999). In contrast, the degree of swelling observed in the auditory fiber terminals was not found to be a significant factor in determining the magnitude of the TTS. Research has demonstrated that kainate-induced swelling of dendrites can recover in a manner similar to the restoration of ABR responses (Zheng et al., 1997), leading to the idea that the swelling of the auditory fibers could correlate with the threshold shift. However, in a study where excitotoxic effects were blocked pharmacologically, the extent of TTS was not altered (Puel et al., 1988).

The effects of noise exposure on the auditory system have been extensively studied, with a focus on the time course of damage to the hair cells and cochlear nerve fibers. While hair cell loss can be detected within a day after exposure, classical studies have shown that cochlear nerve fiber loss is not observed until weeks or even months later (Johnsson 1974; Liberman and Kiang 1978; Bohne and Harding 2000). This time offset in the degenerative process has led researchers to conclude that hair cell damage is the primary effect of noise exposure, and that cochlear nerve fiber loss is a secondary effect that occurs due to the loss of trophic-factor support supplied by the hair cells.

Traditionally, investigators have assessed neural loss in the cochlea by counting the cell bodies of the spiral ganglion cells, which are easy to see in routine histological material assessed with a light microscope. However, this method is not sensitive enough to detect subtle changes in the synapses between hair cells and cochlear nerve fibers (Liberman, 1980; Liberman, 1982b).

Electron microscopy has been used to study the unmyelinated nerve terminals that make synaptic contact with the inner hair cells. In the 1980s, researchers using electron microscopes observed a significant swelling of the postsynaptic terminals of cochlear nerve fibers in ears that had temporary noise-induced threshold shift. (Liberman and Mulroy 1982; Robertson 1983). This swelling was found to be caused by glutamate excitotoxicity, as glutamate is the neurotransmitter at the hair cell synapses (Pujol and Puel, 1999; Matsubara et al. 1996). Given

that the temporary threshold shift observed in the ears was reversible, the swollen terminals were not apparent during post-exposure examinations conducted a few days later, and there was no indication of ganglion cell loss a few weeks post-exposure, leading researchers to believe that the neural damage incurred may be fully reversible through mechanisms such as recovery or regeneration. However, quantifying the synapses with an electron microscope presented a challenge, and as a result, the researchers were unable to carry out quantification.

Recent studies have developed immunostaining techniques to quantify the synaptic contacts between hair cells and cochlear nerve terminals with a light microscope. By using antibodies against a major protein in the presynaptic ribbon and a subtype of glutamate receptor, synapses in normal ears and those exposed to traumatic noise were counted (Kujawa and Liberman, 2009). This method has shown that temporary hearing loss induced by loud noise exposure can damage approximately 50% of the synapses connecting IHCs to the SGNs throughout the affected regions of the cochlea. This synaptopathy occurs despite no loss of hair cells, and the synaptic loss does not recover, i.e., the nerve terminals do not regenerate.

Interestingly, if the post-exposure survival time is extended for months to years, the spiral ganglion cells slowly degenerate despite no loss of hair cells. This phenomenon remained undetected for a long time due to the extreme slowness of the spiral ganglion cell loss.

The discovery of synaptopathy and the loss of spiral ganglion cells has important implications for understanding the mechanisms of noise-induced hearing loss. It suggests that damage to the synapses between hair cells and cochlear nerve fibers may be a critical factor in the development of hearing loss, rather than the death of the nerve cells themselves. The prolonged and gradual nature of the spiral ganglion cell loss has played a significant role in masking the phenomenon and keeping it undetected for an extended duration.

Thanks to the research conducted by Kujawa and Liberman in 2009, it has become evident that cochlear neurons are primarily targeted, with their peripheral synaptic connections being the most vulnerable elements. Furthermore, it has been established that cochlear nerve synapses can be destroyed even when hair cells remain intact. While the threshold shift remains a sensitive metric of underlying hair cell damage, it is relatively insensitive to the diffuse loss of inner hair cell synapses or the cochlear nerve fibers they stimulate. In fact, behavioral detection thresholds

for tones remain relatively unaffected until neural loss exceeds approximately 80-90% (Schuknecht and Woellner, 1955). This implies that cochlear synaptopathy can be prevalent in ears with intact hair cell populations and normal audiograms, which has been termed as "hidden" hearing loss by Schaette and McAlpine in 2011.

The phenomenon has been observed in multiple mammalian species, including humans, and can be caused by various factors such as noise exposure, aging, and certain medications (Wang and Ren, 2012; Ruan et al., 2014; Viana et al., 2015; Rybalko et al., 2015; Singer et al., 2013). Further studies found that in aging mice, cochlear synaptopathy occurs before hair cell loss and threshold shift (Sergeyenko et al., 2013).

In summary, the loss of inner hair cells due to high-level noise exposure, leading to PTS, can be observed within minutes to hours, whereas the loss of spiral ganglion cells is not seen for weeks to months (Spoendlin, 1971; Johnsson, 1974; Lawner et al., 1997). However, when the inner hair cells are missing, it can be challenging to observe the underlying synaptopathy, which refers to the loss of the ribbon synapses. This is where the mouse model of temporary threshold shift becomes essential. When animals are exposed to moderate intensity noise that causes a complete recovery of the ABR thresholds, swelling of the cochlear nerve terminals can be observed in the area of the inner hair cells within few hours after overexposure. This swelling never recovers or regenerates, resulting in a permanent loss of about 40-50% of the ribbon synapses (Kujawa and Liberman, 2009).

1.7.4 First mouse model of TTS: a milestone in NIHL research

In Kujawa and Liberman (2009) mice exposed to noise resulted in a significant loss of synaptic ribbons in the inner hair cells of the cochlea. Specifically, they found that after exposure to a noise level of 100 dB for two hours, there was a 50% reduction in the number of ribbons in the inner hair cells. This reduction was most pronounced in the inner hair cells located in the basal region of the cochlea, which are responsible for detecting high-frequency sounds.

The pioneering work of Liberman and Kujawa has important implications for our understanding of NIHL. The loss of synaptic ribbons is thought to be a key contributor to the degradation of

sound quality and reduced ability to distinguish sounds associated with NIHL. By quantifying the loss of these structures, Liberman and Kujawa provided evidence that noise exposure can result in a significant permanent reduction in the number of ribbons in the inner hair cells of the cochlea, despite a complete recovery of the ABR thresholds when recorded two weeks after the noise exposure. Prior to this study, it was not clear whether synaptic ribbon loss was a feature of NIHL, and if so, to what extent. Although it was understood that NIHL can cause damage to the hair cells in the inner ear, it was not clear what specific structures within the hair cells were affected. Furthermore, using a pair of distinct antibodies (one was targeted against the major protein CtBP2 situated in the presynaptic ribbon on the hair cell side of each synapse, while the other was directed towards a subtype of glutamate receptor, GluR2/3, localized at the tip of the nerve terminal) the study showed that the loss of ribbons was most pronounced in the basal region of the cochlea, which is responsible for detecting high-frequency sounds. This is significant because high-frequency sounds are particularly important for speech perception, and their loss can result in communication difficulties for those with NIHL.

Kujawa and Liberman (2009) used male mice of the CBA/CaJ strain for this study, exposing them at 16 weeks of age to an octave band of noise (8-16 kHz) at 100 dB SPL for 2 hours, and held without further treatment for various post-exposure times, while age-, strain-, and gender-matched animals held identically, except for the exposure, served as controls.

The authors used CBA/CaJ mice in this study because this particular strain of mice has been shown to exhibit excellent cochlear sensitivity and limited age-related elevation in cochlear thresholds. In other words, they have good hearing and do not experience the typical age-related hearing loss that is observed in many other strains of mice.

Despite, no significant gender differences in thresholds were observed between female and male mice in this study, Han et al. (2022) found sex-based differences in susceptibility to NIHL, with male zebrafish showing a greater threshold shift than female zebrafish at some frequencies. In humans, Wang et al. (2021) found that the prevalence of NIHL was significantly higher in male workers (32.4%) than females workers (22.6%) and the severity of hearing loss was also greater in males than in females. Given that a potential reduced susceptibility to noise cannot be

completely ruled out for female mice, it may be prudent to select male mice when quantifying cellular and functional changes following noise exposure or during the aging process.

Zheng, Johnson, and Erway, (1999) provide a comprehensive assessment of hearing function of 80 different inbred strains of mice using ABR threshold analysis, which would help researchers to select appropriate mouse models for hearing research and improve our understanding of the genetic basis of hearing loss. To achieve this goal, the authors measured ABR thresholds in both young (4 week old) and aged (39 week old) mice from each of the 80 strains, at frequencies ranging from 4 kHz to 32 kHz.

While CBA/J mice are vulnerable to otitis media and retinal degeneration, this mouse strain is often preferred as normal controls in hearing research due to its consistent low ABR thresholds, even at an older age of 39 weeks. Along with CBA/CaJ, several recently derived wild-derived inbred strains, including CASA/Rk, CAST/Ei, CE/J, CZECH II/Ei, MOLD/Rk, MOLF/Ei, MOLG/Dn, PERC/Ei, SF/CamEi, and SHR/GnEi, also exhibit low ABR thresholds. However, some inbred strains, when tested before 13 weeks of age, may have normal hearing but could potentially develop late onset or age-related hearing loss.

Similarly, the C57BL/6J strain had normal ABR thresholds until being 33 week old however, by the time they reached 100 weeks, their ABR thresholds had risen to 60 dB above normal means. On the other hand, some inbred strains, such as BUB/BnJ and NOR/LtJ, show a severe hearing loss before 8 weeks of age. These strains are particularly useful for investigating congenital hearing loss and identifying the genes involved in hearing development.

Kujawa and Liberman (2009) used an octave band of noise with a frequency range of 8-16 kHz in their study because this frequency range is most damaging to the hair cells in the cochlea, which are responsible for detecting sound waves and converting them into electrical signals that the brain can interpret as sound. Previous research has shown that noise exposure within this frequency range can cause significant damage to the outer hair cells of the cochlea, leading to hearing loss (Cody and Johnstone, 1981; Liberman and Mulroy, 1982). This frequency range is also common in many occupational and recreational noise exposures, such as loud music and machinery, making it a relevant and important area of study for understanding the mechanisms of noise-induced hearing loss. The results of the study conducted by Cody and Johnstone showed

that exposure to an intense sound stimulus can cause a "half-octave shift" in the tuning of single neurons in the auditory system. The shift in tuning was most pronounced at high sound frequencies and was caused by a reduction in the tuning bandwidth of the neurons. Before exposure to the intense sound stimulus, the neurons showed a sharp tuning curve that responded to a narrow frequency range. After exposure to the stimulus, the tuning curve shifted downward in frequency by approximately half an octave, resulting in a broader tuning bandwidth. The authors propose that the shift in tuning was caused by the loss of outer hair cells in the cochlea, which can occur following exposure to intense sound stimuli. The outer hair cells are responsible for sharpening the tuning curves of the auditory neurons and for amplifying the sound signal. When the outer hair cells are damaged, the tuning curves become broader and the sensitivity of the neurons is reduced. However, Heinz and Young (2003) and Bruce et al. (2003) found evidence to support the idea that the shift was caused by changes in cochlear mechanics, rather than outer hair cell loss. In the second study, Bruce and colleagues used a computational model of the cochlea to simulate the effects of noise exposure on the tuning of auditory nerve fibers. They found that the model was able to reproduce the "half-octave shift" observed in physiological measurements of auditory nerve tuning following noise exposure, suggesting that the shift in tuning is caused by a change in the mechanical properties of the cochlea, specifically a change in the stiffness of the basilar membrane. This change in stiffness causes the tuning curves of the auditory nerve fibers to shift downward in frequency, resulting in the "half-octave shift" observed in physiological measurements. The exact mechanism behind the "half-octave shift" following noise exposure is still a topic of ongoing research and debate in the field of auditory neuroscience. A noise band of 8-16 kHz will have its major consequences in the cochlear region situated approximately half an octave higher, which corresponds to the frequency range of 16-32 kHz. The basilar membrane is wider and more flexible in this region, and the outer hair cells are densely packed, making it more susceptible to damage from noise exposure within this frequency range (Robles and Ruggero, 2001). Previous studies have provided evidence that exposing male mice to 8-16 kHz noise levels below 100 dB SPL for 2 hours can cause temporary threshold shift (TTS) without any visible cellular loss or damage (Wang et al., 2002). Additionally, Kujawa and Liberman (2006) found that mice exposed to 8-16 kHz noise at 100 dB SPL showed a

complete recovery of their auditory brainstem response thresholds within two weeks. Building upon these previous findings, Kujawa and Liberman (2009) developed the first mouse model of TTS in order to investigate noise-induced synaptopathy, also known as the "mouse model of hidden hearing loss".

1.7.5 Therapeutic approaches for NIHL

Noise-induced hearing loss (NIHL) is a growing public health problem that affects millions of people around the world. NIHL can be caused by exposure to loud noise, such as music played at high volumes or working in an environment with excessive sound levels.

There are several therapeutic approaches that have been developed to address this condition, including pharmacological treatments, sound therapies, and surgical interventions (Sha and Shacht, 2017; Ahmed et al., 2022).

The most common treatment for noise-induced synaptopathy is a combination of pharmacological and behavioral therapies. Pharmacological interventions involve the use of drugs to reduce inflammation and improve the health of the inner ear hair cells. Common drugs used in this context include corticosteroids, non-steroidal anti-inflammatory drugs (NSAIDs), antioxidants, and diuretics. These drugs can be administered either before (in experimental animals) or after noise exposure, and they may be effective in reducing the severity of hearing loss and other symptoms associated with the condition (Mutlu et al., 2018; Zloczower et al., 2020; Zloczower et al., 2022). Behavioral therapies, on the other hand, involve lifestyle changes such as reducing exposure to loud noises and wearing hearing protection. Sound therapies, such as the use of noise generators and other devices that produce white noise or other types of soothing sounds, can also be used to help reduce symptoms of noise-induced synaptopathy. These therapies work by providing a background noise that can mask the harmful sounds that are causing damage to the synapses.

Surgical interventions for noise-induced synaptopathy are typically reserved for more severe cases and may include cochlear implantation or other types of surgical procedures that can help to restore hearing at least partially. In addition to these therapeutic approaches, it is also

important to take steps to prevent further damage from noise exposure. This can include wearing earplugs or other protective devices when working in loud environments, avoiding loud noises when possible, and taking breaks from loud noise exposure to give the synapses time to recover. Although medications exist that provide relief from symptoms associated with NIHL such as tinnitus or dizziness, none have yet been able to repair any damaged connections between IHCs and SGNs.

The effects of noise trauma on the auditory system are profound and far-reaching. Research demonstrated that, depending on the exposure parameters, the synapses lost after exposure to noise may not recover over time, even after months, in animal models (Hickman, et al., 2020). Furthermore, as discussed above, the number of dying SGN bodies following a period of intense noise exposure increases with time; this effect is directly correlated with much earlier synaptic loss observed (Kujawa and Liberman, 2009). However, more recent studies exploring this phenomenon in guinea pigs showed that IHC ribbon synapses can partially regenerate after an acoustic insult, suggesting that the ability of IHC ribbon synapses to regenerate after an acoustic insult is species-dependent (Shi et al., 2013). Besides this ability to self-regenerate, promising results show that IHC ribbon synapses might respond well to some pharmacological approaches. To this purpose, it was shown that either infusion or overexpression of neurotrophin-3 supported regeneration of some of the ribbon synapses upon noise exposure insult (Sly et al., 2016; Suzuki et al., 2016). The research on the effects of neurotrophic factors on NIHL has the potential to provide a novel treatment for this type of hearing loss. If the effects of neurotrophic factors on NIHL can be replicated in humans, this could lead to a new and effective treatment for this condition.

Other therapeutic molecules being developed by multiple companies target inflammation, oxidative stress, and apoptosis through a range of mechanisms (Yuan et al., 2015; Ho Pak et al., 2020; Alvarado et al., 2020; Yang et al., 2020). Additionally, these companies are also working on developing therapeutic molecules to address other causes of hearing loss, including regrowing spiral ganglion neurons, restoring hair cells, reconnecting synapses, and implementing gene therapy using adeno-associated virus. While these therapeutic molecules may improve cochlear

implant outcomes, they are not intended to preserve residual hearing (Isherwood et al., 2022; Schilder et al., 2019).

Recently, the discovery of a new compound, AC102, has opened up the possibility of stimulating neuronal regrowth and protecting neurons from injury. The molecule AC102, developed by AudioCure GmbH, entered a Phase I clinical trial in 2020, claiming to reduce apoptosis of outer hair cells after acute trauma and trigger the regeneration of both inner and outer hair cells as well as neurons. Although the exact composition of AC102 has not been made public, this drug is a derivative of the 9-methyl-ß-carboline, which has shown stimulatory, protective, regenerative, and anti-inflammatory effects on dopaminergic neurons in concentration-dependent manner (Polanski et al., 2010). The company is looking to evaluate the potential of AC102 in addressing hearing loss, tinnitus, and trauma from cochlear implant electrode insertion as well NIHL. This compound has also been shown to protect neurons in different animal models of neurodegeneration (Wernicke et al., 2010).

2. Aim of the study

Recent research has demonstrated that prolonged exposure to sound at moderate levels leads to a loss of synapses between the inner hair cells (IHCs) and spiral ganglion neurons (SGNs), which then causes neurodegeneration. This phenomenon has been described in terms of its functional consequences, but there remains much work yet to be done on understanding the underlying cellular mechanisms behind it. In order to gain greater insight into this process, further investigation needs to be conducted with an emphasis on gaining both molecular-level details as well as behavioral observations and functional characterizations from animal models noise exposed.

With this study, I aimed to characterize synaptic changes upon noise exposure under volatile anesthesia and possibly understand the presynaptic mechanisms behind the loss of presynaptic ribbons and the auditory synapses. To accomplish this, I applied system physiology, cell physiology, immunohistochemistry and optical stimulation techniques using mouse models to probe the functional and structural changes in inner hair cells following noise trauma.

Ultimately, the small chemical compound AC102 was tested on my mouse model of noise-induced synaptopathy to explore its potential to prevent ribbon synaptic loss, SGNs degeneration and promote axonal regrowth.

3. Materials and Methods

3.1. Chemicals and buffers

- Modified Ringer's solution (for noise-exposure cell physiology): 110 NaCl, 35 TEA-Cl, 2.8 KCl, 1 $MgCl_2$, 1 CsCl, 10 HEPES, 1.3 $CaCl_2$, and 11.1 D-glucose (pH 7.2, 305 mOsm/l)

- Modified Ringer's solution (for *ex-vivo* optical stimulation): 126 NaCl, 20 TEA-Cl, 2.8 KCl, 1 $MgCl_2$, 1 CsCl, 10 HEPES, 1.3 $CaCl_2$, and 11.1 D-glucose (pH 7.2, 305 mOsm/l)

- Intracellular recording solution (for noise-exposure cell physiology): 130 Cs-gluconate, 10 TEA-Cl, 10 4-AP, 10 HEPES, 1 $MgCl_2$, a well as 300 mg/ml amphotericin B (pH 7.2, 290 mOsm/l)

- Intracellular recording solution (for *ex-vivo* optical stimulation): 135 KCl, 10 HEPES, 1 $MgCl_2$, as well as 300 mg/ml amphotericin B (pH 7.17, 290 mOsm/l)

- PBS (Phosphate Buffer Saline): 137 mM NaCl, 10 mM Na_2HPO_4, 2.7 mM KCl, 2 mM KH_2PO_4 pH 7.4.

- GSDB (Blocking solution): goat serum, 0.3% Triton X-100, 240 mM PB, 4 mM NaCl

- 4% Formaldehyde: Prepared from a 37% initial stock (Carl ROTH), and diluted to the final working concentration of 4% with PBS.

- Mowiol Mounting Medium: 2.4 g Mowiol 4-88 (Carl ROTH) were dissolved into 6 g glycerol with the addition of 12 ml ddH_2O. The solution was stirred for several hours at room temperature. Afterward, 0.2 M Tris pH 8.5 was added into the solution and heated for 1-2 h at 50°C. When Mowiol is dissolved, the solution was centrifuged at 500 x g for 15 min. Finally, 2.5% DABCO (Carl ROTH) was added and the solution was aliquoted.

- Amphotericin B, Streptomyces sp., cat. No. 171375, 100 mg was purchased from Calbiochem (Merck KGaA, Darmstadt, Germany).

- Wash buffer: 20 mM PB, 0.3% Triton X-100, 450 mM NaCl.

- Primary antibodies: mouse anti-CtBP2, IgG1, BD Biosciences, cat. No. 612044; rabbit anti-Homer1, polyclonal, Synaptic Systems, cat. No. 160002; guinea pig anti-Parvalbumin-α, polyclonal, Synaptic Systems, cat. No. 195004. All antibodies were used at dilution of 1:200.

- Secondary antibodies: Goat anti-mouse 488 [IgG, IgA, IgM (H+L)] Invitrogen Cat No. A10667, Goat anti-chicken 568 [IgY (H+L)] Abcam Cat No. Ab175711, Goat anti-rabbit 633 [IgG (H+L)] Invitrogen Cat No. A21070. All antibodies were used at dilution of 1:200.

3.2. Animals

All animals were used in accordance with national animal care guidelines and were approved by the University Medical Center Göttingen board for animal welfare and the animal welfare office of the state of Lower Saxony. Specifically, for the *in-vivo* acoustic noise exposure, C57BL6/J male mice at P21-28 and P35-42 were used.

Recent studies demonstrated that female animals and humans show an increased resilience to NIHL compared to males, due to the protective effects of the estrogen-signaling pathways on modulating peripheral auditory physiology . Young adult 8-week-old male mice have been shown to be affected by acoustic overexposure. This PhD project planned to perform patch clamp of basal IHCs in noise-exposed and not exposed mice. Since patch clamp of 8-week-old mice would certainly add a further challenge to this project, it has been decided to use younger mice, 3- to 4-week-old mice, where electrophysiology is relatively more accessible, and the auditory pathway is fully developed.

For the *ex-vivo* optical stimulation experiments, we crossbred the Ai32 mouse line with the Vglut3-ires-Cre line to obtain expression of the construct specifically in the IHCs. The Ai32 mouse line (B6;129S- *Gt(ROSA)26Sor*$^{tm32(CAG-COP4*H134R/EYFP)Hze}$/J, Nagel et al., 2005; Nagel et al. 2003) contains floxed ChR2 with the H134R point mutation fused to EYFP. The Vglut3-ires-Cre was obtained by knocking in an ires-Cre cassette 3 bases downstream of the Vglut3 stop codon. In this way, Vglut3 and Cre recombinase genes are driven off a bicistronic mRNA. The Cre expression has been characterized by crossbreeding Vglut3-ires-Cre mouse line with a tdTomato reporter mouse line, and found its expression in the IHCs. By doing so, the Ai32-VC-KI mouse line was created.

3.3. Anesthesia

Mice were anesthetized with isoflurane (5% for induction and 2% for maintenance).

The induction was made in a box with a duration of 1-1.5 minutes, and afterward, the animals were transferred onto a custom-designed heating pad to keep the temperature constant. A mask was used to continue applying isoflurane at 2% for the entire duration of the experiment.

During the experiment, ECG recordings were used to measure vital signs such as heart rate and respiration. This allowed us to assess the animal's physiological response in real-time and make any necessary adjustments during the experiment. Care was taken with the use of isoflurane since it has been shown not only to have a well-known depression of the cardiovascular system but also to rapidly and strongly affect the amplitude of neuronal signals.

3.4. Acoustic overexposure

The animals were exposed to an 8–16 kHz band noise, for 2 h at different sound pressure levels (SPL), from 92dB to 96dB, in a sound-exposure box. The noise waveform was created digitally using a TDT System III controlled by a custom-written Matlab routine that was driving speakers to generate 8–16 kHz noise at desired sound intensities, equalized across all frequencies. amplified through (?) and delivered by a loudspeaker (JBL 2402, calibrated using the above-mentioned microphone) placed in front of the animal. The distance between the speaker and the animal's head was kept constant in order to ensure the same intensity of noise exposure for all the animals.

An outline of the experimental paradigm is depicted below:
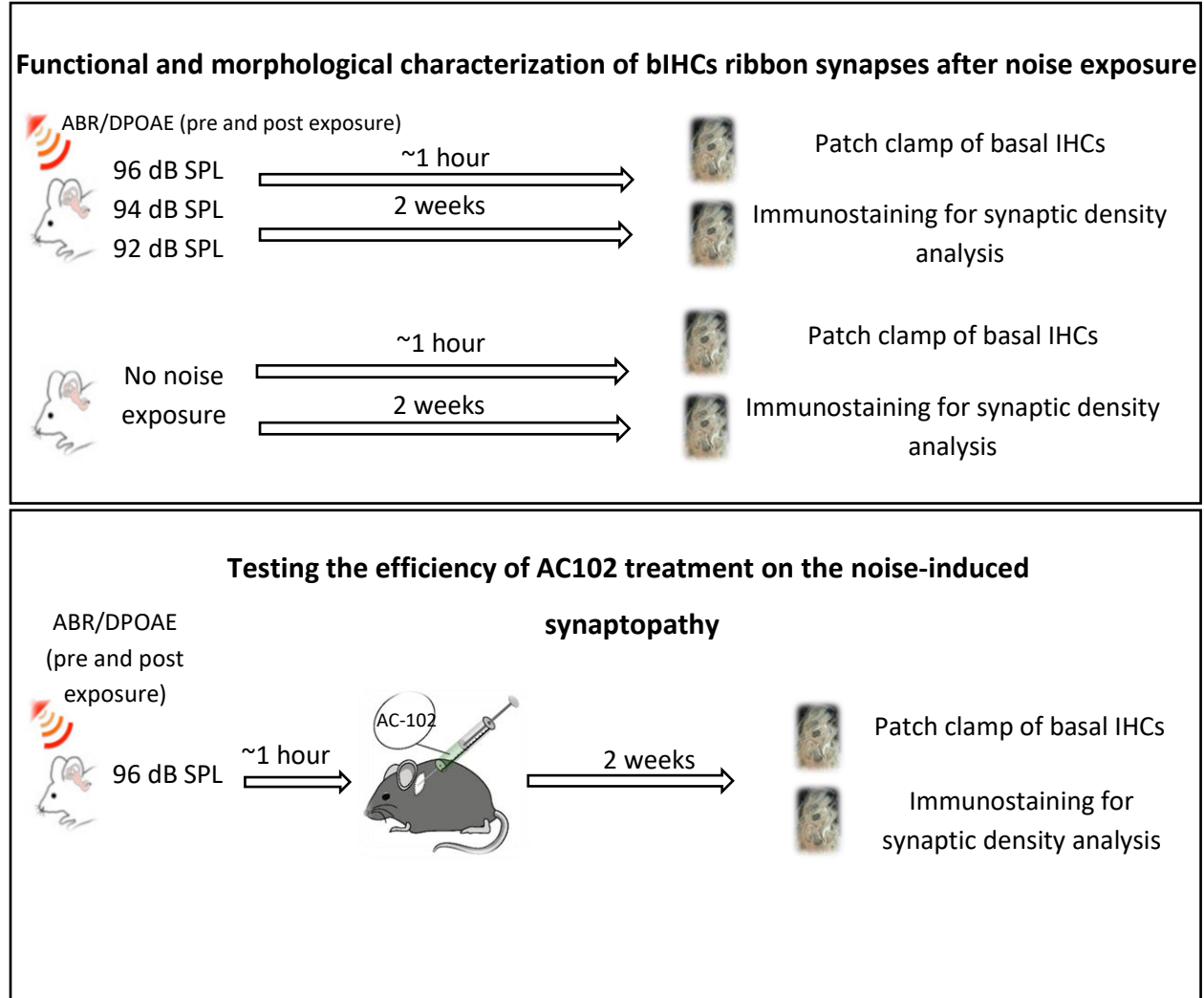
Figure 3.1 Schematic representation of the experimental design

After 2 hours exposure to noise, two groups of mice were sacrificed at different time points and the cochlea was extracted for patch clamp and immunostaining analysis. In the case of testing the drug AC102, mice were injected with the compound via the round window of the cochlea and analyzed for synaptic count two weeks later.

3.5. Hearing tests

After the induction of the anesthesia, the animals were placed onto a custom-designed heating pad that kept the body temperature at 37°C, and their mouth was inserted into the mask for maintenance of the anesthesia.

Hearing was examined both before and after the noise exposure in the "acute group", and also 2 weeks after exposure in the "recovery" group. Non-exposed animals of the same age and gender were used as controls. Auditory Brainstem Responses (ABR) were evoked with tone bursts, presented by a JBL2402 speaker calibrated with a 1/4 inch Brüel and Kjr microphone (model 4939), at 8/12/16/24/32/44 kHz (10 ms plateau, 1 ms cos^2 rise/fall, intensities provided as dB SPL root mean square) at 19 Hz in a free-field configuration, through a TDT III system (Tucker Davis Technologies) together controlled via MatLab. The thresholds were determined by recording the synchronous neural response along the auditory pathway to different sound intensities, given in 5 dB steps, starting from 30 dB up to 90 dB SPL (110 dB for the 44 kHz). Three ABR electrodes (needles) were placed under the skin of the mice at *the vertex (the reference electrode), at the mastoid muscle (the active electrode), and near the tale (the ground electrode).* For each measurement, the difference potential between mastoid and vertex was sampled 1.000 times for 20 ms at 50 Hz, amplified 50.000 times and filtered from 400 to 4.000 Hz, to obtain two separate mean ABR traces. The lowest stimulus intensity that resulted in a reproducible waveform in the two traces was considered to represent the ABR threshold value.

Following the ABR measurements, TDT III system was also used to generate and present stimuli to evoke and measure Distortion Product Otoacoustic Emissions (DPOAEs) to check the functionality of the Outer Hair Cells (OHCs). The two primary tones (frequency ratio f2/f1, 1.2; intensity f2 = intensity f1 + 10 dB with a f1 range of 10-60 dB) were delivered in the ear canal using a custom-made probe containing a MKE 2 microphone (Sennheiser, USA) and two MF-1 speakers.

The frequency combinations to produce otoacoustic emissions were the following:

- f1: 6667, f2: 8000;
- f1: 9444, f2: 11333;
- f1: 13333, f2: 16000;

- f1: 18889, f2: 22667;

- f1: 26667, f2: 32000;

Signals were captured by the microphone (Sennheiser), then amplified and digitalized (DMX 6 Fire, Terratec) and analyzed by Fast Fourier Transformation, and the thresholds were identified using a custom Matlab routine written by Prof. Dr. Nicola Strenzke.

3.6. Frequency mapping

The functional and anatomical effects of noise trauma on the IHCs were explored along the entire cochlea, at given frequency regions (8/16/24/32/44 kHz). To do this, subsections overviews of the Organ of Corti were initially acquired with a 10X air objective (Zeiss LSM 510 META confocal microscope equipped with a 488nm Argon Laser that excites corresponding fluorophores). Then, the images of the subsections were stitched together using a "pairwise stitching" plugin (Preibisch et al. 2009) of the ImageJ software obtaining, eventually, a frequency map of the whole mouse cochlea. This procedure has been performed by Annalena Reitmayer.
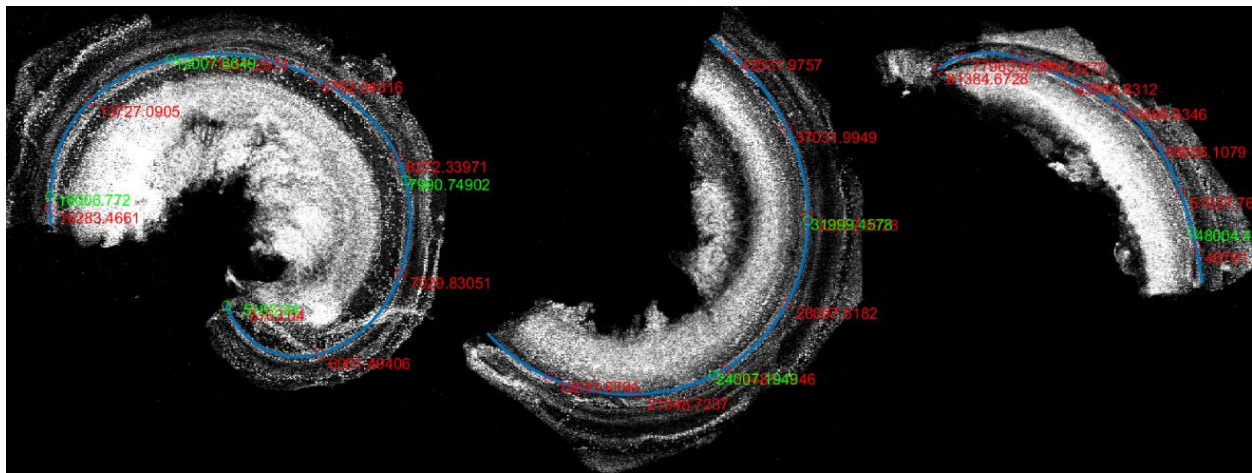
Figure 3.2 Frequency map

Blue lines follow the length of the cochlea along the IHCs. Red and green values represent the frequency values (in Hz) according to Müller et al. (2005). Hair cells and SGNs labeled with calretinin.

A custom-made Matlab routine was then used to measure the total length of the Organ of Corti by interpolating the manually determined points set along the IHCs in the overview image considering the pixel size determined by the microscope. The proportionate tonotopic map was then projected onto the overview image of the mouse cochlea (Müller et al. 2005).

3.7. Dissection of the Organ of Corti

The mice were sacrificed by decapitation under CO_2 anesthesia and the scull was split in two parts. Each part was, then, immersed in a fresh Petri Dish with ice-cooled Modified Ringer's solution containing (in mM): 126 NaCl, 20 TEA-Cl, 2.8 KCl, 1 MgCl2, 1 CsCl, 10 HEPES, 1.3 CaCl2, and 11.1 D-glucose (pH 7.2, 305 mOsm/l) for the optical stimulation of *ex-vivo* apical coils, and 110 NaCl, 35 TEA-Cl, 2.8 KCl, 1 MgCl2, 1 CsCl, 10 HEPES, 1.3 CaCl2, and 11.1 D-glucose (pH 7.2, 305 mOsm/l) for cell physiology of inner hair cells (IHCs).
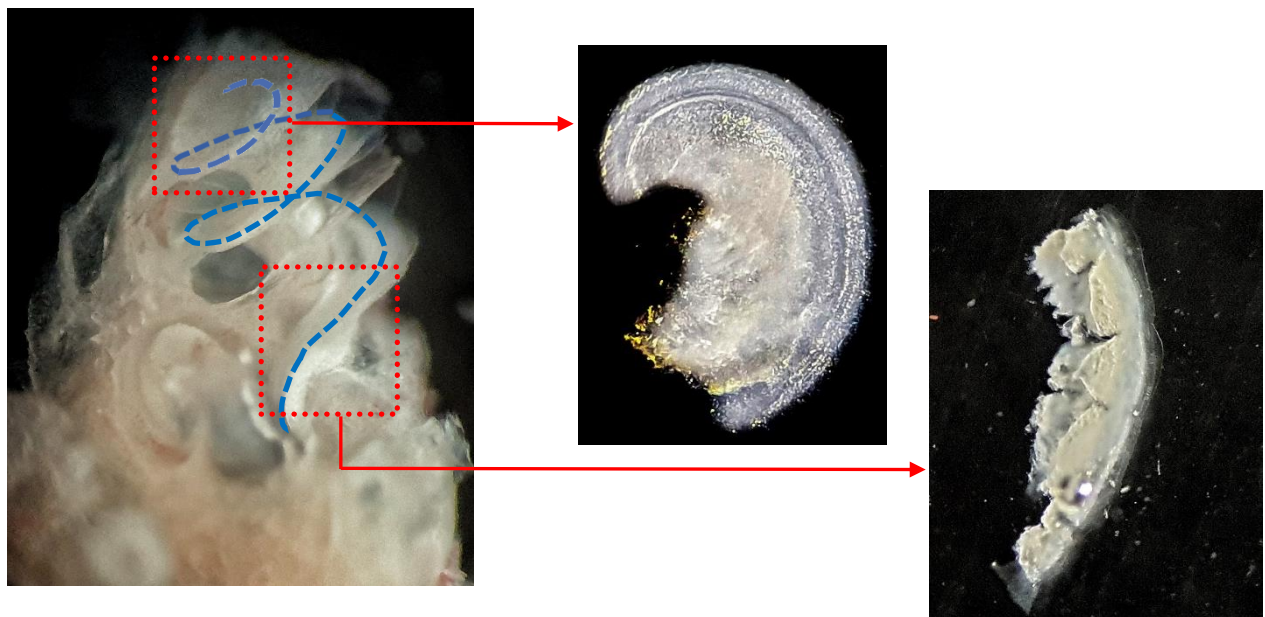
Figure 3.3 Dissected cochlea under brightfield microscopy

An image of a dissected cochlea illustrating the isolated apical and basal turns, captured using brightfield microscopy.

Each hemisphere of the brain was then extracted from the scull and both the cochleae were carefully removed and placed in fresh solutions. At this point, the cochlea was opened using fine forceps either from the apex, to isolate the apical coil of the Organ of Corti, or from the base, to isolate the basal region of the Organ.

The apical or basal coils were then transferred in a chamber for patch-clamp recordings mounted on the stage of either a Zeiss microscope equipped with a 60X water-immersion objective and a camera, perfused with the same extracellular solution used for dissection at a flow rate of approximately 0.5 ml/min., for cell-physiology, or an Olympus BX50WI microscope (Olympus, Hamburg, Germany) equipped with a 60X 60x/0.90 W LUMPlanFI water-immersion objective and a camera, perfused with the same extracellular solution used for dissection at a flow rate of approximately 0.5 ml/min., for the optical stimulation of apical coils.

3.8. Single-IHC electrophysiology

The patch-clamp setup was shielded by a Faraday cage and assembled on a hydraulic air table for vibration isolation (TMC, Peabody, USA). The pipette pressure and the bath level were continuously controlled by an external pump (Lorenz Messgerätebau GmbH) and a SM-5 micromanipulator (Luigs-Neumann) was used to move the pipette. The acquisition of the image was performed with an IMAGO CCD video camera (TILL Photonics) controlled by the Vision 4.0 software (TILL Photonics).

To have electrical access to both the apical and basal IHCs, the tectorial membrane was initially removed, followed by the OHCs, the outer and inner pilar cells and, finally, by the phalangeal cells surrounding the IHCs, applying a gentle and mouth-controlled suction, using soda glass capillaries with decreasing tip diameters. Basal part of the cochlea is much more fragile and hair cells easily swell. Therefore, the removal of supporting tissue was performed very gently to not mechanically perturb the region of the IHCs.

The pipette used for perforated-mode patch-clamp recordings were GB150-8P borosilicate glass capillaries (Science Products, Hofheim, Germany), pulled at a Sutter P-2000 laser pipette puller (Sutter Instrument Company, Novato, USA), having a resistance of 5-7 MΩ.

The pipette solution contained (in mM): 135 KCl, 10 HEPES, 1 MgCl2, as well as 300 mg/ml amphotericin B (pH 7.17, 290 mOsm/l) for the optical stimulation of *ex-vivo* apical coils, and 130 Cs-gluconate, 10 TEA-Cl, 10 4-AP, 10 HEPES, 1 MgCl2, a well as 300 mg/ml amphotericin B (pH 7.17, 290 mOsm/l) for cell physiology of inner hair cells (IHCs). The measurements were done via EPC-10 amplifiers controlled by Patchmaster software (HEKA Elektronik, Germany).

Apical and basal IHCs were patch-clamped at room temperature (20-25°C) in perforated-patch configuration as described previously (Moser and Beutner, 2000), at holding potential of -84 mV. Step depolarization potentials of 10 ms duration from the holding potential of -84 mV to +63 mV in 5 mV increments were used to measure the evoked Ca^{2+}-current and obtain an IV curve.

Membrane capacitance (C_m) was measured using a software-based method of a Lock-in amplifier (Patchmaster, HEKA) together with compensation of pipette and resting cell capacitances by the EPC-10 circuitries. The Lindau-Neher technique was used to measure the capacitance changes (Lindau and Neher,1988). All voltages were corrected for liquid junction potential offline (14 mV). Currents were leak-corrected using a p/10 protocol. Only recordings showing leak currents lower than 35 pA and series resistances lower than 35 MΩ were included in the final analysis.

For the optical stimulation of *ex-vivo* apical coils, current-clamp configuration was used in addition to voltage-clamp to measure the voltage shift upon optical stimulation.

The extraction of the apical turn of the Organ of Corti is a delicate process that requires precision and accuracy. In this experiment, I followed a set protocol to ensure successful retrieval. After sacrificing an animal, I used fine scissors to split both hemispheres of its brain and extracted each cochlea from their respective temporal lobes. To extract the apical turn, I had to break through the bone using fine forceps before gently widening it in order to expose the Organ. Once exposed, I carefully removed its stria vascularis before finally extracting and placing it into a chamber for patch-clamp measurements. Under the microscope, the Organ of Corti appears made by three different rows of OHCs, followed by a row of Outer Pillar Cells (OPCs), another row of Inner Pilar Cells (IPCs), up to the last row of IHCs. On its modiolar side, one can observe myelinated afferent axons belonging to Spiral Ganglion Neurons which give the tissue its soft texture and elasticity.

This unique feature makes subsequent procedures easier as it allows for more precise manipulation with minimal damage or disruption to surrounding structures.

To have access to the IHCs, the OHCs, OPCs and IPCs need to be removed. For this purpose, a gentle suction is applied through glass capillaries with various tip diameters according to the size of the cells to remove. After exposing the IHCs row, a last step needs to be done before patching. The phalangeal cells, placed between two IHCs and wrapping them firmly for nutritional support, need to be gently removed. Now the inner hair cells are ready to be recorded with the patch-clamp technique.

Unfortunately, for the patch-clamp of the basal turn of the Organ of Corti, there are no records available. As such, I have decided to modify an existing technique developed originally for use on apical turns in order to reach my goal. To be able to expose the entire basal region of the Organ of Corti, I decide to open the soft cochlear bone from the oval window. When the stria vascularis became visible, it was carefully removed. Next, the basal turn was carefully dissected using fine forceps and placed under the microscope for subsequent cleaning procedures. Under the microscope, the whole mount appeared smaller in size than the apical coil. Using glass capillaries with the proper tip diameter, I proceeded to remove the OHCs and the OPCs. Particular care was adopted when removing the IPCs, without damaging the IHCs. After successfully removed the phalangeal cells, the bIHCs were ready for patch-clamp exploration.

3.9. Capacitance recordings to measure pre-synaptic neurotransmitter release

Capacitance is the ability of a device to store electric charges. It measures the build-up of charges across two plates. If there are positive charges on one side and negative charges on the other separated by a membrane, for example, that prevents the movement of the charges across the capacitor, it is possible to measure the total amount of charge stored, this value is the capacitance. If the surface of the capacitor increases, the measured capacitance increases as well. And vice-versa. Since the cellular membrane is an electrical insulator that separates opposing charges inside and outside the cell, this makes it a capacitor. Measuring the capacitance of a single IHC is a precise indicator of its size at a given time. When synaptic vesicles fuse with the

cell membrane to release neurotransmitters, a slight increase in the surface area can be measured. In this way, the pre-synaptic activity can be monitored.

The elite technique to measure activity at the pre-synaptic ribbon synapses involves single-cell patch clamp recordings of IHCs. Applying a strong depolarizing current in the IHC through the patch pipette, typically a voltage step from ~ -80 mV to ~ -10 mV, induces voltage-gated Ca^{2+}-channels to open, which causes Ca^{2+} influx into the cell and, consequently, vesicle fusion. The Ca^{2+} current influx and the change of the cellular capacitance (C_m) in response to the depolarization can be simultaneously recorded.

Varying the duration of the depolarization steps makes it possible to observe different kinetic components of exocytosis. Specifically, depolarizations below 20 ms of duration trigger a fast, saturating component of exocytosis, thought to represent the fusion of a restricted synaptic vesicle pool immediately available for release, called "readily releasable pool" (RRP). The estimated number of RRP vesicles is about 11 to 14. On the other side, depolarization longer than 20 ms triggers a more linear component of exocytosis, thought to represent vesicle replenishment, located 20-50 nm away from the plasma membrane and composed of around 30 to 60 vesicles (Beutner and Moser, 2001, 2001; Beutner et al., 2001; Pangrsic et al., 2010; Chakrabarti and Wichmann, 2019).

This capacitance measurement technique can also be used to study certain mutations or treatments that might cause defects in neurotransmitter release.

In the mouse IHCs ribbons vary in shape and size (100–400 nm), and typically appear to be ≤ 200 nm in width (Moser *et al.*, 2006).

3.10. Optical stimulation

The ChR2(H134R)-EYFP fusion protein operates as an unselective cation channel that rapidly activates excitable cells upon illumination with blue light (450-490 nm). Also, the presence of the fluorescent protein allows for clear visualization of the subcellular location of the channelrhodopsin.

The Ai32-VC-KI mouse line used in this work has the distinctive feature to express ChR2(H134R)-EYFP fusion protein exclusively on the membrane of the IHCs, thus enabling them to be selectively stimulated by the appropriate laser wavelength (see above, section 3.2).

After dissectioning, the apical coil of the Organ of Corti was transferred in a recording chamber mounted on the stage of a Zeiss microscope (see section "Dissection of the Organ of Corti") and perfused with the appropriate Modified Ringer's extracellular solution. The dissected piece was first visualized in brightfield illumination imaged with an analog camera (Andor Zyla series camera, from Visitron System GmbH) and displayed on a computer using the VisiView® Microscopy Imaging Software. Then, the frequency region of interest (8-10 kHz) was selected according to the frequency map and stimulated with blue light (488 nm, maximum power rating at 200 mW, Visitron System-Laser Motorized System-MOT100).

Optogenetic stimuli consisted of brief pulses (20ms) of blue laser with 2 different time intervals (70, 650ms) and total exposure durations (20, 30, 45, 60 minutes) at different laser intensities.

3.11. Cochlear fixation, immunostaining, and synaptic count

Immediately after the sacrifice of P21-28 and P35-42 exposed and unexposed mice, the cochleae were extracted from the temporal bones and small holes were made with fine forceps in the apex and the round window. Fixation was performed with 4% FA (freshly diluted in PBS), for 2 minutes. Next, additional holes were made in the middle and the backside of the cochlea followed by another 10 minutes of fixation on ice. To remove the fixative the cochleae were washed 3 times for 5 minutes each in PBS and decalcified in 0.12 M EDTA overnight. The next day the cochleae were washed again in a washing buffer containing 20 mM PB, 0.3% Triton X-100, 450 mM NaCl 3 times for 5 minutes each. Permeabilization in 1% Triton X-100 in PBS was performed for 30 minutes on ice before blocking with GSDB for 2 hours on ice. Next, the cochleae were incubated overnight with the primary antibodies (mCtBP2 for ribbons, chHomer1 for post-synaptic boutons, rbMyo6 for Hair Cells. For the details see the paragraph "Buffers" above). The next day, the cochleae were washed 3 times 5 minutes each in the washing buffer, fixated a third time in freshly-made 4% FA for 2 hours on ice, washed, dissected and the apical, middle and basal regions of the Organ of Corti were carefully isolated. The microdissected pieces were then incubated

with the appropriate secondary antibodies overnight or over the weekend on ice in a light protective box with damp tissue inside to prevent over-drying (anti-m488, anti-ch568, anti-rb647). Afterward, the cochleae were washed in the same way as described before, mounted on a microscope slide with Mowiol, and stored in the fridge. Usually, 10µl of Mowiol was used per each dissected piece. Confocal stacks of the cochlear regions corresponding to 8/16/24/32/44 kHz were collected earliest 24 hours after mounting to ensure stability, on a laser-scanning Leica SP5, confocal microscope equipped with excitation lasers at 488nm, 561nm and 647nm, using a 100x 1.4 NA oil immersion objective, avoiding saturation of the pixel intensity and sampled with a Z-step of 0.20 µm and pixel size of 80 nm in X and Y.

The image stacks were imported in Imaris (Bitplane) where the built-in automated spot detection macro was used for the counting of the pre-synaptic ribbons, labeled with anti-CtBP2, and of the post-synaptic boutons, labeled with anti-Homer1. Juxtaposed pairs of ribbons and boutons were considered as synapses. The total number of ribbons, boutons and synapses per z-stack was then divided per the total number of IHCs, labeled with anti-Myo6, in the stack, so obtaining the cellular density.

For the *ex-vivo optical* stimulation experiments, P15-18 mice have been sacrificed the cochleae were extracted from the temporal bones, the apical and basal regions of the Organ of Corti were isolated and transferred in a recording chamber for optical stimulation as described in the previous paragraph "Dissection of the Organ of Corti". The control groups were left in the chamber, under perfusion with extracellular solution without receiving any optical stimulation.

At the end of the optical stimulation, the dissected pieces were immediately fixed using 4%FA for 20 minutes and washed 3 times for 10 minutes each in PBS at room temperature. The samples were then blocked for 1 hour in with GSDB and incubated overnight in the fridge with the same primary antibodies as above. The next day, the samples were washed 3 times for 10 minutes each in washing buffer and incubated with the same secondary antibodies mentioned before for 2 hours at room temperature. Finally, the samples were washed and mounted in a microscope slide using Mowiol. The image acquisition was done in the same way as for the noise-exposure experiment. Ribbons, boutons and synapses were counted manually using the Image J cell

counter plugin. The total number of the puncta was then divided per the total number of IHCs to measure the cellular density.

3.12. Surgical procedure for AC-102 injection in mice

In contrast to the noise exposed groups, animals received carprofen (5 mg/kg) and buprenorphine (0.1 mg/kg) as a subcutaneous injection for analgesia once before surgery. Animals were anesthetized by inhalation of isoflurane (induction dose 5 vol % isoflurane/air, maintenance dose 0.6-2.5 vol % isoflurane/air). After exposing the animals to noise trauma (as described in xxx) and determining hearing by ABR and DPOAE, the surgery was performed microscopically under aseptic conditions. During and after surgery, the animal was placed on a heated plate (37°C) and the eyes were treated with Bepanthen® ophthalmic ointment to protect against dehydration. The inter-toe reflex was checked to ensure a sufficiently deep anesthesia. The round window was exposed by a retroauricular approach: First, retroauricular fur was shaved and the now exposed skin was disinfected with PVP-iodine and 70% alcohol. After a skin incision of about 1 cm, blunt dissection to the bulla (bony boundary of the middle ear) was performed, whereby obscuring structures (vessels, nerves, musculature) were not cut if possible, but bluntly displaced. The bulla was then opened so that there was a direct view onto the round window. AC-102 injection was performed by an extended microcapillary (opening diameter ~30 µm). The glass capillary was guided by means of a finely adjustable manipulator into the round window niche whereupon it was filled with the drug-containing thermosensitive gel (~1 µl). After the successfully completed surgery, DPOAE were measured again to rule out any major damage to the hearing caused by the procedure. The displaced tissue structures were repositioned and the wound was closed with 4 - 6 single button sutures. Finally, the wound area was disinfected again with PVP iodine. After surgery, the mouse was placed in a warm cage (37°C) for recovery and observed until awakening from anesthesia, after one hour, after 3-6 hours, and on the next day. On the day after surgery, carprofen (5 mg/kg) was administered subcutaneously once for analgesia.

3.13. Statistical analysis

Data analysis was performed using MATLAB (Mathworks), Igor Pro (Wavemetrics), and ImageJ (NIH) software. Means and grand averages are expressed as ±SEM. Statistical analysis was performed using the Igor Pro. The Jarque–Bera and F test were used to determine whether the samples have normal distribution, and equal variance. These tests were then followed by two-tailed Student's t-test, or— when data were not normally distributed and/or variance was unequal between samples—the Mann–Whitney–Wilcoxon test for statistical comparisons between two samples.

4. Results

4.1. Overview of findings

My PhD project tested a novel mouse model of noise-induced auditory synaptopathy. In this model the IHCs ribbon loss is delayed and develops in the absence of any obvious damage to the OHCs. This is contrary to previous mouse models where the synaptic loss was observed immediately after exposure (Kujawa and Liberman, 2009; Lin et al.; 2011; Boero et al., 2020; Hu et al., 2020), and upon temporary threshold shift that recovered within a few days. While noise exposure in my model resulted in approximately 20% loss of ribbons and ribbon synapses in the high-frequency basal part of the cochlea as monitored two weeks after exposure, patch clamp recordings from basal IHCs revealed no difference in the overall synaptic physiology of the IHCs. This finding was surprising given the expectation that the amount of synaptic exocytosis should scale with the number of presynaptic ribbons (Meyer et al., 2010), but in line with the results recently observed in a different noise exposure model that probed the presynaptic function early (t.i. one day) after noise exposure (Boero et al., 2020). These results suggest compensatory presynaptic mechanisms that enhance IHC exocytosis at the remaining ribbon synapses or possibly extrasynaptically. Further investigation into this phenomenon could help elucidate potential protective strategies employed by cells when faced with environmental stressors such as loud noises or other forms of trauma, which can lead to ribbon loss in auditory systems.

In my experiments, the mice were exposed to noise under gas anesthesia. While the exposure to noise levels, frequency range and duration was comparable to studies performing the exposure in awake and freely moving mice, the loss of ribbon synapses in our model was considerably smaller (Kujawa and Liberman, 2009). We attribute this effect to the actue protective effects of the anesthetic isoflurane, which has previously been shown to protect from permanent noise-induced hearing thresholds shift (Kim et al., 2005), while the effect on the ribbon synapses has to my knowledge not been investigated yet. In the future, the mechanisms of the partial protection of the auditory synapses should be further investigated as well as the mechanisms of behind the partially delayed loss of synapses.

We used this mouse model of noise-induced synaptopathy to evaluate the ability of the small chemical compound AC102 in prevention of the auditory synaptic loss due to acoustic trauma. A cohort of mice was exposed to loud noise and then injected with AC102. Comparing the immunohistochemical samples of the organs of Corti immunostained for the IHC ribbon synapses revealed a partial protection (or recovery) of the synapses upon injection of AC102, suggesting its protective effects against noise-induced synaptopathy. Further tests using in-vitro whole-mount apical coils from mouse cochlea showed that acute exposure to AC102 did not significantly alter the synaptic electrical properties of the IHCs, further tests of possible side effects should be tested in the future.

The mouse line expressing ChR2 under the Vglut3 promoter was used to allow for selective stimulation of the inner hair cells in an ex-vivo model. The study attempted to find the optimal light-exposure conditions that would result in synaptic loss while avoiding cellular death. Despite numerous attempts, I was unable to find consistent and reproducible effects on the ribbon synapses. This lack of effect may be due to the difficulty in preserving glutamatergic signaling and afferent boutons during the ex vivo preparation process. Future studies should prioritize the preservation of afferent boutons and, if feasible, focus on testing the basal turn of the cochlea, which seems to be more susceptible to noise (activity)-induced damage as compared to the apical region of the organ of Corti used in the current study.

In conclusion, with my new mouse model of noise-induced hearing loss as a foundation, I am hopeful for future progress toward understanding the complexities of delayed ribbon synaptic loss.

4.2. Synaptic properties of the IHCs from the high-frequency basal cochlea

The patch-clamp technique revolutionized electrophysiology by making it possible to measure currents through ion channels involved in the electrical signaling in excitable cells. Since its development in 1976 by Neher and Sakmann (Neher and Sakmann, 1976), the patch-clamp technique has been extensively used for single-cell electrophysiology recordings. Nowadays, patch-clamp remains the élite technique to describe the electrical properties of all excitable cells

(such as neurons, cardiomyocytes, inner and outer hair cells, etc.), their ion channel conductance and kinetic behavior. The InnerEarLab is one of the pioneers of patch-clamp recordings and membrane capacitance recordings from the rodent IHCs (Moser and Beutner, 2000, Beutner et al., 2001). However, so far, all but one study from the lab (Jean et al., 2020; gerbil cochlea) has investigated the synaptic physiology of the IHCs from the apical turn of the organ of Corti, and none so far investigated mouse basal IHCs. Also elsewhere in the world, there is to my knowledge one lab that can perform the patch-clamp recordings from the basal hair cells (Marcotti et al., 2004; Martelletti et al., 2020). The most challenging task of my PhD work was thus to establish a proper technique to patch-clamp the IHCs located at the basal turn of the mouse organ of Corti.

My initial recordings of bIHCs from p14 old mice using the patch-clamp technique in the perforated mode configuration showed significantly smaller amplitude of the depolarization-evoked Ca^{2+} currents current when compared to the only reference we have in literature (Martelletti et al., 2020). However, the Ca^{2+} dependent exocytosis showed a good overlap between apical and basal IHCs, suggesting a significantly higher efficiency of exocytosis in the basal IHCs for short as well as long depolarization pulses. The calcium current amplitudes increased in the bIHC of 3.5-week-old animals. As compared to the earlier investigation time point, larger capacitance jumps were observed with the longest pulses, perhaps suggesting further maturation of the vesicle replenishment machinery.

Interestingly, at high positive potentials, bIHCs show a smaller outward positive current than the aIHCs. One possibility is that this outward current is generated from the specific K^+ channels called KNCQ4 channels. To rule out the involvement of these channels, I added the selective blocker XE-991 in the extracellular solution during both aIHC and bIHCs recordings. The drug did not appear to change the Ca^{2+} current in response to voltage depolarization.

In line with Martelletti et al. (2020), the size of the basal cells, measured from the value of the membrane capacitance at the beginning of the recording, was significantly smaller compared to that of apical cells. This set of whole-cell perforated patch-clamp recordings demonstrates the
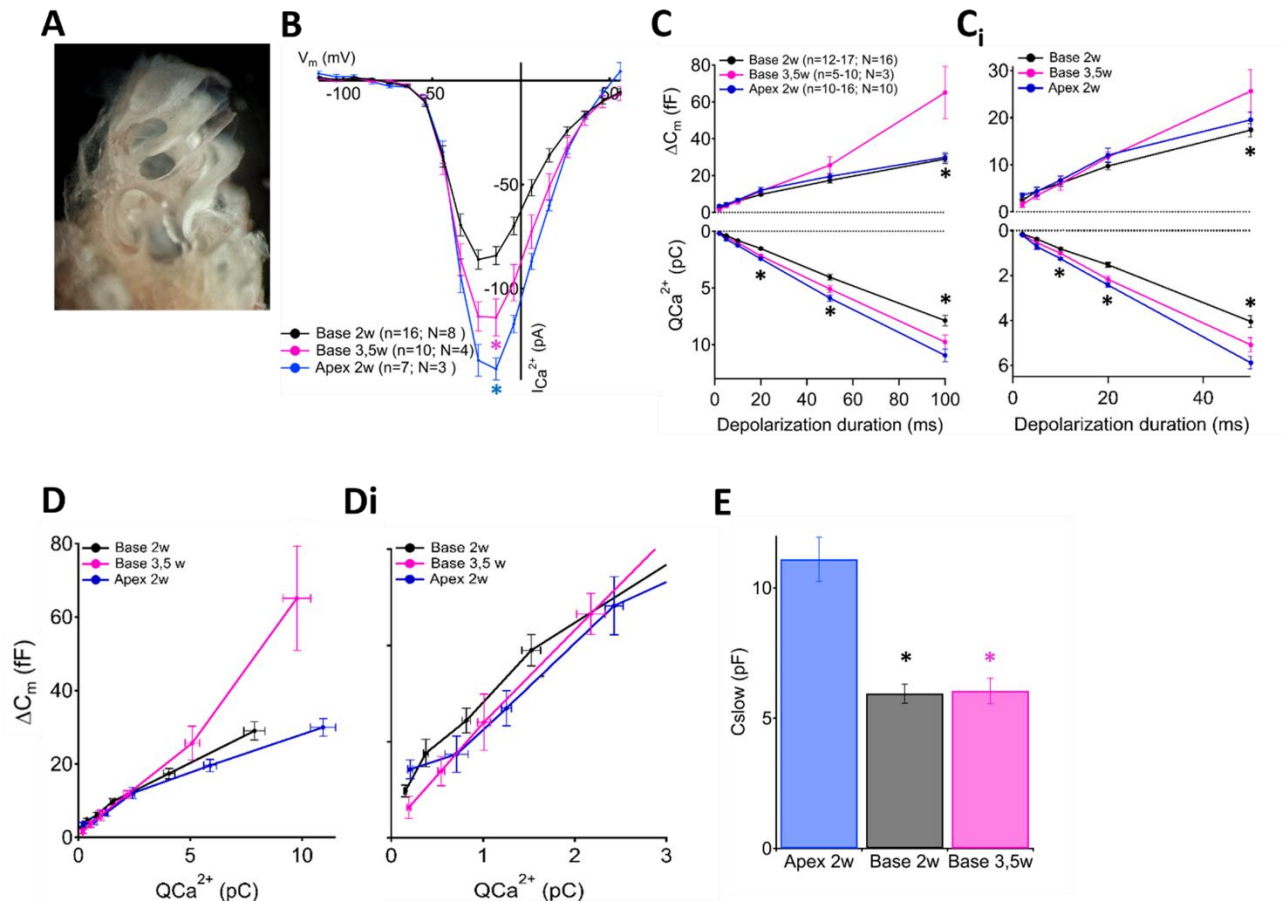
Figure 4.1 Ca²⁺ influx and exocytosis in basal and apical IHCs

(A) Image of a dissected cochlea where the apical, middle and basal turns of the Organ of Corti are visible.

(B) IV-relationship of the whole-cell Ca^{2+} - current in two-week-old basal IHCs and 3,5 week old basal IHCs show reduced current amplitudes compared to apical IHCs ($p<0.05$, t-test). The protocol, consisting of 10 ms steps of 5 mV from -82 to +63 mV.

(C) Cumulative exocytosis (exocytic ΔCm, top) and corresponding Ca^{2+}-charge (QCa, bottom) of 2-week-old bIHC, 3,5-week-old bIHCs and 2-week-old aIHCs as a function of stimulus duration (from 2 to 100 ms to   Vm value activating the maximum Ca^{2+} current influx) shows a reduced QCa in the bIHCs and partially increased ΔCm ($p<0,005$, t-test). (Ci) Inset indicating exocytosis of short pulses.

(D) Relating ΔCm to the corresponding QCa indicates increased Ca^{2+} efficiency of exocytosis in bIHCs. (Di) Inset indicating efficiency of short pulses.

(E) Reduced c-slow value (which indicates the cellular size) in bIHCs compared to the aIHCs ($p<0,05$ t-test).

reliability and efficacy of my procedure for generating reliable recordings from young murine basal IHCs.

My technique produces high quality data which can be used to further explore the properties and function of these cells. Furthermore, this approach could be extended to other cell types, such as basal OHCs.

4.3. Mouse model of noise-induced synaptopathy

The development of an experimental animal model for noise-induced auditory synaptopathy is an important step in understanding the effects of noise on synaptic hair cell physiology and hearing. This was done together with the clinician scientist David Oestreicher and the dentistry student Annalena Reitmeier. To assess cochlear functionality pre- and post-noise exposure, we combined two techniques: the recordings of the auditory brainstem response (ABRs) and the distortion product of otoacoustic emissions (DPOAEs). The ABRs are sound-evoked far field potentials generated by the neural circuits in the ascending auditory pathway, which can be recorded noninvasively using electrodes placed on the scalp (Jewett et al., 1970). ABR recordings can be used to assess the hearing sensitivity by measuring the ABR thresholds. Also, the first wave of the ABR, representing the summed activity of the cochlear nerve (Compound Action Potential), can be used to estimate the density (or rather, functionality) of the SGNs. The second technique, DPOAE, is used to assess the health of the OHCs. It measures the level of the distortion products generated by the OHCs when two tones of different frequencies are presented to the ear simultaneously.

To test the consequences of noise exposure on hearing, the mice in my study were subjected to an 8-16 kHz noise band at 92- or 96-dB SPL for 2 hours under gas anesthesia (see Materials and methods) and tested for hearing. The two intensities were chosen initially to test the effects of a noise trauma presumably causing a temporary (TTS) and a permanent threshold shift (PTS), respectively, which however upon our experiments turned out to both cause a slight PTS (see below). Immediately following an exposure to 92- or 96-dB SPL noise-bands, the ABR analysis
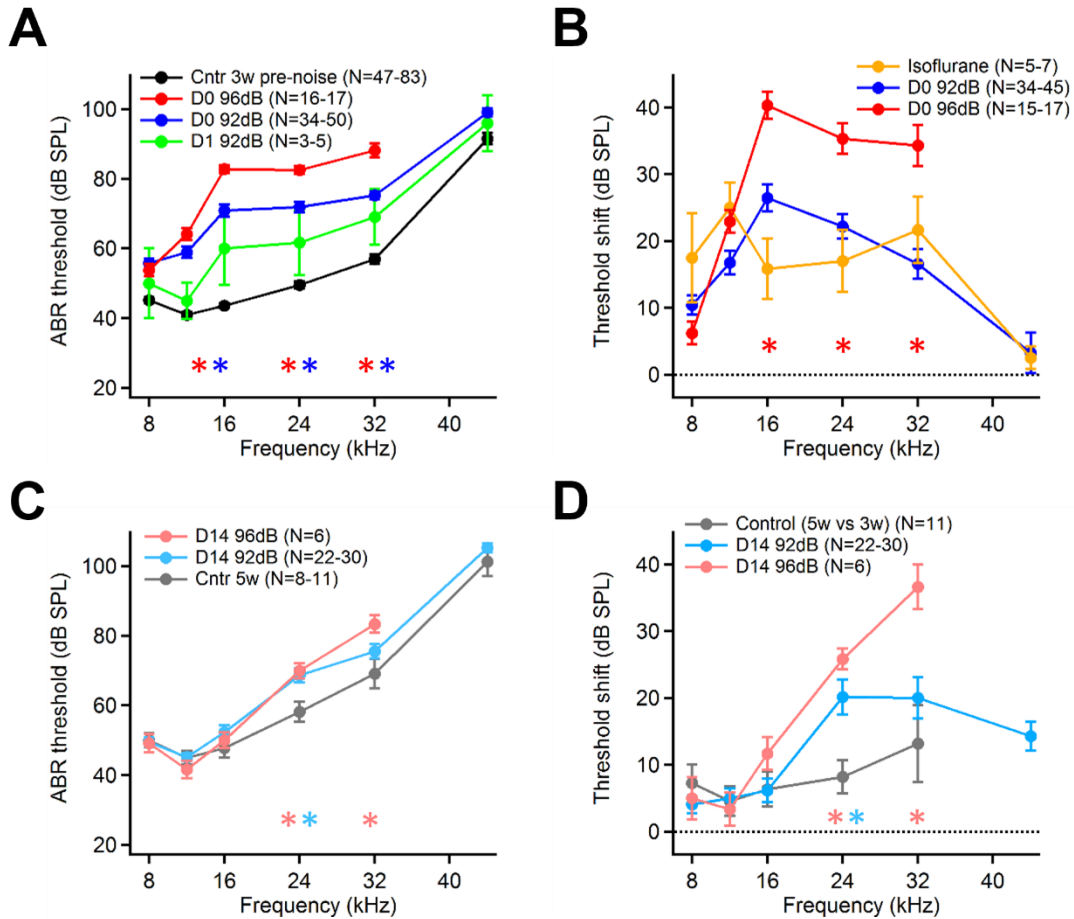
Figure 4.2 ABR responses to tone bursts in noise-exposed mice

(A) ABR thresholds at different noise intensities, recorded both immediately and one day after noise exposure (p<0,05 at all frequencies for both 92 and 96db SPL, t-test), as well as 2 weeks after exposure (C, p<0,05 at 24 and 32 kHz for both 92 and 96db SPL, t-test), as compared to age-matched controls. To exclude possible unrelated errors (e.g. due to middle ear infections, developmental lag, or technical problems), all animals were tested at 3 weeks of age prior to any further experimental procedure (e.g. noise exposure). A group of animals did not undergo neither noise-exposure nor prolonged isoflurane exposure. In this group of animals the hearing was tested again at 5w of age, which further served to estimate the ABR threshold shift between the two control time points (see panel B). Note the permanent shift of ABR thresholds for frequencies 24-32 kHz for both noise exposure levels (C, D).

(B) ABR threshold shifts, as obtained from each animal, for both post noise exposure (top panel, p<0,05 at 16-24-32 kHz for 96 db SPL, t-test) and 2 weeks after (D, p<0,05 at 24-32 kHz for 92 and 96db SPL, t-

test). Note that only 96 dB SPL (red trace) shows a significant threshold shift for frequency >16 kHz when compared with isoflurane exposed control group (orange trace). Note that both noise intensities show a PTS (D). A slight threshold shift is also observed in the non-exposed animals recorded at 3 and 5 weeks of age, likely suggesting an effect of head growth on the ABR thresholds or possibly larger susceptibility to shorter isoflurane exposure (applied during hearing measurement).

revealed a 20-40 dB increase in neural response thresholds at high (≥ 16kHz) frequencies compared to the age-matched control mice (Fig. 4.2 A, B), with slightly smaller elevations observed in DPOAEs (Fig. 4.3, A).

Since prolonged exposure to isoflurane anesthesia can also cause an ABR thresholds shift (Santarelli et al., 2003; Stronks et al., 2010; Cederholm et al., 2012; Bielefeld et al., 2014), I estimated this shift in a cohort of animals that underwent a similar experimental procedure with the hearing tests before and after "exposure" and noise stimulation turned off during the 2-hour "exposure slot". Unfortunately, the absolute ABR thresholds in these animals were unexpectedly and from unknown reasons partially elevated already at the beginning of the experiment and were thus not well comparable to other test groups. To assess the effect of isoflurane, I thus relied on comparison of the threshold shifts before and after the exposure within the same animals. The threshold shift caused by the isoflurane exposure was estimated at ~15-20 dB SPL (Fig. 4.2, B). Thus, only part of the threshold shift as observed by the exposure to 96dB-noise can be attributed to noise-evoked damage to the cochlear structure. In case of a 92-dB noise exposure, the ABR threshold shift was not significantly increased as compared to the shift caused by the isoflurane alone (Fig. 4.2, B). It is thus possible that the damaging effects of this "milder" noise are much smaller and hidden in the variability of the data, or alternatively, 92 dB exposure under isoflurane did not cause any significant immediate cochlear damage, measurable by the ABRs. Both, 92- and 96dB- noise exposure caused a ~20 dB shift in DPOAE thresholds, suggesting a partial defect of the OHCs (Fig. 4.3) as the effects of isoflurane on DPOAE thresholds were suggested as milder (Cederholm et al., Hear Res, 2012).
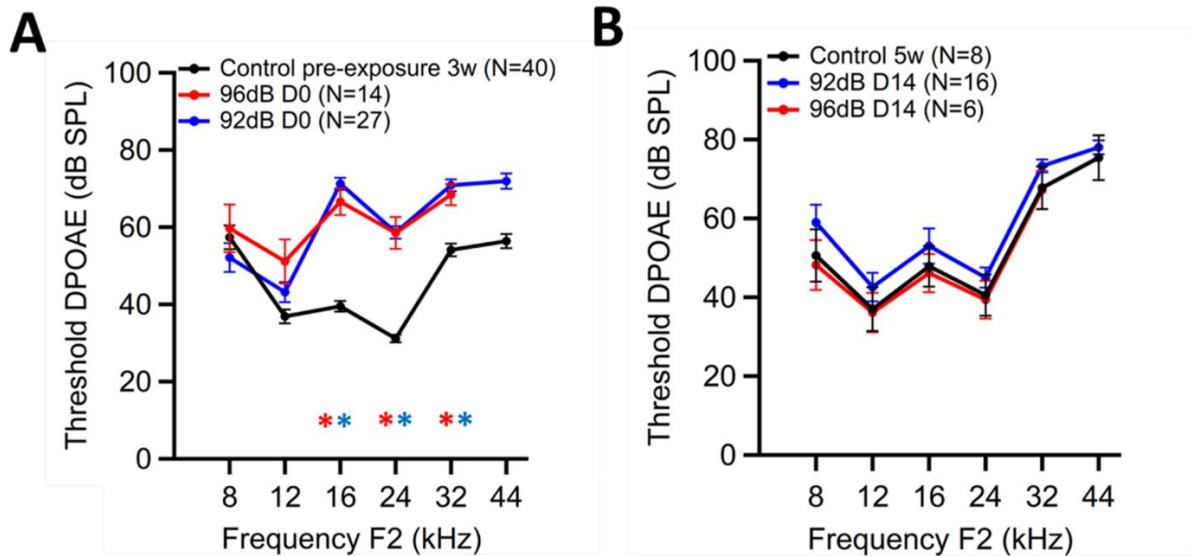
Figure 4.3 DPOAEs responses to tone bursts in noise-exposed mice

(A) DPOAEs show increases in thresholds for frequencies ≥ 16 kHz, for both noise intensities when recorded immediately after noise exposure (p<0,5 at 16-24-32 kHz, t-test). 2 weeks later (B), DPOAE thresholds show complete recovery, suggesting that the remaining ABR threshold shift is not due to OHC dysfunction.

The pattern of cochlear damage observed in Fig. 4.2, which exhibits an upward spread with respect to the exposure spectrum, is characteristic of acoustic injury (Cody and Johnstone, 1981). This phenomenon can be explained by level-dependent nonlinearities in cochlear mechanics, as previously described by Robles and Ruggero (2001).

Two weeks following noise exposure, ABR thresholds did not return to normal values for either of the two noise intensities used, indicating permanent damage to some cochlear structures (Fig. 4.2). While an extensive anatomical exploration of the Organ of Corti was not performed, prior research by Wang et al. (2002) suggests that a noise exposure resulting in a PTS differs from that resulting in a TTS due to irreversible structural damage and hair cell loss, particularly at high noise intensities. Upon tone bursts of 44 kHz, a sizeable ABR wave was only detected at very high sound pressure levels, particularly at 5 weeks of age (thresholds of ~100 dB; see Fig. 4.2). Since our

recording system does not allow measurements above 110 dB SPL and such recordings may cause cochlear damage, we did not attempt to accurately determine a possible threshold shift at this frequency. We next analyzed ABR wave I amplitudes, reporting the sound-evoked synchronized activity of the SGNs. Due to very small amplitudes of the ABR wave I amplitudes as evoked by 32- and 44-kHz tone bursts at 5 weeks of age, which was on the border of the noise of our recordings, we judged these data as unreliable to assess auditory synaptic loss (Fig. 4.4).

Confocal imaging of the sensory epithelium was used to quantify the ribbon synapses connecting the IHCs to the SGNs (this work, including preparation, immunostaining, imaging, and analysis, was performed by the student of dentistry, Mrs. Annalena Reitmeier, and partially by a DNB master student Laura Schoch).

Quantification of the auditory synapses was achieved by marking the presynaptic ribbons with an anti-CtBP2 antibody, the post-synaptic terminal with an anti-Homer 1 antibody, and the IHCs with an anti-Myosin VI (as shown in Figure 4.5). This allowed for a precise determination of synaptic density per each IHC. Confocal z-stacks (as shown in Fig. 4.5, A) were used to count synaptic ribbons in five cochlear regions, and the cochlear location was converted to cochlear frequency based on the mouse map by Taberner and Liberman (2005). In control ears, the mean counts showed a broad peak of around 19 ribbons/IHC in mid-cochlear regions, and slightly declining toward the apical and basal ends (as shown in Fig. 4.5, B). These values are consistent with previously reported data by Kujawa and Liberman (2009) and Kim et al., 2019.

The use of Homer1/CtBP2 double-immunostaining revealed the typical association between the afferent SGN nerve terminals and hair cell synaptic ribbons. In control ears, nearly all IHC ribbons were observed to be connected with a SGN nerve terminal, provided they were adequately isolated to be resolved (as depicted in Fig. 4.5, **A**). In noise-exposed ears, there was no apparent loss of hair cells, either IHCs or OHCs, at any post-exposure time. However, a comprehensive examination of the OHC density has not been carried out. Within 2 hours after the noise trauma, there was no evident sign of synaptic loss in either the pre-synaptic or post-synaptic elements.
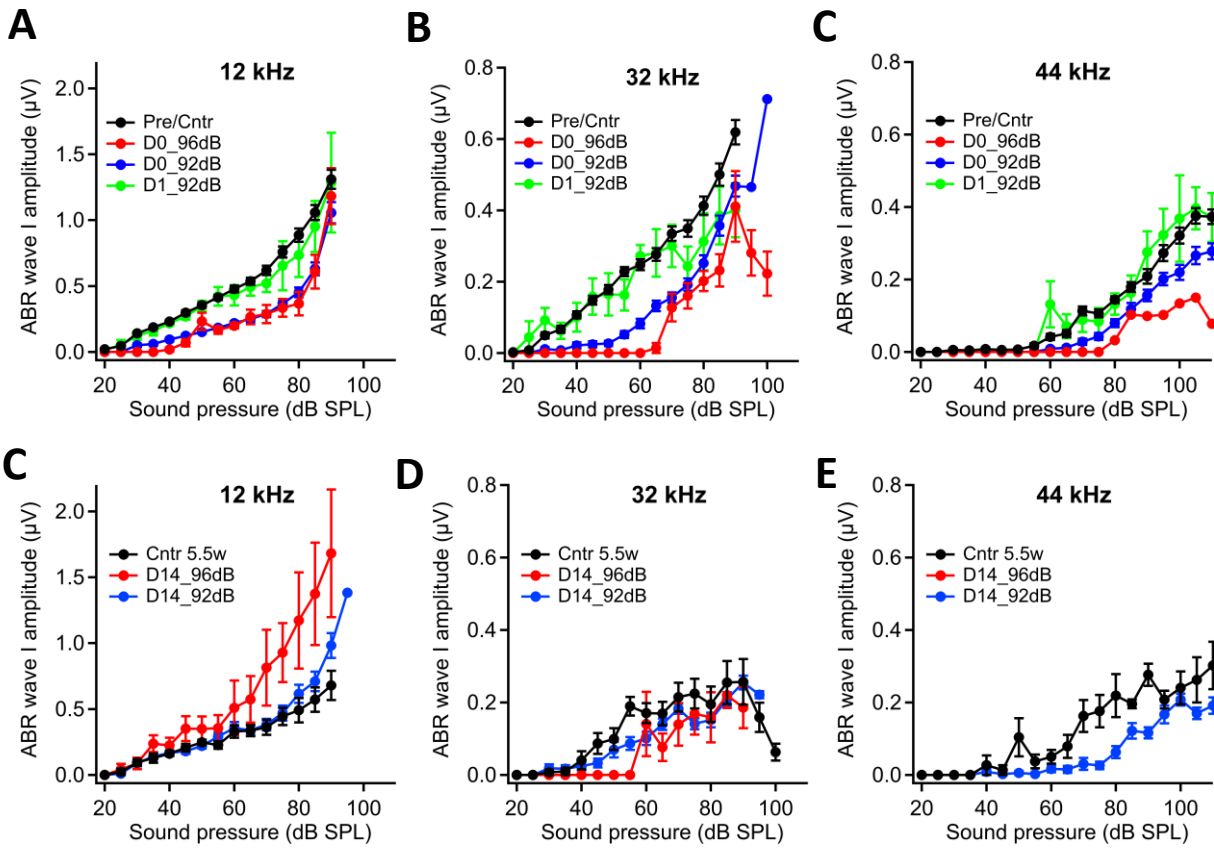
Figure 4.4 Wave I amplitude analysis in noise exposed mice

(A) Average absolute amplitudes of ABR wave I elicited by increasing SPLs tone burst of low frequency region (12 kHz). Amplitudes analyzed both immediately and 1 day after noise exposure. Note the effect of the noise trauma in decreasing the ABR wave I amplitudes ($p<0,05$, t-test). The amplitude analysis conducted two weeks after exposure to the noise (D), was deemed inconclusive due to excessive noise interference. (B) Amplitude analysis for high frequency region (32 kHz), showing significant reduction immediately after noise trauma, but not 1 day after ($p<0,05$, t-test). When repeated two weeks later (E), the data are inconclusive because of excessive noise interference. (C) Amplitude analysis at 44 kHz are inconclusive because of excessive noise interference, both at d0 and at D14 (F).
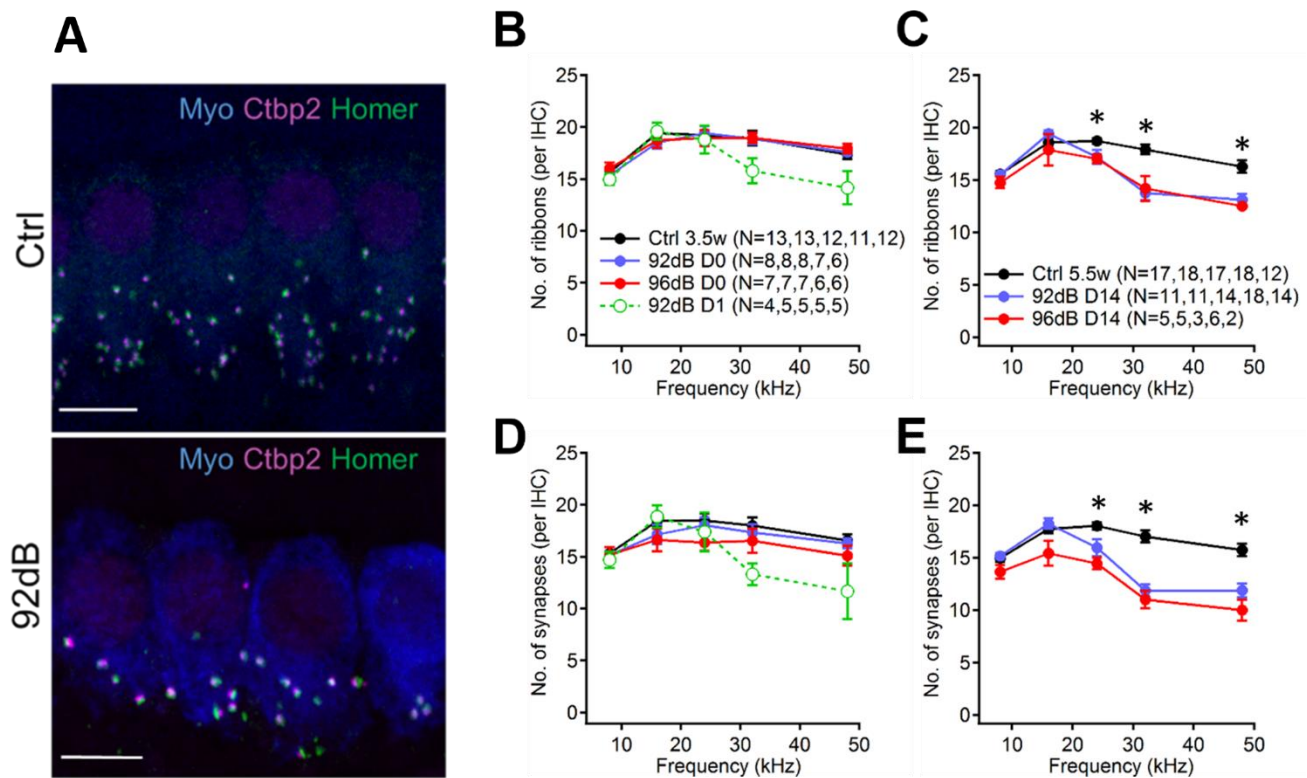
Figure 4.5 Quantification of ribbon synapses in the Organs of Corti of noise-exposed animals

(A)Maximal projections of confocal Z sections of IHCs in the 32 kHz region, immunolabeled for Myo-VI (a marker of IHCs; blue), CtBP2 (a marker of ribbons and nuclei; red), and Homer1 (a marker of postsynaptic density; green) of control (top panel) and 92 dB SPL exposed (bottom panel) mice after 2 weeks from noise trauma. Scale bar 10µm. (B) Quantification of ribbons/IHC and synapses/IHC (D) at D0. Juxtaposed CtBP2 and Homer-1 spots are taken as ribbon synapses. The ribbon and synaptic density in noise exposed mice is comparable to that of non-exposed mice. Data at D1 show a trend towards reduction in both ribbons and synapses. While t-tests suggested a significant reduction, this did not withstand corrections for multiple comparisons. Due to variability, the number of experiments should be further increased. (C) Quantification of ribbons/IHC and synapses/IHC (E) at D14. Note a moderate but significant reduction in the number of ribbon and synapses at 24, 32 and 48 kHz frequency regions in noise exposed mice, irrespective of the noise intensity (p<0,05, t-test, post hoc Holm-Bonferroni correction). (D) Quantification of ribbons/IHC and synapses/IHC (D) at D0. Juxtaposed CtBP2 and Homer-1 spots are taken as ribbon

synapses. The ribbon and synaptic density in noise exposed mice is comparable to that of non-exposed mice. Preliminary data at D1 show a trend towards reduction in both ribbons and synapses, though this reduction is not statistically significant. (E) Quantification of ribbons/IHC and synapses/IHC (E) at D14. Note the mild but significant reduction in the number of ribbon and synapses at 32 and 48 kHz frequency regions in noise exposed mice, irrespective to the noise intensity (p<0,05, t-test).

Degeneration of both presynaptic and postsynaptic elements in the IHC area was also observed one day after exposure, albeit the sample size was insufficient to draw a definitive conclusion. In the high-frequency (32-48 kHz) regions of the noise-exposed ears, the ribbon synapse density was observed to decrease to approximately 14/IHC two weeks after exposure. Conversely, in the lower-frequency (≤24 kHz) regions, no alterations in the ribbon synapse density were observed (Fig. 4.5, **B**). According to the results of other groups, the amplitude of the ABR wave I should approx. scale with the number of ribbon synapses (e.g. upon aging in Sergeyenko et al., 2013; see also CAP amplitudes in Jeffers et al., 2021). It would thus be expected that a ~20-25% loss of ribbon synapses as observed in this work, is accompanied by a similar reduction in the wave I amplitude, which however is not observed in our data (Fig. 4.4, **E**). While this discrepancy is hard to reconcile, it is possible that overall, very small ABR wave signals at high frequencies at the border of the recording noise, not supporting reliable analysis of the peak amplitudes, together with the variability, precluded observation of a small reduction in the ABR wave amplitudes. Finally, considering the limitations as described above, the tendency for reduction in the ABR growth functions was observed in some of the data obtained at D14 with 32- and 44-kHz stimulation (Fig. 4.4).
In conclusion, the results indicate that exposure to 92- and 96-dB SPL noise-bands caused significant and permanent damage to cochlear structures, particularly in the high-frequency regions. Despite no apparent loss of hair cells, a reduction in synaptic density was observed, suggesting noise-induced damage to the ribbon synapses connecting IHCs to SGNs.

4.4. Ribbon synapse functionality after noise exposure reveals possible compensatory mechanisms to the delayed synaptic loss

To gain more insights into the functional alteration occurring at the level of the ribbon synapses between the IHCs and the SGNs following noise trauma, I then performed perforated whole-cell patch clamp recordings on basal Inner Hair Cells from noise-exposed and control mice (at tonotopic position of approx. 40-50 kHz). This enabled me to accurately measure synaptic transmission and biophysical properties of the voltage-gated Ca2+channels in response to various depolarization durations and depolarization potentials, respectively, and observe how they change following exposure to acoustic trauma.
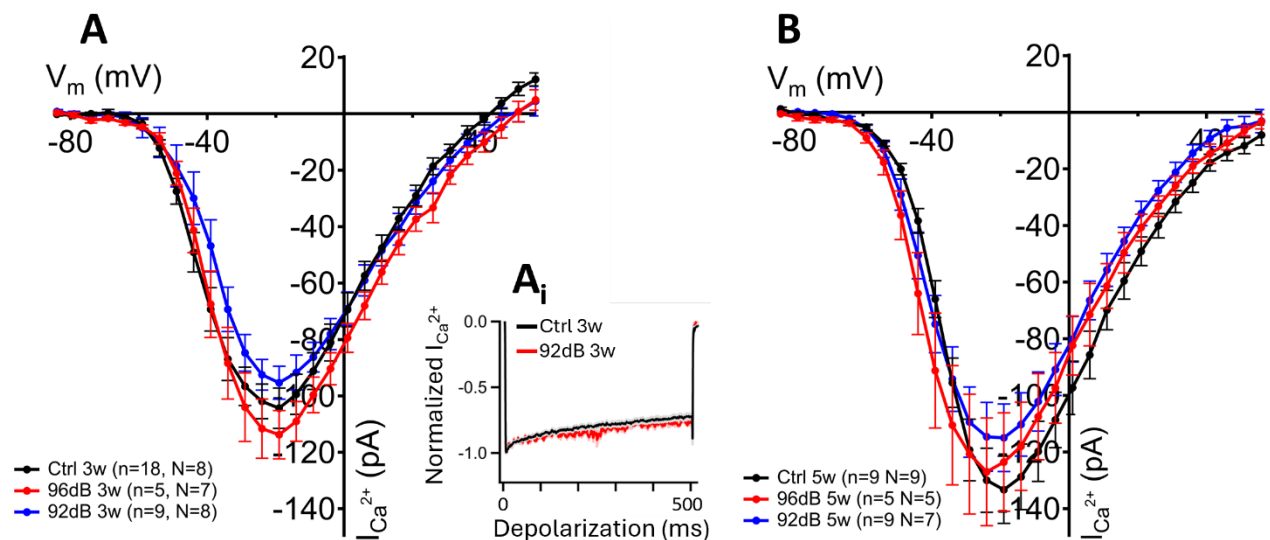
Figure 4.6 IHC Ca^{2+} influx measured post-noise exposure and two weeks later.

(A) IV-relationship of the IHCs whole-cell Ca^{2+} current show comparable current amplitudes in exposed and unexposed mice. The black line represents IHCs from unexposed mice, while the red and blue lines represent IHCs from mice exposed to noise at 96 dB SPL and 92 dB SPL, respectively. (Ai), overlapping kinetics of inactivation after acute noise exposure.

(B) IV-relationship recorded after two weeks show comparable Ca^{2+} current amplitudes between in noise exposed and unexposed mice.

Whenever possible, the same animals were used to assess the synaptic density as well as IHC synaptic physiology to obtain most comparable results. On the day of exposure, the Ca^{2+} current amplitudes seemed unaffected by the noise trauma for any of the two noise SPLs used (Fig. 4.7 A). This data is consistent with the observation of no synaptic loss on the day of exposure (Fig 4.7) and further suggests no obvious noise-induced effects on the biophysical properties of these channels (such as voltage-dependence of activation, kinetics of inactivation; see e.g. example current recording in Fig. 4.7, Ai).

To monitor the kinetics of calcium-dependent exocytosis, I then applied a series of depolarization pulses of variable durations using the voltage that evoked the inward calcium currents with the largest amplitude, as assessed from the IVs (Fig. 4.7). As previously described (Beutner and Moser, 2001) depolarizations below 20ms of duration trigger a fast, saturating component of exocytosis, thought to represent the fusion of a restricted synaptic vesicle pool immediately available for release, called the "readily releasable pool" (RRP). On the other side, longer depolarizations trigger a more linear component of exocytosis, thought to represent the fusion of vesicles upon vesicle replenishment (Beutner and Moser, 2001, 2001; Beutner et al., 2001; Pangrsic et al., 2010; Chakrabarti and Wichmann, 2019). The results of my membrane capacitance recordings, obtained within a few hours after exposure, suggest that, within the scope of our mouse model, acute noise trauma does not seem to grossly impact the fast or slow component of exocytosis nor the Ca^{2+} efficiency of exocytosis. Nevertheless, enhanced exocytosis, along with increased total Ca^{2+} influx, can be observed following exposure to 96 dB SPL for short and a trend for long depolarizations. Conversely, data upon exposure to 92 dB SPL exhibis a tendency towards decreased exocytosis and Ca^{2+} influx in response to all applied depolarization durations, although the differences are not statistically significant. Cumulatively, this data suggests no noise-evoked acute disruption of IHC ribbon synapses in our experimental conditions, on the contrary, the strongest stimulation tested even suggests slightly enhanced exocytosis, which is possibly due to temporarily disrupted control of presynaptic activity early.
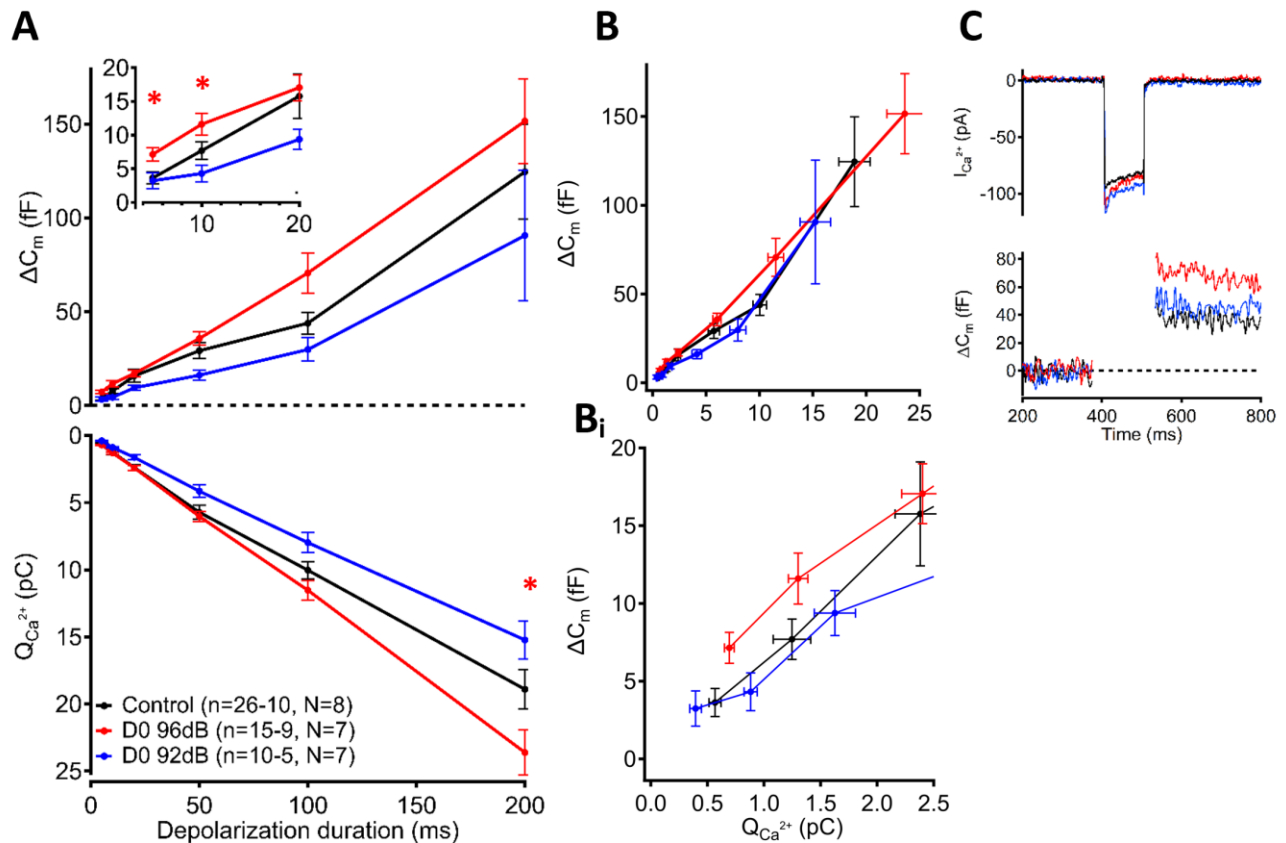
Figure 4.7 IHC exocytosis in acute noise exposed mice

(A) Cumulative IHCs exocytosis (exocytic ΔCm, top) and corresponding Ca^{2+}-charge (QCa, bottom) of not exposed mice in black, 96 dB SPL exposed mice in red and 92 dB SPL exposed mice in blu as a function of stimulus duration (from 2 to 100 ms to -14 mV) unaltered in noise exposed mice at D0. Note the increased efficiency of Ca^{2+} current in triggering the exocytosis at 2, 5 and 10 ms depolarization durations for 96 dB SPL (Ai, $p<0.05$, t-test). (B) Cumulative exocytosis and corresponding Ca^{2+}-charge are enhanced in noise exposed mice. (Bi) Efficiency of Ca^{2+} dependent exocytosis at brief depolarization durations. (C) Representative Ca^{2+} currents (top) and Cm changes (bottom) in IHCs in response to 100ms depolarizations.
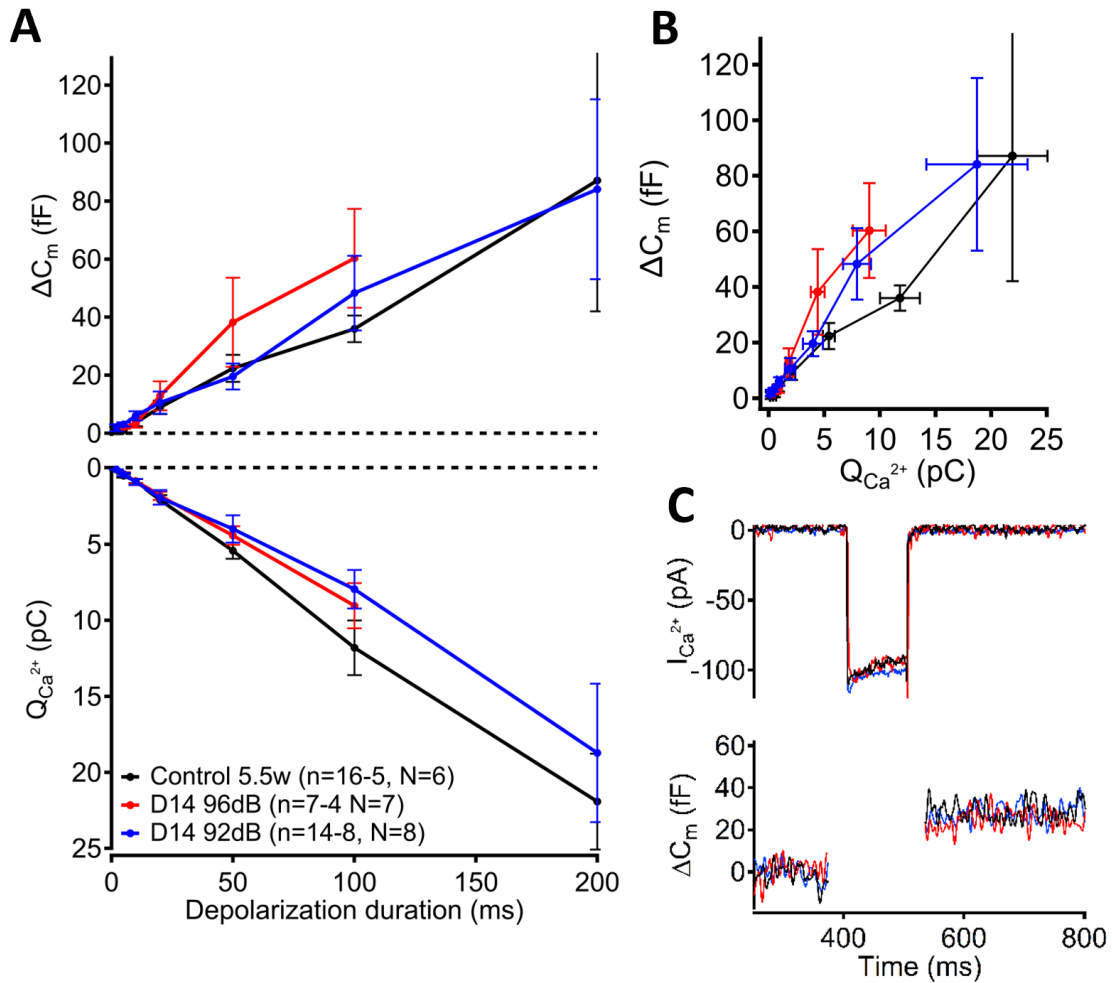
Figure 4.8 IHC exocytosis measured two weeks after noise exposure

(A)Cumulative IHCs exocytosis (exocytic ΔCm, top) and corresponding Ca^{2+}-charge (QCa, bottom) of not exposed mice (in black), 96 dB SPL exposed mice (in red) and 92 dB SPL exposed mice (in blu)) as a function of stimulus duration (from 2 to 100 ms to -14 mV) unaltered in noise exposed mice at D14. (B) Cumulative exocytosis and corresponding Ca^{2+}-charge recorded at D14 are unaltered in noise exposed mice. (C) Representative Ca^{2+} currents (top) and Cm changes (bottom) in IHCs in response to 100ms depolarizations.

Surprisingly, two weeks following noise exposure, patch clamp recordings revealed no significant changes in ribbon synapse functionality, despite a moderate but significant decrease in synaptic density at high frequency tonotopic positions as identified by immunofluorescence (Fig. 4.6). This observation implies that the residual ribbon synapses might undergo compensatory mechanisms

to maintain the overall synaptic functionality. This is consistent with the data observed by Boero et al. (2021) where exposure to loud noise caused an increase in IHC exocytosis (but upon very different exposure parameters in the apical cochlea one day after exposure, see Discussion). At present it is not clear, if there are additional, ribbonless AZs, formed at the plasma membrane. To address this possibility, an additional staining, using a presynaptic marker for AZ protein bassoon and/or for calcium channels in combination with ribbon-specific markers could be used to identify possible formation of ribbonless AZs. Indeed, orphan CaV1.3 immunofluorescent spots Since isoflurane may affect the function of the voltage-gated calcium channels (Study et al., 1994; White et al., 2005; Hao et al., 2020), I tested whether this could convolute the patch-clamp results obtained upon noise exposure. For this, I conducted an additional set of patch-clamp recordings in the basal IHCs of mice exposed to isoflurane for the same duration as the noise-exposed mice. The results revealed no significant changes in the calcium current amplitudes or voltage-dependence of activation in the presence or absence of prior prolonged exposure to isoflurane (Fig 4.10).

While we observed no significant effect of isoflurane on the calcium currents approx.. 1 hour after the end of isoflurane exposure (comparable to our first recordings in the IHCs from the noise-exposed animals), which validates the use of non-exposed controls, this data does not suggest isoflurane has no acute effects on the IHC synaptic function. It is quite likely that the putative effect of the anesthetic has dissipated by the time the patch clamp experiment were initiated. Indeed, isoflurane is a volatile anesthetic that rapidly dissipates after exposure cessation. 1 hour after the end of isoflurane exposure (comparable to our first recordings in the IHCs from the noise-exposed animals), which validates our use of non-exposed controls, this data does not suggest isoflurane has no acute effects on the IHC synaptic function. Thus, to determine whether isoflurane anesthesia has a direct effect on calcium channel and ribbon synapse activity during noise exposure, it is necessary to record the electrical activity of IHCs during acute application of isoflurane. In the future, thus, in vitro recordings will need to be devised to safely apply isoflurane in the extracellular solution while monitoring the (synaptic) activity of the IHCs by patch clamp.
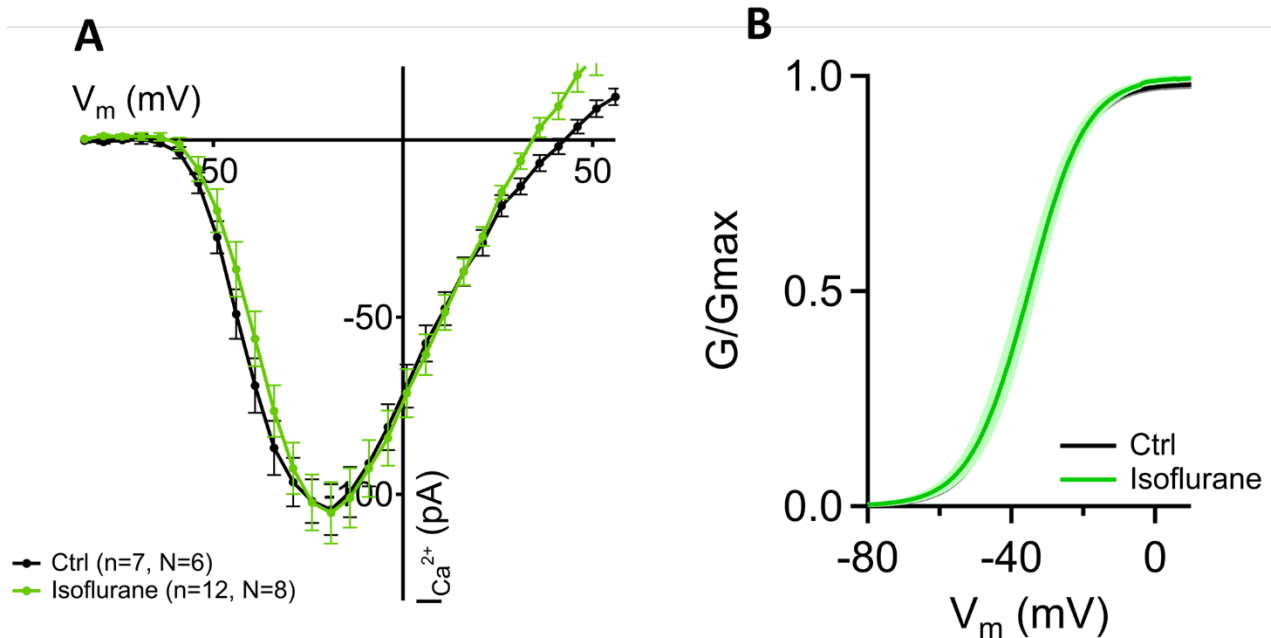
Figure 4.9 Isoflurane exposure does not affect calcium channel properties in basal inner hair cells

(A) IV-relationship of the whole-cell Ca^{2+} - current in previously anesthetized mice and not. The evoked Ca^{2+} current amplitudes in response to step depolarization potentials recorded from mice exposed to isoflurane are comparable with from unexposed mice. The protocol, consisting of 10 ms steps of 5 mV from -82 to +63 mV.

(B) Fractional activation of the whole-cell Ca^{2+}-current derived from the IV-relationships in (A) was fitted to a Boltzmann function. The panel shows overlapping voltage-dependent Ca^{2+} channel activation in isoflurane exposed and not animals.

Thus, to determine whether isoflurane anesthesia has a direct effect on ribbon synapse activity during noise exposure performed under anesthesia, it is necessary to record the electrical activity of IHCs during isoflurane exposure. In the future, *in vitro* recordings will need to be devised to safely apply isoflurane in the extracellular solution while monitoring the (synaptic) activity of the IHCs through the patch clamp pipette.

4.5. Assessing the efficacy of AC102 in protecting IHCs ribbon synapses following noise trauma

The discovery of a new compound, AC102, has opened up the possibility of stimulating neuronal regrowth and protecting neurons from injury (Polanski et al., 2010; Wernicke et al., 2010; Keller et al., 2020). This compound is currently undergoing tests of possible therapeutic protection of hair cells, ribbon synapses and/or SGNs in animal models of hearing loss, including noise-trauma and sudden hearing loss models. As such, it is undergoing preclinical trials with promising initial results. In order to further explore this potential therapeutic option for noise-induced hearing loss I tested AC102 in my mouse model of noise-induced synaptopathy. The purpose was to determine its efficacy at preventing synaptic loss due to acoustic trauma as well as any potential side effects that may arise from its use or administration protocol.

To ensure reliable results I planned on using a combination of hearing sensitivity measurements along with immunofluorescence staining which will allow us to detect changes within individual cells over time following administration of AC102. As indicated by the guidelines of the company, Dr. David Oestreicher injected the compound diluted in the termosensitive gel through the tympanic membrane to deposit it on the round window of mice previously exposed to 92 dB SPL noise. The injections were performed on the day of exposure, following the hearing tests upon noise trauma. In the future, later time points will be tested to assess the suitable maximal time window of putative therapeutic approach with this drug. As previously shown by the company, the compound can diffuse through the porous membrane of the round window into the inner ear. Two weeks after noise exposure and application of the medication, the ABR recordings were performed in all mice, followed by ribbon synapse staining for further analysis (immunohistochemistry experiments performed with the help of Mrs. Laura Schoch).

The results revealed no significant difference between ABR thresholds in noise-exposed animals with or without treatment with the AC102. While this may suggest that the early application of AC102 can not protect against mild ABR threshold shift as observed in our noise-exposed control animals, possible surgery-evoked mechanical damage to the cochlear tissue in particular at the cochlear base can currently not be excluded.
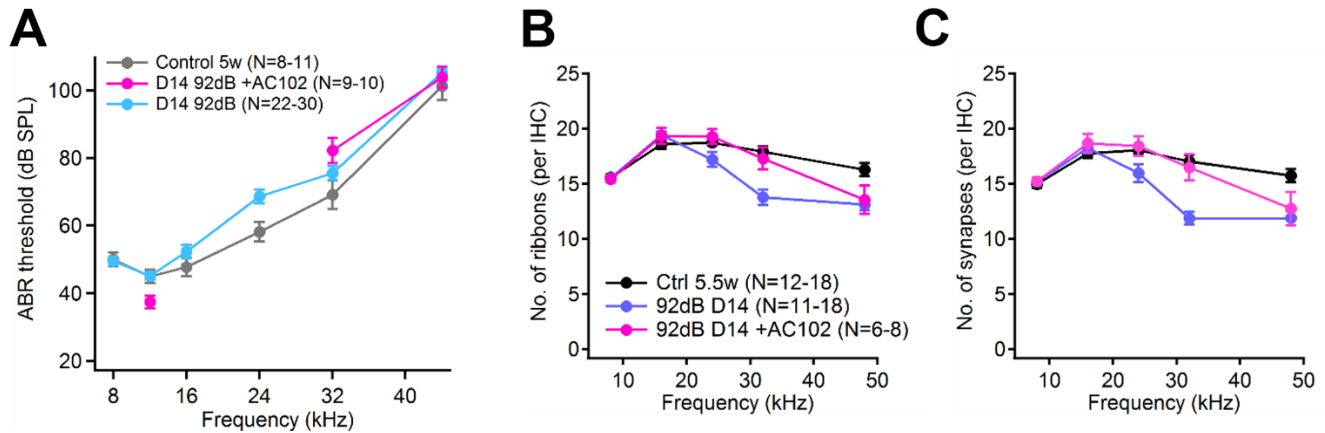
Figure 4.10 Auditory brainstem responses to tone bursts in noise-exposed mice after administration of AC102

(A)ABR thresholds of mice exposed to 92 dB SPL noise with (pink trace) or without treatment with the AC102 (blue), recorded at D14. According to these data, AC102 does not seem to ameliorate the permanent threshold shift at high frequency regions (32 kHz), however a possible mechanical damage during operational procedure can at present not be excluded).

(B) IHC ribbon density seems to recover well after administration of AC102 at 32 kHz, but not 44 kHz tonotopic region.

(C) The recovery of synapses (in this case, postsynaptic boutons) is not observed at any of the two noise-affected frequencies.

A caveat of the present experiments is that so far, the results of the AC102 application were compared to non-injected controls rather to controls with sham injections (t.i. the gel vehicle without the active compound). In the future, this along with further tests of AC102 should best be performed in the noise conditions that show higher degree of synaptopathy to ease the analysis and interpretation of data.

Prior research has proposed that AC102 may exert its influence on post-synaptic compartments at the level of neuronal bodies, stimulating the transcription of crucial neurotrophic factors such as BDNFα (Wernicke et al., 2010). This mechanism could potentially account for the compound's observed neuronal regrowth and protective effects as observed in the animal model of Alzheimer (Polanski et al., 2010). In the context of the cochlea, it is postulated that AC102 could act on the

SGNs, promoting the expression of key transcription factors that may protect or regenerate synaptic terminals following noise trauma. Increased numbers of ribbons, on the other hand, may be related to direct protective or regenerative effects of the medication on the ribbons, or indirect effects through protection against postsynaptic loss. Since we observed a putative recovery of the synaptic ribbon numbers at the 32-kHz tonotopic region in the absence of a complete recovery of the respective postsynaptic elements, our data favors the former hypothesis of a direct protective or regenerative effect on the presynaptic ribbons.

Finally, I conducted an in-vitro investigation to assess the acute impact of AC102 on IHC synaptic function. For these experiments, I selected to work with the apical region of the Organ of Corti due to technical ease of the patch-clamp recordings in comparison to basal IHCs. The compound was dissolved in an extracellular solution at concentrations previously estimated by the company to occur in the perilymph upon in vivo application on the round window, and whole-cell perforated patch clamp recordings were subsequently performed in these cells.

The findings revealed that acute exposure to AC102 did not significantly alter the synaptic electrical properties of the IHCs, neither in terms of Ca^{2+} channel properties nor synaptic vesicle release. My data thus suggests no adverse acute effects of the drug on the IHC synaptic function.

4.6. Optogenetic overstimulation of ex-vivo Organ of Corti

Noise-induced synaptopathy is a condition that results from overexposure to loud noises and can lead to synaptic loss. The mechanism behind noise-induced synaptopathy begins with excessive stimulation of the hair cells. High intensity sounds cause greater depolarisation of the IHC plasma membrane, which in turn leads directly to excessive release of glutamate molecules, resulting in increased neural activity that can eventually determine excitotoxicity at the level of the SGN terminals and their subsequent loss (Puel at al., 1998; Kim et al., 2019; Hu et al.,2020).

To gain a better understanding of the molecular processes involved, I proposed developing an in vitro mouse model using the Ai32VC-KI mouse line expressing channelrhodopsin 2 (ChR2) in the inner hair cells (IHCs), under the Vglut3 promoter (Fig. 4.13).
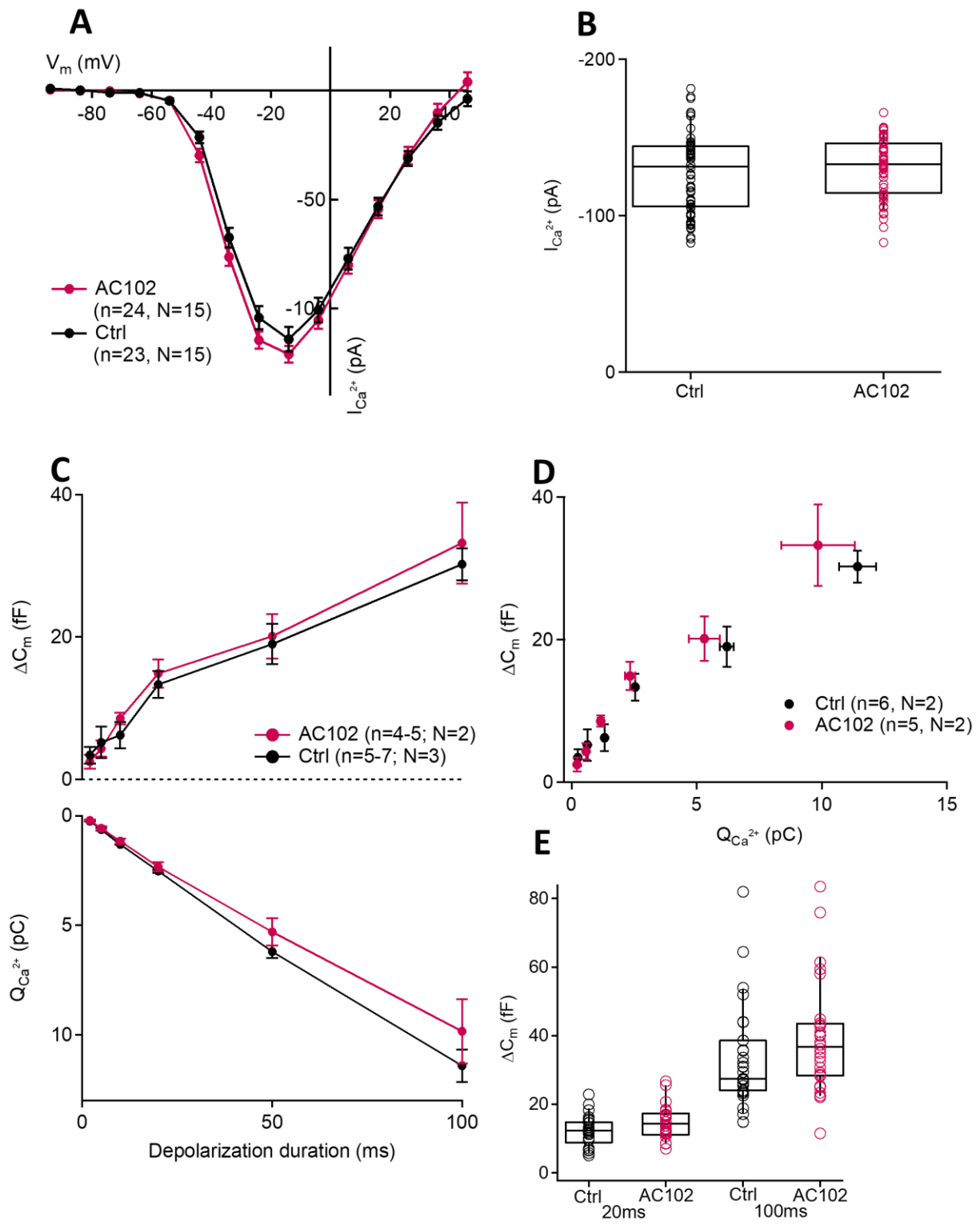
Figure 4.11 Acute exposure to AC102 did not significantly alter the IHCs synaptic functionality

(A) IV-relationship of the whole-cell Ca^{2+} current in control IHCs (n=23 cells, N=15) and in presence of AC102 (n=24 cells, N=15) show comparable current amplitudes. The protocol, consisting of 10 ms steps of 10 mV from -82 to +63 mV.

(B) IHC peak Ca^{2+} currents at -14 mV are overlapping between control IHCs and perfused with AC102.

(C) Cumulative IHCs exocytosis (exocytic ΔCm, top) and corresponding Ca^{2+}-charge (Q_{Ca}, bottom) of control IHCs (n=5-7 cells, N=3) and perfused with AC102 (n=4-5 cells, N=2) as a function of stimulus duration (from 2 to 100 ms to -14 mV) are comparable.

(D) Relating ΔCm to the corresponding Q_{Ca} indicated comparable Ca^{2+} efficiency of exocytosis between control IHCs and after AC102 perfusion.

(E) Cumulative IHCs exocytosis upon 20ms (reflecting the exocytosis of the RRP) and 100 ms (reflecting the replenishment of the synaptic vesicles) in control IHCs and after perfusion with AC102 shows comparable results.

By illuminating with blue light at 488 nm, it should be possible to repetitively stimulate the IHCs and thus mimic a prolonged excessive stimulation during noise exposure. Such optogenetic overstimulation, if successful, could then be used as a tool for studying changes in ribbon synaptic density associated with acoustic overexposure.

To test for possible effects of optogenetically-evoked overstimulation, I performed immunohistochemistry in combination with confocal microscopy to detect and visualize potential structural synaptic IHC alterations. The first results of my research provided evidence that the apical coils of the Organ of Corti show a longer survival rate than those in the basal region. Based on this, I decided to use this more robust region of the cochlea for optogenetic stimulation as it is likely to yield better and more reliable results. Furthermore, due to longer viability, there is a potential for further experimentation with different pharmacological interventions in the apical cochlear area, which could lead to new discoveries about the molecular processes involved in the noise-induced synaptopathy.

Drawing upon this initial knowledge, optical stimulation of the apical turns was commenced. Initially, the specimens were exposed for a duration of 45 minutes, utilizing a light exposure time of 20 ms and an interpulse interval of 650ms. The selection of the time interval and the exposure

time was based on previously conducted research on the same mouse line by a different laboratory, demonstrating the complete repolarization of the inner hair cells (IHCs) following optical stimulation of the ChR2 within a time frame of less than 50 ms from the end of the optical stimulation, and that membrane depolarization achieved its peak approximately 20 ms after stimulation and subsequently began to gradually repolarize, suggesting the deactivation of the ChR2 (Chakrabarti et al., 2022).

This information guided my decision to adopt an exposure time of 20 ms and an interpulse time interval of 70 ms for the optical stimulation of the samples in this experiment. The interpulse interval was determined by a technical constraint within our laser stimulation software, precluding further reduction of the time interval. Prior to commencing the exposure of the CRE+ mouse line to blue light, a group of CRE- mice lacking the expression of the ChR2-YFP construct were subjected to a 60-minute exposure to blue light at 80% laser power. No evidence of cellular phototoxicity was observed in these mice, thereby providing an essential experimental control.

The findings in CRE+, ChR2-expressing mice revealed no alteration in the ribbon density subsequent to optical stimulation at any of the laser powers examined (Fig 4.14). Interestingly and unexpectedly, only a small fraction of the spiral ganglion neuron (SGN) terminals survived for an hour in our ex-vivo conditions. The survival of SGNs did not improve despite my several attempts to improve the conditions (e.g. different techniques of organ isolation/preparation, or different types of solutions).
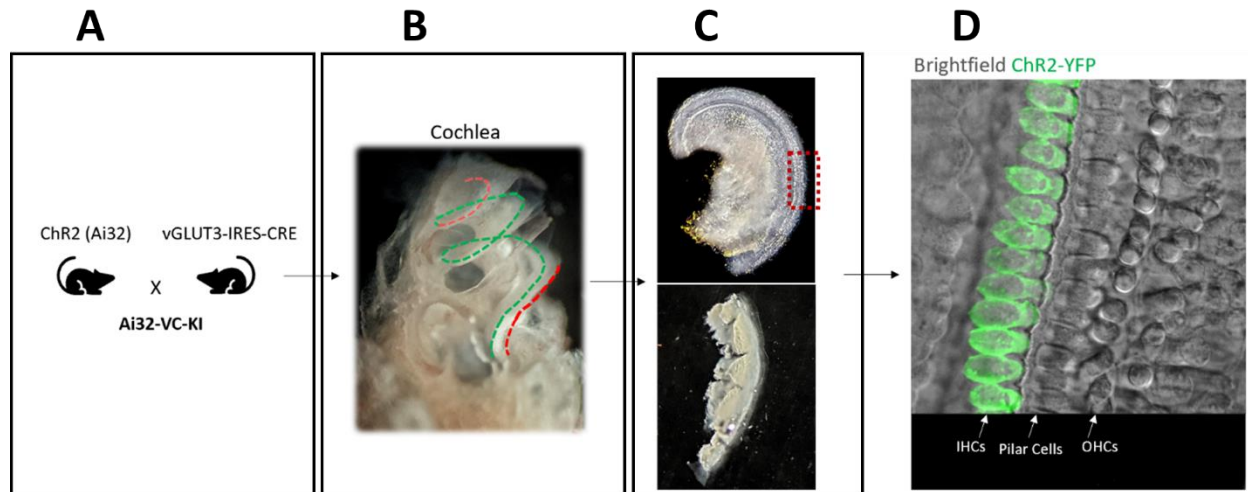
Figure 4.12 ChR2-YFP positive IHCs in the Ai32-VC-KI mouse line

(A) The Ai32 mouse line was crossbred with the Vglut3-ires-Cre line to obtain expression of the construct specifically in the IHCs.

(B) Picture of the dissected cochlea showing the apical and basal regions (red dashed lines) used for the experiments.

(C) Apical turn (top panel) and basal turn (bottom panel) of the Organ of Corti under the brightfield microscope.

(D) Apical turn under spinning-disk microscope. X63 zoom. ChR2-YFP positive IHCs in green.
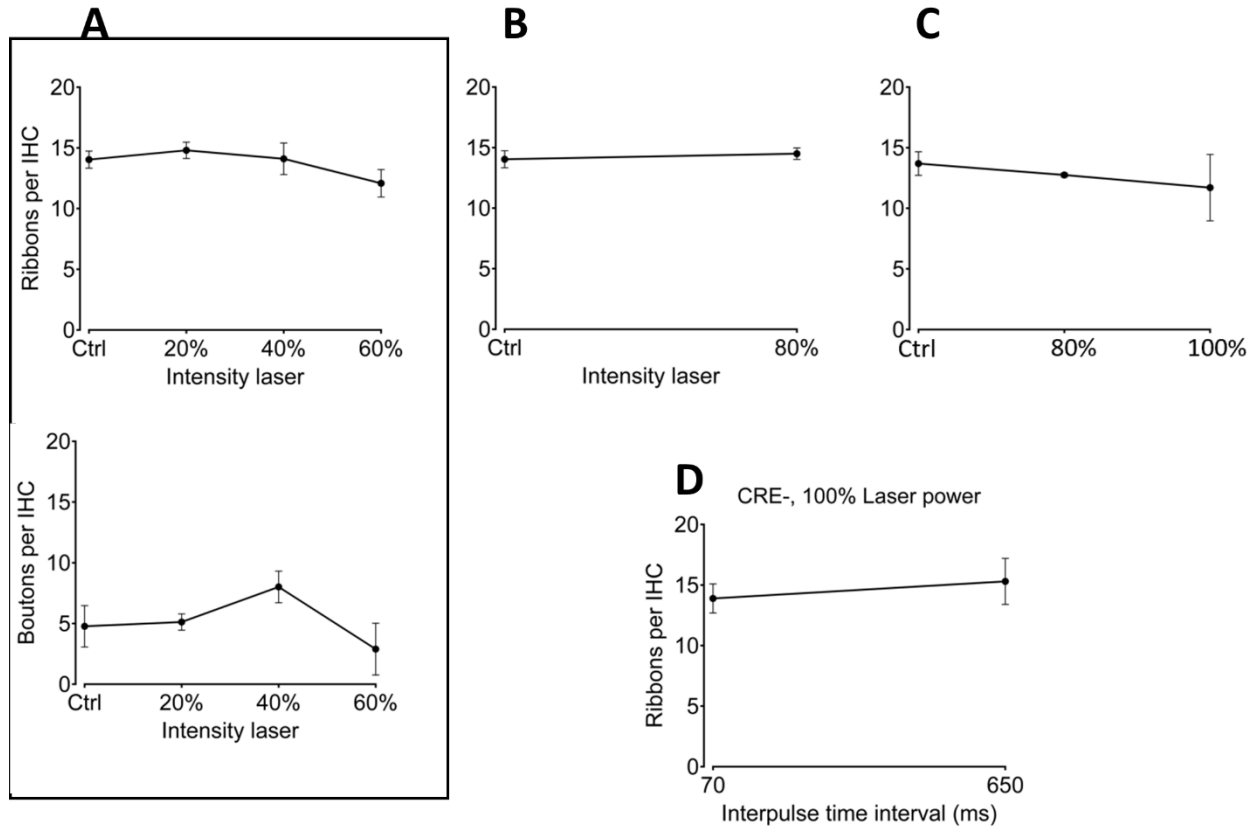
Figure 4.13 Optogenetic Stimulation of IHCs does not affect ribbon density in ex-vivo conditions

(A) IHC ribbon (top panel) and post-synaptic terminals' density (bottom panel) showing no alteration after optical stimulation in function of laser power. The stimulation parameters were as following: 20 ms exposure time; 650 ms interpulse time intervals; 45 min total exposure time. Note how only a small fraction of the SGN terminals survives in the ex-vivo preparation.

(B) IHC ribbon density showing no alteration after optical stimulation following optical stimulation with 80% of the laser power. The stimulation parameters were as following: 20 ms exposure time; 70 ms interpulse time intervals; 45 min total exposure time.

(C) IHC ribbon density showing no alteration after optical stimulation following optical stimulation with 80% and 100% of the laser power. The stimulation parameters were as following: 20 ms exposure time; 70 ms interpulse time intervals; 60 min total exposure time.

(D) CRE- mouse line exposed to 100% laser power doesn't show significant ribbon loss after 60 min.

Ctrl   Stimulated

CtBP2 Homer1 ChR2-YFP
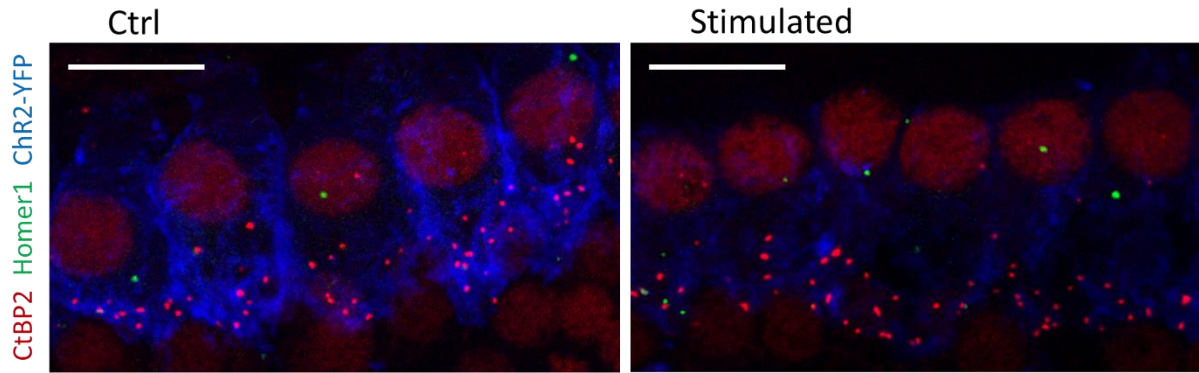
Figure 4.14 Confocal z sections show no ribbon IHC loss

Maximal projections of confocal Z sections of non-stimulated (left panel) and stimulated IHCs (right panel) did not reveal any substantial loss of IHC ribbons following a 60-minute exposure to blue light at 80% laser power. This observation was made using CtBP2, a marker of ribbons and nuclei in red, and Homer1, a marker of postsynaptic density in green. Scale bar 10μm.

5. Discussion

The primary objective of this project was to create a mouse model that could demonstrate a reliable and clear loss of ribbon synapses after exposure to noise trauma under anesthesia. We observed a mild but consistent delayed loss of ribbon synapses at the high frequency region, prompting us to employ this model for functional analysis.

Drawing inspiration from the successful mouse model developed by Kujawa and Liberman (2009), see introduction section, I have decided to utilize their work as a foundational starting point for the development of a novel mouse model specific to the characteristics of my project. As reported by Zheng, Johnson, and Erway (1999), male C57bl/6J mice, in conjunction with the CBA/CaJ strain, have been identified as ideal models for investigating the effects of noise exposure on the cochlea due to their normal ABR thresholds at 33 weeks of age. In light of the technical challenges associated with single cell electrophysiology recording (patch clamp) from inner hair cells (IHCs) located in the basal region, particularly in cases where recordings must be performed immediately following noise exposure and again after a 2-week interval (when the effects were described to be permanent; Liberman et al., 2015), I have opted to begin noise exposure in weaned male animals at the age of 3-4 weeks as the experiments in older animals become progressively more challenging.

There are several different noise exposure paradigms that have been used in animal studies to investigate the effects of noise on the auditory system. The use of an octave band of noise with a frequency range of 8-16 kHz has been widely employed in animal research to study the effects of noise exposure on the auditory system (Liberman and Kiang, 1978; Liberman and Mulroy, 1982; Liberman and Dodds, 1984a; Liberman and Dodds, 1984b; Liberman and Kiang, 1984; Zheng, Johnson, and Erway, 1999; Kujawa and Liberman, 2006; Kujawa and Liberman, 2009; Kujawa et al, 2011; Kujawa and Liberman, 2015; Liberman et al, 2015; Suthakar and Liberman, 2021). One of the advantages of using the 8-16 kHz octave band of noise in animal research is its specificity in targeting the high-frequency region of the cochlea, which is particularly vulnerable to noise-induced hearing loss (Cody and Johnstone, 1981; Liberman and Mulroy, 1982). Other noise paradigms such as continuous pure tone, intermittent noise, and white noise have also been employed. However, all of these paradigms have important limitations when studying the

effects of noise trauma on the Organ of Corti. Continuous pure tone exposure involves exposure to a single tone at a constant frequency and intensity over an extended period of time (Hakuba et al, 2000; Tan et al, 2007). While this paradigm can be useful for investigating the effects of specific frequency components on hearing, it may not accurately reflect real-world noise exposure patterns and, it may not account for the potential effects of noise exposure at multiple frequencies. Theopold's study (1978) uncovered a correlation between the frequency band of the noise and the extent of cochlear damage. Specifically, the study demonstrated that when the animals were exposed to an octave band of noise, the region of the cochlea that was damaged was significantly wider compared to the damage caused by a continuous pure tone noise.

Intermittent noise exposure involves repeated episodes of noise exposure with periods of rest in between. While this paradigm can better mimic real-world noise exposure patterns, it can be more difficult to control and standardize the duration and intensity of each exposure episode, and it may not fully account for the cumulative effects of noise exposure over time. Intermittent noise exposure allows the auditory system to recover between noise phases, which may explain the reduced damage observed (Chen et al, 1998; Campo and Lataye, 1992; Clark et al., 1987; Clark and Bohne, 1992; Fredelius and Wersall, 1992; and Patuzzi, 1998). Campo and Lataye (1992) and Clark and Bohne (1992) have suggested that the recovery period may allow for restoration of the endolymph and normalization of the ionic environment in the inner ear, reducing the likelihood of damage to the hair cells.

Finally, white noise exposure involves exposure to noise that contains equal power across all frequencies. Although this noise paradigm can offer a comprehensive and wide-ranging stimulus to evaluate hearing function across all frequencies, it may not precisely simulate real-life noise exposure patterns. Furthermore, it can be challenging to regulate the frequency composition of the noise.

After conducting a comprehensive literature review and carefully considering my research objective to establish a mouse model of acoustic trauma that displays synaptopathy without cellular loss, I have determined that the 8-16 kHz noise band paradigm is the most suitable. This decision was further guided by the previous tests of the laboratory that failed to find a noise

paradigm evoking a clear (permanent) synaptopathy in the apical cochlea, which would have otherwise been much easier to assess by in vitro electrophysiology (see below).

5.1 Functional comparison between apical and basal IHCs

To create an effective animal model of noise-induced hearing loss, it is essential to understand the tonotopic distribution of vulnerability to noise in the cochlea. Observing synaptic damage in the apical cochlea has so far either failed (previous attempts in our lab), or demands very high levels of noise, causing very strong PTS (see Boero et al., 2021). Furthermore, in this study, the loss of ribbons was only temporary (Boero et al.; 2021). Testing the effects of hidden hearing loss (with no PTS) or in the presence of at most mild PTS, thus does not seem possible in that part of the cochlea, which is otherwise well accessible to in vitro electrophysiological investigation. The basal part of the cochlea, on the other hand, which processes high-frequency sounds, is reportedly most vulnerable to noise exposure. Thus, the majority of studies on noise-induced hearing loss and in particularly a hidden hearing loss, focused on noise paradigms that damage high frequency hearing. In the mice, thus, often a 8-16 kHz noise band is chosen (see e.g. Kujawa and Liberman, 2009; Liberman et al., 2015; Liu et al., 2019; Kim et al., 2019; Hu et al.2020). Noise exposure in this octave band is typically most synaptopathic for the tonotopic cochlear regions between 24 and 50 kHz (see e.g. Liberman et al., 2015). Any of these regions is not easily accessible to in vitro patch-clamp as during the excision these parts of the organ of Corti are extremely prone to mechanical damage. In my initial tests, I determined that the preservation of the tissue is better in the wholemount of the basal part of the cochlea, containing the tonotopical region around 40-50kHz, as compared to tonotopical regions towards the mid of the cochlea (e.g. 24-32 kHz). I thus decided to focus my experiments in the 40-50kHz tonotopic region. Performing a patch clamp of IHCs in the basal region is challenging but crucial for investigating the functional and anatomical alterations of the ribbon synapses following noise exposure. Thus, the first and most challenging step of this project was to establish a protocol to successfully record ionic currents and monitor exocytosis in the basal IHCs.

In my initial attempts to perform patch clamp recordings of basal inner hair cells (bIHCs), I used young mice aged 13-15 days. This approach was chosen due to the fact that at this developmental

stage, the cochlear bone is not as hard, making it easier to perform dissections of the basal region as compared to older mice (>p21), where dissections can become increasingly challenging. To establish a robust experimental baseline for my investigation, age-matched mice were euthanized and patch clamp recordings of apical inner hair cells (aIHCs) used as comparison. This approach was selected due to the established reliability of these recordings within our laboratory. Initial recordings of bIHCs showed significantly smaller depolarization-evoked Ca2+ current amplitudes as well as calcium charge transfer (QCa) when compared to the age-matched aIHCs. On the other side, Ca2+-dependent exocytosis appeared to overlap between apical and basal IHCs, suggesting a significantly higher efficiency of Ca2+ -triggered exocytosis at both short depolarization durations (<20 ms), which reflects the exocytosis of the RRP, and long (>20ms), which reflects the replenishment of the vesicles. In the bIHCs of slightly older, p21-28, mice, the Ca2+ current amplitudes approached, but were still smaller as compared to the 2w-old apical IHCs, while the difference was no longer significant when inspecting the QCa. However, the Ca2+-dependent exocytosis was significantly higher for longest pulses. These results suggest further increase in the efficiency of exocytosis upon long depolarizations in the bIHCs, which may be due to further development of the bIHC synaptic physiology and enhanced vesicle replenishment. This finding aligns with the research of Johnson et al. (2008) and Johnson et al. (2009), who studied the tonotopic variation in the Ca2+ dependence of neurotransmitter release and vesicle pool replenishment in gerbil ribbon synapses. The authors found that the Ca2+ efficiency of exocytosis improved in both apical and basal IHCs with maturation, with a more pronounced improvement in the basal IHCs. Johnson et al. (2008) suggested that vesicle pool refilling could become rate-limiting for vesicle release in adult IHCs, with high-frequency cells able to sustain greater release rates (Johnson et al. 2008).

5.2 Noise trauma and its effect on auditory function

The development and investigation of different animal models of noise trauma are important steps towards understanding the different manifestations of noise over-exposure, including the possible different impacts on IHC ribbon synapses. In this study, two groups of mice were exposed to an octave noise band (8-16kHz) for 2 hours at either 96 or 92 dB SPL. The hearing sensitivity

and cochlear amplification was measured before and after the exposure using ABR and DPOAE, respectively, while the animals were anesthetized with isoflurane (up to 2%).

The ABR thresholds recorded immediately after the noise exposure showed varying degrees of change depending on the intensity of the noise (~40 dB vs ~20 dB SPL threshold shift upon 96- and 92dB-noise exposure, respectively). Prolonged exposure to isoflurane alone appeared to temporarily increase the thresholds by ~20 dB SPL. This suggests that only with the highest noise intensity paradigm used (96 dB SPL) part of the threshold increase could be safely attributed to noise trauma, while possible modest acute effects upon 92dB-exposure, if present, could not be separated from the effects of volatile anesthetic. The ABR W1 amplitude, which reflects the synchronous activity of the auditory nerve fibers, also displayed a considerable reduction in the 96 dB SPL group of mice. Assessment of OHCs activity using DPOAE threshold and amplitude analyses, revealed a significant reduction in OHCs activity immediately after noise exposure. This decrease in OHCs activity suggests that exposure to both 96 and 92 dB SPL noise intensity of 96 dB SPL had affected OHCs function. However, it is important to note that the combined effect of isoflurane anesthesia and noise exposure might have contributed to the observed changes in the OHC function. The control DPOAE experiments in mice exposed to isoflurane but not noise were unfortunately of too poor quality for reliable comparison. To distinguish between the possible effects of isoflurane and noise exposure, these control experiment thus need to be repeated in the future. Judged by the published data, the effects of isoflurane on DPOAE thresholds are less pronounced as compared to the effects on the ABR thresholds (Cederholm et al., 2012;).

In a cohort of animals, the hearing tests were repeated two weeks after initial noise exposure, both noise-exposed groups of mice demonstrated evidence of mild PTS at high frequencies. IN addition, a moderate loss of ribbon synapses was detected in the high-frequency tonotopical regions two weeks after noise exposure, independent of the noise intensity. This loss seemed to be slightly delayed in comparison to other studies (e.g. Liberman, Kujawaa), as it was not observed immediately after noise exposure. Limited amount of data on D1 samples however may suggest that the loss of ribbon synapses is evident by approx. 24 hours after noise exposure. There are two critical aspects highlighted by these findings.

Firstly, as previously observed and suggested (Liberman and Dodds, 1984; Wang et al., 2002) the noise exposure typically damages cochlea at the tonotopic frequency regions above the frequencies of the applied noise band, typically starting an octave above the lower edge of the noise band (e.g. in our case, 8 kHz). In our model, at low-frequency regions (<16 kHz), no functional alterations of signal transduction were observed, consisted with an idea of such "octave shift". From 16 kHz onwards, the damaging effect of noise exposure became visible in the ABR thresholds (with a trend at 16kHz, and a significant increase in the ABR threshold at 24 and 32 kHz). Noise exposure can cause reversible and irreversible damage of the cochlear structures, for example a temporary threshold shift (TTS) or a permanent threshold shift (PTS), but also temporary stereociliary damage or synaptic damage with or without (partial) recovery/repair. A noise-induced PTS has been ascribed to anatomical alterations of stereocilia, perforation of the reticular lamina with the consequent mixture of perilymph and endolymph, decreased endocochlear potential, and cellular loss (Wang et al., 2002). A TTS, on the other hand, is believed to mainly reflect a temporary collapse of supporting cells (Wang et al., 2002).

Secondly, in our experimental conditions, we could not evoke the so called hidden hearing loss, which has first been observed and described by Kujawa and Liberman (Kujawa and Liberman, 2009) as a TTS with permanent loss of a subpopulation of ribbon synapses. While exposure to either 92 or 96 dB noise caused a comparable loss of ribbon synapses as well as comparable minor PTS, lower SPL noise values not shown in this thesis but tested preliminary in the lab (90 dB SPL), that results in no PTS did not result in a significant loss of ribbon synapses. This means that in our experimental conditions, a significant loss of ribbon synapses was only observed in the presence of at least a mild PTS. One possibility to explain the above observations could be the effect of isoflurane on auditory nerve fibers. Isoflurane was reported to reduce the excitability of SGNs (Cederholm et al., 2012), possibly attenuating an over-excitation during noise exposure. Since over-excitation of SGNs terminals during acoustic overexposure according to recent data seems essential for triggering presynaptic ribbon loss (Kim et al., 2019; Hu et al., 2020), it is plausible to hypothesize that the same noise intensity that would induce TTS and consequently ribbon loss in awake animals may not be sufficient to overstimulate SGNs under isoflurane exposure, resulting in no ribbon loss with milder noise SPL levels. In this scenario, to

induce ribbon loss, the intensity of the noise needs to be increased, ultimately creating a PTS. In summary, this is essentially what our new mouse model demonstrates. A TTS specific for the frequency region of 16 kHz, for both 92 and 96 dB SPL, does not exhibit any ribbon loss. On the contrary, cochlear regions ≥24 kHz showing a PTS also display approx.. 20% ribbon loss. It is possible that noise of further increased SPLs (e.g. 100 dB SPL) might induce a larger PTS and a greater ribbon loss. However, caution should be exercised with higher intensity exposures, as hair cells might be lost, or the stereocilia heavily damaged, resulting in an early block of the MET already during noise exposure, which may potentially even lead to a situation that reduced hair cell activation and consequently "protects" ribbon synapses. Our model of of noise-evoked auditory synaptopathy is perhaps most interesting in the observation that even though protective effects of isoflurane are postulated, our results indicate that a moderate ribbon synapse loss can even be observed when little or no ABR threshold shift is evident immediately after noise exposure, as it in particularly the case with our 92 dB exposure. Auditory synaptopathy is typically observed in conditions that show at least 20, but more often 40 dB of initial ABR threshold shift immediately after noise exposure that typically is of transient nature and recovers within a few days (see e.g. Liberman and Kiang, 1978; Liberman and Dodds, 1984; Kujawa and Liberman, 2006; Kujawa and Liberman, 2009;Furman et al., 2013; Liberman and Kujawa, 2017; Fernandez et al., 2020). So far, I am not aware of a study that would demonstrate a loss of ribbon synapses can also occur with little to no obvious immediate threshold shift. While the interpretation of our threshold shift immediately noise exposure is complicated due to confounding effects of isoflurane and noise trauma, it is still likely that the ABR threshold shift, if present, is at most mild upon 92 dB exposure. Our data thus suggests that, at least in the presence of volatile anesthetic isoflurane, a small but significant noise-evoked ribbon synapse loss seems disconnected from an immediate ABR threshold shift. This observation is to my knowledge novel and should open a path for future investigations. One intriguing interpretation for this observation is that in conditions where the function of the OHCs and MET is well preserved during the entire duration of prolonged noise exposure, this may cause a relatively larger synaptic damage as the hair cells may remain in the "overexcited state" for prolonged period of time (as compared to an alternative situation where an early noise-evoked damage to stereocilia or the

OHCs may attenuate hair cell depolarization still during the noise exposure, effectively shortening the time of damaging hair cell and postsynaptic over-excitation)

5.3 Mechanisms underlying IHCs ribbon loss in noise

The amount of synaptic loss was comparable between the two different noise intensities used, and selective for the high frequency regions (>24 kHz). However, despite these results match with those from Kujawa and Liberman (2009), two important differences should be noted. The first is the amount of the synaptic loss, almost 20% percent in this study against the almost 50% observed by Kujawa and Liberman (2009). Secondly, the time course of the synaptic loss, two weeks after the noise exposure (or likely by D1) in this study against a few hours in the Kujawava and Liberman study (according to personal communication, approx.. 2 hours). Interestingly, this "fast" synaptic loss seems to occur in other studies where mice are exposed to moderate intensity noise that determines a TTS (Sebe et al., 2017; Kim et al., 2019; Hu et al., 2020; Boero et al., 2021). This suggest that any molecular mechanism underlying the death of the ribbon synapses would occur relatively fast, within few hours after the noise or even during the exposure itself. On the other hand, the present study shows a delayed ribbon synaptic loss, suggesting the involvement of possible different molecular mechanisms of those involved in the fast synaptic loss.

Since three decades researchers tried to unravel the mechanism at the base of the synaptic neuropathy observable upon noise exposure. The predominant hypothesis sees glutamate as the main factor responsible of the synaptic loss. Glutamate is essential for normal auditory function, but excessive glutamate release can be neurotoxic and can lead to synaptic loss and neuronal death (Choi, 1988). Excessive glutamate release can occur in response to various types of stimuli, including noise exposure, ototoxic drugs, and other insults to the auditory system. The to be due to a combination of increased glutamate release from IHCs and reduced uptake of glutamate by glial cells (Kujawa and Liberman, 2009). A second line of evidence supporting the glutamate toxicity hypothesis is that blocking glutamate receptors with antagonists can prevent or reduce noise-induced hearing loss (Ruel et al., 2005; Sebe et al, 2010; Hu et al., 2020). For example, Riluzole, an FDA-approved drug used to treat amyotrophic lateral sclerosis, has been shown to

protect against noise-induced hearing loss by inhibiting glutamate release (Ruel et al., 2005). Other drugs that target glutamate receptors or glutamate transporters are also shown to be effective in preventing or reducing noise-induced hearing loss. For instance, Sebe et al. (2010) provides evidence for the presence of CP-AMPARs at the mature hair cell ribbon synapse in different species, including zebrafish, rat, and bullfrog. The researchers used a combination of in vivo electrophysiological and Ca2+ imaging approaches in zebrafish larvae to demonstrate that hair cell stimulation leads to robust Ca2+ influx into afferent terminals, and prolonged application of AMPA causes excitotoxicity and loss of afferent terminal responsiveness. Furthermore, blocking CP-AMPARs protects terminals from excitotoxic swelling (Sebe et al, 2010; Hu et al., 2020). A third line of evidence is that cochlear perfusion of the AMPA/kainate antagonist, kynurenate, can protect against noise-induced swelling of cochlear nerve terminals contacting IHCs (Ruel et al., 2005). This swelling is thought to be due to excessive glutamate release and the resulting activation of glutamate receptors on the cochlear nerve terminals.

Insults other than noise lend support to the glutamate toxicity hypothesis. For example, aminoglycoside antibiotics, which are commonly used to treat bacterial infections, can cause both hair cell loss and synaptic loss in the cochlea (Ruan et al., 2014; Oishi et al., 2015). Studies have shown that aminoglycosides can cause glutamate release and glutamate toxicity in the cochlea (Smith, 1999). Similarly, impulse noise exposure, which is characterized by short-duration, high-intensity sound pulses, can also cause synaptic loss in the cochlea (Cho et al., 2013). Excessive activation of ionotropic glutamate receptors, particularly the AMPA receptors, can lead to calcium influx into the postsynaptic neuron and the activation of downstream signaling pathways that can lead to synaptic loss and neuronal death (Lau and Tymianski, 2010). The calcium influx can activate proteases, such as calpains and caspases, which can cleave cytoskeletal and synaptic proteins and lead to synaptic loss (Fonseca et al., 2016). In addition, excessive activation of AMPA receptors can lead to the internalization of the receptors and the reduction in the number of functional receptors at the synapse (Cull-Candy et al., 2006). This reduction in functional receptors can lead to a decrease in synaptic strength and eventually to synaptic loss. While it is evident that noise trauma-induced synaptic loss requires glutamate release and subsequent over-activation of glutamatergic receptors, predominantly CP-AMPA

receptors, situated in the terminals of the Spiral Ganglion, the precise molecular mechanisms of ribbon loss remain uncharted.

Ubiquitin-mediated proteolysis may be one potential candidate mechanism for the degradation of proteins. This process involves the tagging of a protein that requires degradation with a small protein known as ubiquitin, which is facilitated by a series of enzymes. This post-translational modification directs the protein to the proteasome, a complex of proteins that rapidly breaks down the protein through proteolysis (Voges et al., 1999). In vitro experiments measuring proteasomal activity have demonstrated that the proteasome can degrade proteins within a matter of minutes (Beckwith et al., 2013). This could potentially explain why synapse loss is observed immediately after the noise insult. Inhibition of ubiquitination in the Drosophila melanogaster neuromuscular junction has been linked to increased neuronal excitability (Martin et al., 2016), which suggests a possible role for ubiquitination in the regulation of IHC presynaptic activity. Additionally, it is possible that nitric oxide (NO), a signaling molecule, is involved in this process. NO is involved in various cellular processes, including the uncoupling of the gap junction system in Deiter's cells, the regulation of blood flow, and immune response (Green et al., 1990; Rörig and Sutor, 1996; Jiang et al., 2004). NO is also implicated in synaptic transmission, with neuronal NO-synthase linked to glutamate receptors, and activation of these receptors resulting in NO formation (Dawson et al., 1991). Following noise exposure, the concentration of NO in the cochlea has been shown to increase, inhibiting mitochondrial respiration (Shi et al., 2007). Studies on mice lacking NO-sensitive guanylate cyclase show that while their hearing function is normal, they exhibit less sensitivity to noise exposure, with lower elevation of auditory brainstem response thresholds, but similar elevation of distortion product otoacoustic emissions thresholds compared to wildtype animals. Moreover, these mice show lower ribbon loss than wildtype animals. Möhrle and colleagues reported that NO activates guanylate cyclases, inducing an elevation of cyclic guanosine monophosphate (cGMP) in IHCs but not in outer hair cells (OHCs) (Möhrle et al., 2017). These data suggest that NO affects IHC function, and its production is increased following intense activity associated with noise trauma. Furthermore, NO activates guanylate cyclases, producing cGMP, which acts as a second messenger to activate stress-related signaling cascades (Ma et al., 2015).

Another potential mechanism that may contribute to synapse loss in IHCs is oxidative stress. Reactive oxygen species (ROS) are generated in response to various stressors, including noise exposure, and can cause cellular damage by oxidizing lipids, proteins, and DNA (Le Prell et al., 2007). ROS have been shown to cause degeneration of cochlear hair cells, including the loss of synapses (Ohlemiller et al., 1999).

Contrary to the results showed on Kujawa and Liberman 2009, the mouse model used in this study shows a reliable synaptic loss only a later time point. The reasons must be attributable to the either the paradigm of noise exposed or the anesthesia. On one hand, it is plausible that increasing noise exposure intensity could lead to a more noticeable loss of ribbon synapses, potentially occurring immediately after exposure. On the other hand, it is also possible that the delayed loss of ribbon synapses is due to the protective effect of anesthesia, or perhaps a combination of both factors. It can be hypothesized that mild-intensity noise, causing a temporary shift in ABR/DPOAE thresholds by a few dB SPL (e.g., 10-15 dB SPL), combined with the protective effect of a volatile anesthetic like isoflurane, may activate stress-induced cellular signaling pathways (such as ROS, cGMP/PKG signaling, ubiquitination, etc.) that accumulate over hours or days, ultimately leading to the degradation of ribbon synapses. Additionally, if histological analysis is conducted at a later time point, such as one month after the noise trauma, it might reveal cellular loss as well.

An alternative more intriguing hypothesis, arising from this investigation suggests that a mild noise exposure accompanied by pharmacological protection may trigger distinct molecular mechanisms leading to delayed ribbons loss, which differs from those proposed to explain immediate ribbons loss.

5.4 Functional alteration of IHCs ribbon loss in noise

To further investigate the functional alterations occurring at the level of ribbon synapses between the inner hair cells (IHCs) and the spiral ganglion neurons (SGNs) following noise trauma, whole-cell perforated patch clamp recordings on basal inner hair cells from noise-exposed and non-exposed mice were performed.

The results indicate that exposure to noise did not impact the biophysical properties of Ca2+ channels. Specifically, Ca2+ currents and voltage activation kinetics of Ca2+ channels remained unchanged after the noise trauma. Following the 96 dB SPL noise exposure, a significant increase of Ca2+ dependent exocytosis was detected on the day of exposure at 5, 10, and 100 ms depolarization duration. Importantly, despite the increase in exocytosis, there were no significant changes in Ca2+ influx, suggesting higher IHC efficiency of exocytosis.

One possible explanation for the observed increase in exocytosis after noise exposure is related to potential mechanisms of synaptic plasticity. Several studies have provided anatomical evidence suggesting that synaptic rearrangements on sensory hair cells occur at different conditions, for example after noise exposure or in aging mice (Shresta et al., 2018; Stamataki et al., 2006; Jiang et al., 2015; Zachary and Fuchs, 2015; Jeng et al., 2021). In aging mice, despite showing degeneration of up to 50%, ribbon synaptic plasticity can be observed in the form of an increase in the size of the presynaptic ribbons, which is accompanied by a higher density of Ca2+ currents and sustained exocytotic responses, indicating a synaptic release potentiation (Peineau et al., 2021). Interestingly this synaptic release potentiation is observed also in mice noise exposed (Boero et al, 2021). The increase in the size of the presynaptic ribbons in aging mice is associated with larger Ca2+ microdomain amplitude and larger density of Ca2+ currents. Heterogeneity in the Ca2+ channels coupling and in their voltage activation was suggested to influence the properties of ANFs. Ribbons in the modiolar side were shown to activate at more negative potentials. However, no evidence of a voltage-shift in the voltage-dependence of Ca2+ channels with aging has been found. Instead, the increase in Ca2+ entry and stronger time-inactivation of the Ca2+ currents may be responsible for the larger Ca2+ microdomains (Grant and Fuchs, 2008; Vincent et al., 2017). Also, a higher synaptic vesicles density at the active zone of the IHC ribbon synapses is associated with an increase in the size of presynaptic ribbons in aging mice, as indicated by an EM study (Stamataki et al., 2006). This higher synaptic vesicle density may account for the larger and more sustained exocytotic responses observed in IHCs from old C57BL/6J mice. Moreover, the greater capacity to sustain secondarily releasable pool (SRP) exocytosis in old IHCs with larger ribbons would reduce the level of firing adaptation of the

auditory fibers, which could explain the altered recovery from short-term adaptation in old C57BL/6J mice (Walton et al., 1995).

Despite this study solely analyzing the cellular density of the ribbon synapses without examining their volume or shape, it is conceivable that the observed enhancement of CA^{2+} dependent exocytosis may be linked to an increase in the size of the ribbon synapse. This phenomenon could be attributed to plasticity on the ribbon synapses resulting from vesicle repositioning around Ca^{2+} channels following acute noise exposure. For instance, recent studies have demonstrated changes in the accumulation of intracellular membranes and synaptic vesicle counts in afferent synapses of inner hair cells following noise exposure (Bullen et al., 2019). Furthermore, mouse models exposed to noise have shown an increased number of available synaptic vesicles and associated increase in exocytosis events (Boero et al., 2021).

Finally, these phenomena may be also underlined by changes in the vesicular Ca^{2+} sensors as a result of acoustic trauma, such as the possible effects on expression levels of otoferlin or synaptotagmin-IV (Beurg et al., 2010; Johnson et al., 2010).

Surprisingly, two weeks after exposure, no significant alteration in the functionality of ribbon synapses was observed, despite a significant reduction in their density as revealed by immunofluorescence. The difference between the findings from the histology and physiology data suggests compensatory mechanisms in the noise-exposed IHCs. However, we can not exclude a more technical explanation that may account for this discrepancy. If all ribbons in an IHC are considered to function identically, the loss of approx.. 20% of the ribbons, should result in a concomitant 20% decline of exocytosis, which may be lost in the cell-to-cell variability. It has to be noted; however, that while not yet entirely proven, the data by other labs suggested that noise preferentially "damages" large ribbons on the modiolar side of the IHC (Liberman et al., 2015) presumably driving more exocytosis at larger presynaptic calcium clusters (Frank et al., 2009; Ohn et al., 2016; Ozcete and Moser, 2020). Assuming that similar preference of ribbon damage occurs in our experimental model, theoretically larger than 20% effect on the exocytosis could be expected. While a detailed spatial analysis of the distribution of the remaining ribbons was currently not performed, it is still possible that the variability on our patch-clamp recordings from this delicate region of the cochlea is still too large to detect such differences, in particular,

if combined with the compensatory changes, as described above (e.g. increase of ribbon volume with possible increase in exocytosis). In terms of calcium currents, previous immunohistochemical studies demonstrated the presence of orphan calcium clusters (Kim et al., 2019), presumably at the sites where the ribbon and the postsynaptic terminal were damaged and degraded. Thus, a loss of ribbons may not necessarily be associated with a loss of calcium channel clusters, still, calcium channels properties could be affected by noise or they may redistribute in the plasma membrane (including extrasynaptically). While we cannot distinguish between these possibilities, our calcium current analysis revealed no noise-evoked differences on the whole-cell level. To better address the questions of how the presynaptic calcium signaling and synaptic vesicle release changes in noise exposed IHCs, future experiments need to be performed at the level of the single AZs.

It is worth to mention that a mild but detrimental effect of a prolonged exposure to volatile anesthetic sevoflurane, can induce neurotoxicity in the developing brain, and, as reported very recently (Li et al., 2022) in the developing cochlea as well. Indeed, it has been reported that multiple sevoflurane exposures during early development led to slightly elevated hearing thresholds across all frequency regions tested and a ~10% reduction in the number of ribbon synapses in the inner hair cells at 3 months of age. Additionally, the length of these ribbons was significantly decreased in sevoflurane-exposed mice. The authors proposed that sevoflurane exposure during the neonatal period could increase oxidative stress, causing damage to hair cells and their ribbon synapses. Previous research has also demonstrated that sevoflurane exposure can induce oxidative stress in the brain, potentially extending to the cochlea (Allaouchiche et al., 2001; Piao et al., 2020; Xu and Qian, 2020). Another potential mechanism suggests that sevoflurane exposure might disrupt the balance between excitatory and inhibitory neurotransmitters in the cochlea, resulting in synaptic connectivity imbalances and reductions in hair cell ribbon synapses. Earlier studies have shown that sevoflurane exposure can alter neurotransmitter balance in the developing brain, which could similarly impact the cochlea (Li et al., 2020; Mapelli et al., 2021).

There are, however, notable differences differences between my study and Li et al.'s (2022) research. Their study focused on young, immature animals, suggesting that repetitive (3x)

sevoflurane exposure could affect synaptic development. In contrast, our study involved animals with more matured ribbon synapses and different exposure parameters, using a similar anesthetic at lower concentrations. Moreover, Li et al. reported changes in Vhalf of Ca^{2+} channels two weeks after repetitive exposure, whereas our study did not find such changes immediately after prolonged exposure or in combination with noise exposure.

The impact on ribbons and postsynaptic elements also varied between the study conducted by Li et al. (2022) and my own findings. Specifically, the effect on ribbons was found to be considerably milder in Li et al. (2022), resulting in only a 10% loss. Conversely, my data showed ~20% losses on both pre- and postsynaptic sides when a combination of isoflurane and noise exposure was administered.

It should be further noted that a separate set of experiments (not shown in my thesis) involving exposure to 90dB SPL (N=2-4, 4 for most frequency regions) at D14 showed no loss of ribbon synapses. These animals were subjected to comparable exposure to isoflurane, which did not result in loss of ribbon synapses when compared to our controls.

Taken together, these findings indicate that the synaptopathy as observed in my study can not be attributed to isoflurane exposure. They further suggest that either the effects as observed by Li and colleagues (2022) are more critical in the period of cochlear development while older cochleae are less prone to such damage. Alternatively, the different levels of exposure, and different anesthetic may underlie the different outcomes. However, it is imperative to conduct additional controls in the future to clearly test the potential effects of isoflurane on ribbon synapses. Regardless of the outcome of these controls, the results will provide crucial insights into our understanding of the possible protective (e.g., against noise-evoked synaptopathy during surgical drilling) or damaging effects of prolonged/repetitive exposure to inhalation anesthetics. This understanding is not only relevant for animal research beyond the early developmental stage but also potentially to better understand the complex effects of inhalation anesthetics in humans.

5.5 Efficacy of AC102 in protecting IHCs ribbon synapses following noise

AC102, a recently developed molecule by AudioCure GmbH, entered Phase I clinical trials in 2020 with the hypothesis of reducing apoptosis of outer hair cells following acute trauma and promoting regeneration of both inner and outer hair cells, as well as neurons. While the exact composition and mechanism of action of AC102 remain undisclosed, patents filed by the company suggest that it is a 9-methyl-ß-carboline that has demonstrated stimulatory, protective, regenerative, and anti-inflammatory effects on dopaminergic neurons in previous studies (Polanski et al., 2010). AudioCure GmbH is evaluating the efficacy of AC102 in treating hearing loss, tinnitus, and trauma from cochlear implant electrode insertion, as well as its potential to protect neurons in animal models of neurodegeneration (Wernicke et al., 2010). The mechanism of action of the 9-methyl-beta-carboline is not fully understood, but it is thought to rely on modulating the activity of certain transcription factors. For example, one study found that 9-methyl-beta-carboline increased the expression of brain-derived neurotrophic factor (BDNF) and nerve growth factor (NGF) in the hippocampus of rats, possibly by activating the transcription factor cyclic AMP response element-binding protein (CREB) (Wernicke et al., 2010).

Based on the so far observed effects, AC102 may exert its effects pre- or post-synaptically by potentially offering protective effects against noise-evoked damage or by supporting regeneration upon synaptic damage. Our results support the hypothesis of putative benefitial effects of the drug upon noise exposure, however further experiments including vehicle controls, dose effects and different time points of drug application need to be tested and validated. We further tested whether AC102 has any adverse, direct acute effects on the IHC (synaptic) function. The results of my in vitro patch-clamp experiments have indicated that the AC102 does not affect the properties of Ca^{2+} -channels or Ca^{2+} dependent exocytosis in the presynaptic IHCs.

5.6 Ex-vivo optical stimulation of IHCs

One of the key mechanisms by which noise exposure damages the SGNs is through an increased release of the neurotransmitter glutamate from the IHCs (Mao and Chen, 2021; Boero et al., 2021; Hu et al., 2020; Kim et al., 2019; Sebe et al., 2017; Hakuba et al., 2000). Excess glutamate

release may overstimulate SGNs, leading to hyperexcitability, damage, and ultimately cell death, causing hearing loss and other auditory impairments (Puel et al., 1998; Pujol and Puel., 1999).

To investigate the molecular processes involved in noise-induced synaptopathy in more detail, I set to develop and test an in vitro mouse model of hair cell over-excitation by using the Ai32VC-KI mouse line expressing channelrhodopsin 2 (ChR2) in the inner hair cells (IHCs). Blue light at 488 nm was used to repetitively stimulate the IHCs, to mimick the prolonged continuous stimulation as expected in vivo upon noise exposure. The idea was that such optogenetic overstimulation, if achievable, could serve as an in vitro model of the auditory synaptopahty, where pre- and post-synaptic overstimulation may also be achieved in separation and in combination with pharmacological treatment of the putative molecular mechanisms involved in the loss of synapses, these could be tested in more detail. I opted to test the possibility of using acute organs of Corti for this purpose, as the culturing of the organs of Corti at the age when mice can hear is not yet feasible. To test whether prolonged optogenetic stimulation can evoke the loss of ribbon synapses in vitro, I used immunohistochemistry in combination with confocal microscopy. None of the light-exposure parameter combinations tested resulted in reliable and reproducible effects on ribbon synapses.

The ribbon synapses' resistance to overstimulation of IHCs may possibly be explained by the low survival rate of the afferent fibers and boutons in my ex vivo preparations, as observed by the immunostaining of the synaptic boutons or afferent fibers. Despite efforts to better preserve postsynaptic spiral ganglion (SGN) boutons, only a fraction of afferent fibers and boutons seem to have survived in my ex vivo acute whole-mount organ of Corti preparations 1 hour after organ excision. Recent in vivo studies suggest that glutamatergic signaling and activation of postsynaptic glutamate receptors in the SGN boutons may be required for the induction of activity-dependent ribbon loss, potentially through retrograde signaling from postsynaptic boutons (Kim et al. 2019; Hu et al., 2020). It is thus possible that the lack of reliable loss of ribbons in our in vitro model was due to the lack of putative retrograde signals from the SGN boutons. If so, the mechanism of postsynaptic loss and associated activation os signaling cascade may differ in the case of mechanical damage (e.g. cutting of the SGN) and excitotoxicity. Indeed, in the old

studies using mechanical destruction of the auditory fibers no loss of ribbons was reported (Mackenzie and Wolfenden, 1955).

To enhance the potential of this tool as an in vitro model of overstimulation-evoked auditory synaptopathy, it is essential to prioritize efforts towards improving the preservation of afferent boutons. This could lead to more accurate and reliable results in future studies.

The apical region of the cochlea, which codes for low frequencies, has been reported to be less vulnerable to noise exposure compared to more basal regions that encode higher frequencies (see e.g. Boero et al.; relatively modest and reversible loss of ribbons was observed in the apical cochlea only upon very high levels, t.i. 120 dB SPL, of noise stimulation, causing considerable PTS). While this may be due to the mechanical properties of the cochlea, it is further possible that the apical IHCs are intrinsically less vulnerable to over-excitation, as well. Therefore, further experiments should be performed using the basal turn of the cochlea, where however the preservation of the tissue is significantly more challenging, to investigate the potential effects of overstimulation on ribbon synapses in this region. Another alternative to the use of acutely isolated organs, is the organotypic culture. While a better preservation of postsynaptic fibers may be achieved in the organotypic culture, a possible caveat with using the cultures is that these can so far only be generated from early postnatal and thus immature organ of Corti. While signs of maturation in the culture have been documented (e.g. Vogl et al), the validity of such approach would first need to undergo extensive testing, as well. Overall, the molecular mechanisms underlying noise-induced synaptopathy are still only partially understood and should be investsigated in the future also to identify potential therapeutic targets. It would be easiest to investigate the molecular pathways and the kinetics of the ribbon changes in vitro. Thus, the quest to develop the proper model for noise-evoked auditory synaptopathy continues.

Additionally, the apical region of the cochlea, which codes for low frequencies, has been reported to be less vulnerable to noise exposure compared to more basal regions that encode higher frequencies. Therefore, further experiments should be performed using the basal turn of the cochlea, where the preservation of the tissue is more challenging, to investigate the potential effects of overstimulation on ribbon synapses in this region. Overall, these findings highlight the

need for more research to better understand the molecular mechanisms underlying noise-induced synaptopathy and identify potential therapeutic targets for this condition.

5.7 Impact of isoflurane anesthesia on hearing sensitivity

A prolonged exposure to isoflurane anesthesia (for a duration equivalent to that of the noise-exposed cohort), revealed an acute ABR threshold shift of approximately 20 dB SPL, indicating a discernible temporary impact of the anesthetic agent on auditory transmission.

Previous studies have shown that isoflurane can induce auditory threshold shift in mice, guinea pigs and rats which is believed to originate from disrupted OHC amplification or auditory nerve transmission (Sheppard et al., 2018; Bielefeld, 2014; Cederholm et al., 2012; Ruebhausen et al., 2012; Stronks et al., 2010). The molecular effects of isoflurane on OHCs, IHCs and auditory nerve are not fully understood, but several hypotheses have been proposed based on the available evidence (Cederholm et al., 2012; Ruebhausen et al., 2012). Isoflurane has been shown to have a dose-dependent suppressive effect on the ABR in rats, with higher doses and longer durations resulting in greater suppression, and its effects were greater than ketamine anesthesia (Bielefeld, 2014; Cederholm et al., 2012; Ruebhausen et al., 2012; Stronks et al., 2010). Similarly, isoflurane anesthesia has a greater suppressive effect on DPOAEs (Sheppard et al., 2018); However, in a separate study by Cederholm et al. (2012), the initial DPOAE thresholds and growth functions were similar for both anesthetics. After 60 minutes, DPOAE thresholds increased for both groups, but the effect was significantly greater with ketamine anesthesia. The reported effects largely depend on the amount of anesthetic, low levels of isoflurane anesthesia may reportedly result in no significant threshold shift (Bourian lab), but may, as experienced during my PhD work, be hard to achieve in young mice as it does not seem compatible with sufficient depth of anesthesia to support undisturbed measurements. These effects are likely to be mediated by the modulation of multiple molecular targets in the auditory system, including ion channels, neurotransmitter receptors, intracellular signaling pathways, and gene expression.

Clinical concentrations of volatile anesthetics like isoflurane have been found to inhibit voltage-gated sodium channels, Nav, in isolated rat nerve terminals and neurons, dorsal root ganglion (DRG) neurons, hippocampal neurons, as well as in heterologously expressed mammalian Nav

subunits (Ouyang et al., 2003; Perouansky et al., 2004; Zhou et al., 2009; Sand et al., 2017). Patch-clamp recordings of nerve terminals have shown that isoflurane reduces action potential amplitude and accelerates the inactivation of the sodium currents, leading to a reduction in the excitability of the nerve fibers and significantly effecting the transmitter release and hence the synaptic transmission (Perouansky et al., 2004; Wu et al., 2004; OuYang et al., 2005; Zhou et al., 2009; Sand et al., 2017). Isoflurane inhibits multiple mammalian Na+ channel isoforms, including Nav1.2, Nav1.4, Nav1.6, Nav1.5, and Nav1.8 (Rehberg et al., 1995; Stadnickaet al., 1999; Shiraishi et al., 2004; OuYang et al., 2007; OuYang et al., 2009; Herold et al. 2010; Purtell et al., 2015). Isoflurane suppresses Nav mainly by stabilization of inactivated state of Nav and delay recovery from steady-state inactivation (Zhou et al., 2019). Along with the transit components of the Nav current, clinically relevant concentrations of isoflurane also inhibit the persistent component of Nav currents in hippocampal pyramidal neurons. These results suggest that volatile anesthetics have the potential to directly modulate the intrinsic excitability of presynaptic neurons (Zhao et al., 2019). The Nav1.6 sodium channel is a voltage-gated ion channel that plays a critical role in the generation and propagation of action potentials in neurons. It is highly expressed in the central nervous system and has been shown to play a key role in synaptic transmission and plasticity. Recent studies have shown that Nav1.6 is also present in auditory nerve fibers, which are responsible for transmitting sound signals from the cochlea to the brain (Hossain, 2005; Kim and Rutherford, 2016; Quinn et al., 2021). The inhibition of Nav1.6 channels in auditory nerve fibers can lead to a reduction in the firing rate of auditory nerve fibers, as well as a decrease in the amplitude of the action potentials generated (Meredith et al., 2021). The reduction in firing rate of auditory nerve fibers can result in a decrease in the sensitivity of the auditory system to sound stimuli. This can manifest as an increase in ABR thresholds. Despite extensive understanding of the effects of isoflurane on Nav channels, there remains a dearth of knowledge regarding its impact on auditory nerve fibers and subsequent signal transmission.

Other than binding to the Nav channels, isoflurane has been shown to modulate the activity of voltage-gated potassium channels in the nervous system (Steinberg et al., 2014; Zhou et al., 2015; Lazarenko et al., 2010). These channels play a critical role in the regulation of the membrane potential and the firing properties of the neurons, and their modulation by isoflurane can lead to

changes in the neuronal excitability and synaptic transmission. For example, a study by Berg-Johnsen and Langmoen (1990) investigated the effects of isoflurane on the voltage-gated potassium channels in rat hippocampal neurons. The authors found that isoflurane increased the activity of the potassium channels, leading to a hyperpolarization of the membrane potential and a reduction in the neuronal excitability. The molecular mechanisms underlying the effects of isoflurane on potassium channels are not fully understood, but several studies have suggested that the drug may interact with specific domains or subunits of the channels (Barber et al., 2012). Spiral ganglion neurons (SGNs) express several types of potassium channels, which contribute to the regulation of their excitability and firing properties. One of the potassium channels expressed by SGNs is the Kv3.1 channel, which is a high-threshold, rapidly activating and inactivating channel (Kim et al., 2021). Kv3.1 channels are known to play a role in the generation of high-frequency firing in SGNs, which is important for the encoding of sound information (Oak and Yi, 2014). Another potassium channel expressed by SGNs is the Kv1.1 channel, which is a low-threshold, slowly activating and inactivating channel. Kv1.1 channels are involved in the regulation of resting membrane potential and contribute to the control of SGN firing patterns (Smith et al., 2015; Reijntjes and Pyott, 2016). Enhancing the activity of Kv3.1 channels in SGNs would lead to an increase in their firing frequency and a more regular firing pattern. This is because Kv3.1 channels are responsible for repolarizing the neuron after an action potential, which allows the neuron to fire at high frequencies without entering a refractory period (Labro et al., 2015; Boddum et al, 2017). While the exact effects of isoflurane on the potassium channels of SGNs are not well understood, previous studies on other neurons, such as hippocampal neurons, have shown that isoflurane can cause hyperpolarization of the membrane potential and a reduction in neuronal excitability (Labro et al., 2015; Boddum et al, 2017). Therefore, it is hypothesized that similar effects may be expected in SGNs, although more research is needed to fully understand the specific effects of isoflurane on the Kv channels of these neurons. Given the existing evidence that isoflurane can induce membrane hyperpolarization and decrease neuronal excitability, it is plausible to speculate that these effects may contribute to an increase in the thresholds of ABR and DPOAE, as well as a reduction in their amplitudes. However, it is important

to acknowledge that this is still a hypothetical explanation and further studies would be needed to validate this hypothesis.

In addition to their presence on the axonal membrane of auditory nerve fibers, K+ channels are also present in the hair cells of the inner ear, where they play a crucial role in the transduction of auditory signals. The resting membrane potential in hair cells is primarily determined by the activity of the KCNQ4 channels, which are the main type of K+ channels in the OHCs (Kubish et al., 1999). Along with KNCQ4 channels, OHCs express two other types of potassium channels, SK2 and BK channels, located near the cholinergic synapse between the efferent olivocochlear fibers and the OHCs (Rohmann et al., 2015). These channels are Ca^{2+} dependent K+ channels, and their activation is triggered by the increase in cytoplasmic Ca2+ that occurs when the nAChR channels open in response to acetylcholine released by the efferent fibers (Rohmann et al., 2015). The increase in cytoplasmic Ca2+ activates the SK2 and BK channels, which in turn hyperpolarize the OHCs, reducing their sensitivity to sound stimuli (Rohmann et al., 2015).

The presence of isoflurane, which has been shown to potentiate the conductance of Kv channels and increase their open probability, on the OHCs, would increase the conductance of all the K+ channels, including the KCNQ4 channel, SK2 channel, and BK channel, resulting in an increase in K+ efflux from the cell, leading to hyperpolarization of the membrane potential. This hyperpolarization would reduce the driving force for Ca2+ entry into the OHCs, resulting in a decrease in neurotransmitter release and a reduction in the sensitivity of the OHCs to sound stimuli. When the nAChRs on OHCs are activated by neurotransmitters released by the medial olivocochlear fibers, it results in an increase in intracellular Ca2+ levels (Fuchs, 2014; Rohmann et al., 2015). This increase in Ca2+ levels cause the BK and SK2 channels in the OHCs to become more conductive, leading to a greater efflux of K+ ions and subsequent hyperpolarization of the membrane potential (Fuchs, 2014; Rohmann et al., 2015).

This hyperpolarization further reduces the sensitivity of the OHCs to sound stimuli, and at the same time, it also strengthens the inhibitory effect of the medial olivocochlear fibers on OHC activity. In other words, the activation of BK and SK2 channels by the Ca2+ ions amplify the negative feedback loop, leading to a decrease in the responsiveness of OHCs to sound (Kong et al., 2008; Wersinger et al., 2010; Fuchs, 2014; Rohmann et al., 2015).

The IHCs in the mammalian cochlea possess two types of voltage-dependent K+ channels, the (BK) Ca2+-activated K+ channels and the SK2 channels, and a small amount of KCNQ4 (Marcotti et al., 2004; Nam et al., 2015). These channels play a crucial role in regulating the excitability and neurotransmitter release of IHCs. The SK2 channels in IHCs are activated by an increase in intracellular Ca2+ levels, which occurs when the IHC is depolarized and Ca2+ ions enter the cell through voltage-gated calcium channels. Activation of SK2 channels leads to an outward flow of K+ ions, which hyperpolarizes the cell membrane (Marcotti et al., 2004). This reduces the amount of neurotransmitter released by the IHCs, leading to a decrease in the firing rate of the auditory nerve fibers and a decrease in the sensitivity of the auditory system (Marcotti et al., 2004).

Similarly, the BK channels in IHCs are also activated by an increase in intracellular Ca2+ levels, but their activation leads to a more significant efflux of K+ ions due to their larger conductance (Pyott and Duncan, 2016). This results in a more profound hyperpolarization of the cell membrane and a larger reduction in the amount of neurotransmitter released by the IHCs. The activation of BK channels also plays a role in shaping the dynamics of the receptor potential and the MET current in IHCs, which can affect the firing rate and temporal coding of auditory nerve fibers (Oliver et al., 2003).

The mechanisms by which isoflurane affects the function of IHCs are not fully understood, and there are currently no data available regarding modulation of the BK and SK2 channels by this anesthetic agent. Given that isoflurane has been shown to enhance the conductance of Kv channels, it follows that the exclusive dependence of SK2 channels on intracellular Ca2+ for activation is unlikely to be affected by this mechanism, while BK channels can be modulated by both voltage and Ca2+. Consequently, it is reasonable to propose that isoflurane may elevate the conductance of BK channels in IHCs, leading to membrane hyperpolarization. This effect on IHCs could reduce the release of neurotransmitters, which may have implications for hearing function. It is possible that the aforementioned increase in BK channel conductance in IHCs due to isoflurane administration could be a contributing factor to the observed reduction ABR amplitudes and increased thresholds. This effect on IHCs and subsequent reduction in neurotransmitter release could affect the fidelity of the neural signals transmitted to the brain, resulting in a decrease in auditory sensitivity.

Beside binding and modulating Nav and Kv channels, isoflurane has also been shown to affect Ca2+ channels (Merin, 1986). At the IHC synapse, Ca2+ enters via the Cav1.3 L-type voltage-dependent Ca2+ channel and is responsible for triggering exocytosis (Pangrsic et al., 2018). Isoflurane has been shown to affect the activity of various types of calcium channels, including the L-type calcium channels (Study, 1994). Several studies have demonstrated that isoflurane can inhibit L-type calcium currents in various types of cells, including dorsal root ganglion (DRG) neurons, guinea pig ventricular myocytes, rabbit cardiac myocytes, and rat ventricular myocytes (Eskinder et al., 1991; Kameyama et al., 1999; Camara et al., 2001). In guinea pig ventricular myocytes, isoflurane inhibited L-type calcium currents in a concentration-dependent manner (Charlesworth et al., 1994). This effect was reversible upon washout of the anesthetic. One proposed mechanism by which isoflurane might affect Cav1.3 channels is by decreasing the channel opening and enhancing the rate for channel closing and inactivation (Harris et al., 2000; Camara et al., 2001). This effect has been observed in various types of neurons, including human neuronal cells and rat spinal cord motor neurons. Isoflurane has also been shown to reduce the peak amplitude of L-type CaV channels in neurons (Eskinder et al., 1991; Kameyama et al., 1999). In rat DRG neurons, isoflurane can inhibit L-type Cav currents through enhancing current inactivation and prolonging recovery time after inactivation (Eskinder et al., 1991; Kameyama et al., 1999).

The available evidence suggests that isoflurane exposure can potentially impair the functioning of the auditory nerve by reducing the Ca2+ current entering into the IHCs through the L-type Cav 1.3 channels, thereby compromising the ability of the auditory nerve to detect and respond to sound stimuli. This phenomenon is thought to occur due to the reduction in the number of synaptic vesicles released, resulting in a decrease in the activity of the auditory nerve.

Exposure to high-intensity noise can cause damage to the auditory system by triggering an excessive release of neurotransmitters, leading to oxidative stress and cell death (Mao and Chen, 2001; Le Prell et al., 2007). The hypothesis that isoflurane could reduce the activation of L-type Ca 1.3 channels, thereby protecting the synapses from overexcitation, is plausible.

The observed phenomenon of increased thresholds of ABR and reduction of suprathreshold Wave 1 amplitudes can potentially be explained by the inhibition of L-type Cav 1.3 channels following exposure to isoflurane, in conjunction with previously described effects.

Post-synaptically, glutamate receptors are involved in the transmission of excitatory signals in the brain. Among these receptors, N-methyl-D-aspartate (NMDA) receptors play a critical role in synaptic plasticity (Hunt and Castillo, 2013). AMPA receptors are a subtype of ionotropic glutamate receptors that mediate fast excitatory neurotransmission in the central nervous system. They are composed of four subunits, GluA1-4, which can combine in various combinations to form the functional receptor complex (Jane, 2007). The cochlear afferent synapses between inner hair cells and auditory nerve fibers contain the AMPAR subunits GluA2, 3, and 4 (Hu et al., 2020; Walia et al., 2021). Two different types of AMPA receptors can be distinguished based on the presence of the subunit GluA2: the GluA2-lacking AMPARs, that are Ca2+-permeable (CP-AMPARs), and the GluA2-containing AMPARs, that are Ca2+-impermeable (CI-AMPARs), (Hu et al., 2020). Recent studies have found that the CP-AMPARs can be antagonized to prevent trauma to ANF synapses without affecting baseline measurements of cochlear function (Hu et al., 2020; Walia et al., 2021). NMDA receptors are also found on the post-synaptic terminal's membrane of the auditory afferents, but its function is not well described (Zhang-Hooks et al., 2016; Bing et al., 2015

The function of both NMDA and AMPA receptors can be modulated by volatile anesthetics, as the isoflurane (Ogata et al., 2006; Alkire et al., 2008; Carino et al., 2012). Isoflurane has been shown to block NMDA-stimulated currents, potentially by interfering with NMDA receptor channel function (Yang et al., 1991; Ogata et al., 2006; Alkire et al., 2008;). Inhibition of AMPA receptor responses has been shown to reduce excitotoxicity and protect against neuronal damage (Guo and Ma, 2021). In one study, the application of isoflurane to cultured cortical neurons was found to reduce the toxicity of AMPA receptor agonists (Kimbro et al., 2000; Li et al., 2002). This reduction in excitotoxicity was correlated with a decrease in the amplitude of AMPA receptor-mediated currents, indicating that isoflurane may protect against excitotoxicity by inhibiting the function of AMPA receptors (Kimbro et al., 2000; Li et al., 2002). Isoflurane's neuroprotective effects have also been observed in vivo. Pretreatment with isoflurane in a rat

model of global ischemia reduced neuronal injury and improved neurological outcomes (Xiao et al., 2015). This effect was associated with a decrease in the expression of AMPA receptor subunits in the hippocampus, suggesting that isoflurane may reduce excitotoxicity by inhibiting the expression and/or function of AMPA receptors in vivo (Xiao et al., 2015).

While acute inhibition of NMDA receptors is not expected to have immediate consequences on the activity of SGN terminals, because of their slow activation and deactivation kinetics, on the other hand, acute inhibition of AMPA receptors is expected to have significant effects on the firing rate or synchronization of SGNs. Inhibition of AMPA receptors by isoflurane is expected to decrease the amplitude of excitatory postsynaptic currents (EPSCs), resulting in a reduction of the firing rate and decreased synchronization of SGN fibers. This effect is likely to be more pronounced in high-frequency regions of the cochlea, where the firing rates of SGNs are highest. The ABR threshold shift and the reduction of the W1 amplitudes observed in isoflurane-anesthetized mice are likely due to the effect of the anesthetic on the AMPA receptors rather than the NMDA receptors.

Γ-aminobutyric acid (GABA) is the major inhibitory neurotransmitter in the central nervous system, where is primarily synthesized and released by specialized inhibitory interneurons located in the olivocochlear complex. In the cochlea, GABAergic transmission plays a critical role in regulating the excitability of the auditory nerve fibers and shaping their responses to sound stimuli (Maison et al., 2006). GABA acts on postsynaptic GABAa and GABAb receptors expressed on auditory nerve fibers, reducing their firing rate and increasing their temporal precision (Maison et al., 2006).

As for the GABA receptors, also the nicotinic acetylcholine receptor (nAChR) inhibits the signal transmission (Maison et al., 2010). Activation of the nAChR by acetylcholine, which is released by the efferent neurons of the medial olivocochlear (MOC) pathway during exposure to intense sound, leads to the opening of the small conductance calcium-activated potassium channel (SK2) and the large conductance calcium-activated potassium channel (BK), which allow K+ ions to flow out of the OHCs. This efflux of K+ ions hyperpolarize the OHCs, leading to a decrease in their electromotility and associated amplification of sound. This mechanism is thought to be protective during acoustic overexposure (Maison et al., 2010; Fuchs and Lauer, 2019).

GABAa and GABAb receptors, together with nAChR receptors, are critical targets of general anesthetics, in particular for the volatile ones (Scheller et al., 1997; Topf et al., 2003; Jia et al., 2008). Most effects of general anesthetics on GABAergic synaptic transmission are postsynaptic or extrasynaptic on GABA receptors compared to presynaptic glutamatergic transmission modulation. The effects of volatile anesthetics on GABA receptors are relatively complex, with most of them enhancing the amplitude and prolonging the duration of GABA-induced synaptic inhibition (Topf et al., 2003; Jia et al., 2008). In contrast, volatile anesthetics and ketamine have been identified as the most potent inhibitors of nAChRs at clinically relevant doses (Xu et al., 2000; Yamashita et al., 2005). Isoflurane has been shown to inhibit the function of nAChRs through direct interaction with the receptor subunits and modulation of the surrounding lipid membrane (Minami et al., 1994).

A prolonged exposure to isoflurane anesthesia, as observed in this study, may result in the potentiation of both the GABA- and nACh-mediated inhibition of auditory nerve activity and outer hair cell amplification, respectively. However, it is challenging to conclusively establish this mechanism as a potential cause for the observed increase in threshold of the ABR and distortion DPOAE.

In conclusion, as detailed in this paragraph, isoflurane anesthesia can significantly impact signal transmission and transduction in the auditory system at various levels. These effects include hyperpolarization of outer and inner hair cells, reduced synaptic vesicle exocytosis at inner hair cell-spiral ganglion neuron synapses, and decreased activation of auditory nerve fibers. It is possible that other mechanisms may also be involved in the observed decrease in ABR amplitudes and threshold shift following exposure to isoflurane.

6. Conclusions and next

I development of a novel mouse model of noise-induced synaptopathy through the use of moderate-level noise exposure under isoflurane anesthesia. Here, I aimed to characterize the presynaptic mechanisms behind ribbon loss and understand how noise overexposure causes this phenomenon. Through the use of system physiology, cell physiology, immunohistochemistry, and optical stimulation techniques in mouse models, we were able to gain deeper insights into the underlying mechanisms of ribbon loss due to acoustic overexposure.

Two groups of mice were exposed to 92- and 96-dB SPL noise-bands for two hours their ABRs and DPOAEs analyzed immediately after exposure and two weeks later. The results showed a significant increase in neural response thresholds at high frequencies compared to age-matched control mice, with slightly smaller elevations observed in DPOAEs. However, when compared to the isoflurane-exposed group, the threshold elevation was approximately 20 dB and only observed for the 96 dB SPL paradigm. These findings suggest that isoflurane exposure can impact both ABR and DPOAE thresholds, with only the 96 dB SPL paradigm causing an obvious immediate cochlear damage. Hearing thresholds partially recovered (in 96-dB group), but a mild shift of hearing sensitivity was observed two weeks after exposure with either of the noise levels, suggesting mild permanent threshold shift not involving OHC damage.

Confocal imaging of the sensory epithelium showed that in pre-exposure ears, nearly all IHC ribbons were observed to be connected with a nerve terminal, provided they were adequately isolated to be resolved. Immediately after the noise trauma, there was no evident sign of synaptic loss in either the pre-synaptic or post-synaptic elements. Two weeks after exposure, a moderate (~20%) reduction in the synaptic density in the high-frequency regions (>24 kHz) was observed in the noise-exposed ears for both of the noise intensities examined (92 dB SPL and 96 dBSPL). Degeneration of both presynaptic and postsynaptic elements in the IHC area was already indicated one day after exposure, albeit the sample size was insufficient to draw a definitive conclusion.

Further investigations using whole-cell perforated patch clamp recordings on basal IHCs revealed that acute noise trauma did not cause gross changes in the biophysical properties of calcium channels or the fast and slow kinetics of exocytosis. However, enhanced exocytosis and increased

total calcium influx was observed in response to short and prolonged depolarization durations following exposure to 96 dB SPL, while exposure to 92 dB SPL exhibited a tendency towards decreased exocytosis and calcium influx in response to all applied depolarization durations. Interestingly, two weeks after noise exposure, patch clamp recordings revealed no substantial changes in ribbon synapse functionality despite a decrease in synaptic density observed through immunofluorescence. This observation suggests that the residual ribbon synapses might exhibit compensatory mechanisms or part of the vesicle release happens extrasynaptically, perhaps at ribbonless AZs or even outside AZs. Future investigations should explore higher noise intensities (> 100 dB SPL) to detect more pronounced functional alterations in electrophysiology experiments, which would increase our knowledge of the molecular mechanisms involved in hearing loss caused by noise trauma. Isoflurane appears to play a protective role in ribbon loss due to noise trauma, but further experiments are needed to determine its impact on ribbon synapse activity and its effect on response to noise exposure. Performing patch clamp recordings of voltage-dependent Ca^{2+} currents and exocytosis in IHCs that have been extracellularly perfused with isoflurane could provide valuable insights into the potential impact of isoflurane on ribbon synapse functionality during acoustic overstimulation. Finally, the application of a small chemical compound AC102 in the round window niche of noise-exposed animals supports the hypothesis that this drug may partially prevent noise-induced synaptopathy. In the future, the effective therapeutic time window for application of this drug needs to be further tested as well as the underlying mechanisms of the drug action in the damaged cochlea.

Bibliography

Activity-dependent depression of neuronal sodium channels by the general anaesthetic isoflurane—British Journal of Anaesthesia. (n.d.). Retrieved March 15, 2023, from https://www.bjanaesthesia.org/article/S0007-0912(17)31248-5/fulltext

Adams, J. C. (2009). Immunocytochemical Traits of Type IV Fibrocytes and Their Possible Relations to Cochlear Function and Pathology. JARO: Journal of the Association for Research in Otolaryngology, 10(3), 369–382. https://doi.org/10.1007/s10162-009-0165-z

Age-related Hearing Loss: GABA, Nicotinic Acetylcholine and NMDA Receptor Expression Changes in Spiral Ganglion Neurons of the Mouse—PMC. (n.d.). Retrieved March 12, 2023, from https://www.ncbi.nlm.nih.gov/pmc/articles/PMC3935603/

Aging after Noise Exposure: Acceleration of Cochlear Synaptopathy in "Recovered" Ears—PMC. (n.d.). Retrieved February 11, 2023, from https://www.ncbi.nlm.nih.gov/pmc/articles/PMC4429155/

Alvarado, J. C., Fuentes-Santamaría, V., & Juiz, J. M. (2020). Antioxidants and Vasodilators for the Treatment of Noise-Induced Hearing Loss: Are They Really Effective? Frontiers in Cellular Neuroscience, 14. https://www.frontiersin.org/articles/10.3389/fncel.2020.00226

Amanipour, R. M., Zhu, X., Duvey, G., Celanire, S., Walton, J. P., & Frisina, R. D. (2018). Noise-Induced Hearing Loss in Mice: Effects of High and Low Levels of Noise Trauma in CBA Mice. Annual International Conference of the IEEE Engineering in Medicine and Biology Society. IEEE Engineering in Medicine and Biology Society. Annual International Conference, 2018, 1210–1213. https://doi.org/10.1109/EMBC.2018.8512525

Anderson, D. J., Rose, J. E., Hind, J. E., & Brugge, J. F. (1971). Temporal position of discharges in single auditory nerve fibers within the cycle of a sine-wave stimulus: Frequency and intensity effects. The Journal of the Acoustical Society of America, 49(4), Suppl 2:1131+. https://doi.org/10.1121/1.1912474

Ashmore, J. (2002). Biophysics of the cochlea – biomechanics and ion channelopathies. British Medical Bulletin, 63(1), 59–72. https://doi.org/10.1093/bmb/63.1.59

Audiology, C. A. of. (2021). Cochlear Excitotoxicity 101. Canadian Audiologist, 8(1). https://canadianaudiologist.ca/cochlear-101/

Auditory-Nerve Activity in Cats Exposed to Ototoxic Drugs and High-Intensity Sounds—Nelson Y. S. Kiang, M. Charles Liberman, Robert A. Levine, 1976. (n.d.). Retrieved March 18, 2023, from https://journals.sagepub.com/doi/10.1177/000348947608500605

Baumgart, J. P., Zhou, Z.-Y., Hara, M., Cook, D. C., Hoppa, M. B., Ryan, T. A., & Hemmings, H. C. (2015). Isoflurane inhibits synaptic vesicle exocytosis through reduced Ca2+ influx, not Ca2+-exocytosis coupling. Proceedings of the National Academy of Sciences of the United States of America, 112(38), 11959–11964. https://doi.org/10.1073/pnas.1500525112

Bazard, P., Frisina, R. D., Acosta, A. A., Dasgupta, S., Bauer, M. A., Zhu, X., & Ding, B. (2021). Roles of Key Ion Channels and Transport Proteins in Age-Related Hearing Loss. International Journal of Molecular Sciences, 22(11), 6158. https://doi.org/10.3390/ijms22116158

Becker, L., Schnee, M. E., Niwa, M., Sun, W., Maxeiner, S., Talaei, S., Kachar, B., Rutherford, M. A., & Ricci, A. J. (2018). The presynaptic ribbon maintains vesicle populations at the hair cell afferent fiber synapse. ELife, 7. https://doi.org/10.7554/eLife.30241

Berg-Johnsen, J., & Langmoen, I. A. (1986). The effect of isoflurane on unmyelinated and myelinated fibres in the rat brain. Acta Physiologica Scandinavica, 127(1), 87–93. https://doi.org/10.1111/j.1748-1716.1986.tb07879.x

Berg-Johnsen, J., & Langmoen, I. A. (1990). Mechanisms concerned in the direct effect of isoflurane on rat hippocampal and human neocortical neurons. Brain Research, 507(1), 28–34. https://doi.org/10.1016/0006-8993(90)90517-F

Bharadwaj, H. M., Verhulst, S., Shaheen, L., Liberman, M. C., & Shinn-Cunningham, B. G. (2014). Cochlear neuropathy and the coding of supra-threshold sound. Frontiers in Systems Neuroscience, 8, 26. https://doi.org/10.3389/fnsys.2014.00026

Bielefeld, E. C. (2014). Influence of dose and duration of isoflurane anesthesia on the auditory brainstem response in the rat. International Journal of Audiology, 53(4), 250–258. https://doi.org/10.3109/14992027.2013.858280

Bing, D., Lee, S. C., Campanelli, D., Xiong, H., Matsumoto, M., Panford-Walsh, R., Wolpert, S., Praetorius, M., Zimmermann, U., Chu, H., Knipper, M., Rüttiger, L., & Singer, W. (2015). Cochlear NMDA Receptors as a Therapeutic Target of Noise-Induced Tinnitus. Cellular Physiology and Biochemistry, 35(5), 1905–1923. https://doi.org/10.1159/000374000

Boddum, K., Hougaard, C., Xiao-Ying Lin, J., von Schoubye, N. L., Jensen, H. S., Grunnet, M., & Jespersen, T. (2017). Kv3.1/Kv3.2 channel positive modulators enable faster activating kinetics and increase firing frequency in fast-spiking GABAergic interneurons. Neuropharmacology, 118, 102–112. https://doi.org/10.1016/j.neuropharm.2017.02.024

Boero, L. E., Payne, S., Gómez-Casati, M. E., Rutherford, M. A., & Goutman, J. D. (2021). Noise Exposure Potentiates Exocytosis From Cochlear Inner Hair Cells. Frontiers in Synaptic Neuroscience, 13, 740368. https://doi.org/10.3389/fnsyn.2021.740368

Bohne, B. A., & Harding, G. W. (2000). Degeneration in the cochlea after noise damage: Primary versus secondary events. The American Journal of Otology, 21(4), 505–509.

Bommakanti, K., Iyer, J. S., & Stankovic, K. M. (2019). Cochlear Histopathology in Human Genetic Hearing Loss: State of the Science and Future Prospects. Hearing Research, 382, 107785. https://doi.org/10.1016/j.heares.2019.107785

Bourien, J., Tang, Y., Batrel, C., Huet, A., Lenoir, M., Ladrech, S., Desmadryl, G., Nouvian, R., Puel, J.-L., & Wang, J. (2014). Contribution of auditory nerve fibers to compound action potential of the auditory nerve. Journal of Neurophysiology, 112(5), 1025–1039. https://doi.org/10.1152/jn.00738.2013

Bowman, P. D., Rarey, K., Rogers, C., & Goldstein, G. W. (1985). Primary culture of capillary endothelial cells from the spiral ligament and stria vascularis of bovine inner ear. Retention of several endothelial cell properties in vitro. Cell and Tissue Research, 241(3), 479–486. https://doi.org/10.1007/BF00214566

Brandt, A., Striessnig, J., & Moser, T. (2003). CaV1.3 channels are essential for development and presynaptic activity of cochlear inner hair cells. The Journal of Neuroscience: The Official Journal of the Society for Neuroscience, 23(34), 10832–10840. https://doi.org/10.1523/JNEUROSCI.23-34-10832.2003

Bruce, I. C., Sachs, M. B., & Young, E. D. (2003). An auditory-periphery model of the effects of acoustic trauma on auditory nerve responses. The Journal of the Acoustical Society of America, 113(1), 369–388. https://doi.org/10.1121/1.1519544

Budak, M., Grosh, K., Sasmal, A., Corfas, G., Zochowski, M., & Booth, V. (2021). Contrasting mechanisms for hidden hearing loss: Synaptopathy vs myelin defects. PLoS Computational Biology, 17(1), e1008499. https://doi.org/10.1371/journal.pcbi.1008499

Bullen, A., Anderson, L., Bakay, W., & Forge, A. (2018). Localized disorganization of the cochlear inner hair cell synaptic region after noise exposure. Biology Open, 8(1), bio038547. https://doi.org/10.1242/bio.038547

Buran, B. N., Strenzke, N., Neef, A., Gundelfinger, E. D., Moser, T., & Liberman, M. C. (2010). Onset coding is degraded in auditory nerve fibers from mutant mice lacking synaptic ribbons. The Journal of Neuroscience: The Official Journal of the Society for Neuroscience, 30(22), 7587–7597. https://doi.org/10.1523/JNEUROSCI.0389-10.2010

Butler, B., & Lomber, S. (2013). Functional and structural changes throughout the auditory system following congenital and early-onset deafness: Implications for hearing restoration. Frontiers in Systems Neuroscience, 7. https://www.frontiersin.org/articles/10.3389/fnsys.2013.00092

Canlon, B. (1988). The effect of acoustic trauma on the tectorial membrane, stereocilia, and hearing sensitivity: Possible mechanisms underlying damage, recovery, and protection. Scandinavian Audiology. Supplementum, 27, 1–45.

Carricondo, F., & Romero-Gómez, B. (2019). The Cochlear Spiral Ganglion Neurons: The Auditory Portion of the VIII Nerve. The Anatomical Record, 302(3), 463–471. https://doi.org/10.1002/ar.23815

Cederholm, J. M. E., Froud, K. E., Wong, A. C. Y., Ko, M., Ryan, A. F., & Housley, G. D. (2012). Differential actions of isoflurane and ketamine-based anaesthetics on cochlear function in the mouse. Hearing Research, 292(1–2), 71–79. https://doi.org/10.1016/j.heares.2012.08.010

Chapochnikov, N. M., Takago, H., Huang, C.-H., Pangršič, T., Khimich, D., Neef, J., Auge, E., Göttfert, F., Hell, S. W., Wichmann, C., Wolf, F., & Moser, T. (2014). Uniquantal release through a dynamic fusion pore is a candidate mechanism of hair cell exocytosis. Neuron, 83(6), 1389–1403. https://doi.org/10.1016/j.neuron.2014.08.003

Charlesworth, P., Pocock, G., & Richards, C. D. (1994). Calcium channel currents in bovine adrenal chromaffin cells and their modulation by anaesthetic agents. The Journal of Physiology, 481(3), 543–553. https://doi.org/10.1113/jphysiol.1994.sp020462

Chen, F.-Q., Zheng, H.-W., Hill, K., & Sha, S.-H. (2012). Traumatic Noise Activates Rho-Family GTPases through Transient Cellular Energy Depletion. The Journal of Neuroscience, 32(36), 12421–12430. https://doi.org/10.1523/JNEUROSCI.6381-11.2012

Chen, G.-D., McWilliams, M. L., & Fechter, L. D. (1999). Intermittent noise-induced hearing loss and the influence of carbon monoxide. Hearing Research, 138(1), 181–191. https://doi.org/10.1016/S0378-5955(99)00157-4

Chung, J. W., Ahn, J. H., Kim, J. Y., Lee, H. J., Kang, H. H., Lee, Y. K., Kim, J. U., & Koo, S.-W. (2007). The effect of isoflurane, halothane and pentobarbital on noise-induced hearing loss in mice. Anesthesia and Analgesia, 104(6), 1404–1408, table of contents. https://doi.org/10.1213/01.ane.0000261508.24083.6c

Clark, W. W., Bohne, B. A., & Boettcher, F. A. (1987). Effect of periodic rest on hearing loss and cochlear damage following exposure to noise. The Journal of the Acoustical Society of America, 82(4), 1253–1264. https://doi.org/10.1121/1.395261
Comparing the electrophysiological effects of traumatic noise exposure between rodents | Journal of Neurophysiology. (n.d.). Retrieved November 24, 2022, from https://journals.physiology.org/doi/full/10.1152/jn.00081.2021

Conn, P. M. (Ed.). (2008). Sourcebook of models for biomedical research. Humana Press.
Consciousness and Anesthesia | Science. (n.d.). Retrieved March 16, 2023, from https://www.science.org/doi/10.1126/science.1149213

Cooper, N. P. (1998). Harmonic distortion on the basilar membrane in the basal turn of the guinea-pig cochlea. The Journal of Physiology, 509 (Pt 1)(Pt 1), 277–288. https://doi.org/10.1111/j.1469-7793.1998.277bo.x

Costalupes, J. A., Young, E. D., & Gibson, D. J. (1984). Effects of continuous noise backgrounds on rate response of auditory nerve fibers in cat. Journal of Neurophysiology, 51(6), 1326–1344. https://doi.org/10.1152/jn.1984.51.6.1326

Crawford, A. C., & Fettiplace, R. (1981). An electrical tuning mechanism in turtle cochlear hair cells. The Journal of Physiology, 312, 377–412. https://doi.org/10.1113/jphysiol.1981.sp013634

Cui, Y., Sun, G.-W., Yamashita, D., Kanzaki, S., Matsunaga, T., Fujii, M., Kaga, K., & Ogawa, K. (2011). Acoustic overstimulation-induced apoptosis in fibrocytes of the cochlear spiral limbus of mice. European Archives of Oto-Rhino-Laryngology: Official Journal of the European Federation of Oto-Rhino-Laryngological Societies (EUFOS): Affiliated with the German Society for Oto-Rhino-Laryngology - Head and Neck Surgery, 268(7), 973–978. https://doi.org/10.1007/s00405-011-1484-3

Dallos, P., & Harris, D. (1978). Properties of auditory nerve responses in absence of outer hair cells. Journal of Neurophysiology, 41(2), 365–383. https://doi.org/10.1152/jn.1978.41.2.365

Dallos, P., Zheng, J., & Cheatham, M. A. (2006). Prestin and the cochlear amplifier. The Journal of Physiology, 576(Pt 1), 37–42. https://doi.org/10.1113/jphysiol.2006.114652

de Sousa, S. L. M., Dickinson, R., Lieb, W. R., & Franks, N. P. (2000). Contrasting Synaptic Actions of the Inhalational General Anesthetics Isoflurane and Xenon. Anesthesiology, 92(4), 1055–1066. https://doi.org/10.1097/00000542-200004000-00024

Dew, L. A., Owen, R. G., & Mulroy, M. J. (1993). Changes in size and shape of auditory hair cells in vivo during noise-induced temporary threshold shift. Hearing Research, 66(1), 99–107. https://doi.org/10.1016/0378-5955(93)90264-2

Dierich, M., Altoè, A., Koppelmann, J., Evers, S., Renigunta, V., Schäfer, M. K., Naumann, R., Verhulst, S., Oliver, D., & Leitner, M. G. (2020). Optimized Tuning of Auditory Inner Hair Cells to Encode Complex Sound through Synergistic Activity of Six Independent K+ Current Entities. Cell Reports, 32(1), 107869. https://doi.org/10.1016/j.celrep.2020.107869

Differential effects of noise exposure between substrains of CBA mice | Elsevier Enhanced Reader. (n.d.). https://doi.org/10.1016/j.heares.2021.108395

Ding, D. L., Wang, J., Salvi, R., Henderson, D., Hu, B. H., McFadden, S. L., & Mueller, M. (1999). Selective loss of inner hair cells and type-I ganglion neurons in carboplatin-treated chinchillas. Mechanisms of damage and protection. Annals of the New York Academy of Sciences, 884, 152–170. https://doi.org/10.1111/j.1749-6632.1999.tb08640.x

Dynamic loss of surface-expressed AMPA receptors in mouse cortical and striatal neurons during anesthesia—Carino—2012—Journal of Neuroscience Research—Wiley Online Library. (n.d.). Retrieved March 16, 2023, from https://onlinelibrary.wiley.com/doi/10.1002/jnr.22749

Effect of periodic rest on hearing loss and cochlear damage following exposure to noise: The Journal of the Acoustical Society of America: Vol 82, No 4. (n.d.). Retrieved March 18, 2023, from https://asa.scitation.org/doi/10.1121/1.395261

Effects of acoustic trauma on the representation of the vowel /ɛ/ in cat auditory nerve fibers: The Journal of the Acoustical Society of America: Vol 101, No 6. (n.d.). Retrieved March 18, 2023, from https://asa.scitation.org/doi/10.1121/1.418321

Effects of Isoflurane on N-Methyl-D-Aspartate Gated Ion Channels in Cultured Rat Hippocampal Neuronsa—YANG - 1991—Annals of the New York Academy of Sciences—Wiley Online Library. (n.d.). Retrieved March 16, 2023, from https://nyaspubs.onlinelibrary.wiley.com/doi/10.1111/j.1749-6632.1991.tb33851.x

Encoding sound in the cochlea: From receptor potential to afferent discharge. (n.d.). Retrieved February 27, 2023, from https://physoc.onlinelibrary.wiley.com/doi/epdf/10.1113/JP279189

Evans, E. F. (1972). The frequency response and other properties of single fibres in the guinea-pig cochlear nerve. The Journal of Physiology, 226(1), 263–287.

Falasca, V., Greco, A., & Ralli, M. (n.d.). Noise Induced Hearing Loss: The Role of Oxidative Stress.

Fernandez, K. A., Guo, D., Micucci, S., De Gruttola, V., Liberman, M. C., & Kujawa, S. G. (2020). Noise-induced Cochlear Synaptopathy with and Without Sensory Cell Loss. Neuroscience, 427, 43–57. https://doi.org/10.1016/j.neuroscience.2019.11.051

Fernandez, K. A., Jeffers, P. W. C., Lall, K., Liberman, M. C., & Kujawa, S. G. (2015). Aging after noise exposure: Acceleration of cochlear synaptopathy in "recovered" ears. The Journal of Neuroscience: The Official Journal of the Society for Neuroscience, 35(19), 7509–7520. https://doi.org/10.1523/JNEUROSCI.5138-14.2015

Fernandez, K. A., Watabe, T., Tong, M., Meng, X., Tani, K., Kujawa, S. G., & Edge, A. S. (2021). Trk agonist drugs rescue noise-induced hidden hearing loss. JCI Insight, 6(3). https://doi.org/10.1172/jci.insight.142572

Fetoni, A. R., De Bartolo, P., Eramo, S. L. M., Rolesi, R., Paciello, F., Bergamini, C., Fato, R., Paludetti, G., Petrosini, L., & Troiani, D. (2013). Noise-induced hearing loss (NIHL) as a target of oxidative stress-mediated damage: Cochlear and cortical responses after an increase in antioxidant defense. The Journal of Neuroscience: The Official Journal of the Society for Neuroscience, 33(9), 4011–4023. https://doi.org/10.1523/JNEUROSCI.2282-12.2013

Fettiplace, R. (2017). Hair Cell Transduction, Tuning, and Synaptic Transmission in the Mammalian Cochlea. In Comprehensive Physiology (pp. 1197–1227). John Wiley & Sons, Ltd. https://doi.org/10.1002/cphy.c160049

Fettiplace, R., & Fuchs, P. A. (1999). Mechanisms of hair cell tuning. Annual Review of Physiology, 61, 809–834. https://doi.org/10.1146/annurev.physiol.61.1.809

Fine structure of the intracochlear potential field. I. The silent current. - PMC. (n.d.). Retrieved March 15, 2023, from https://www.ncbi.nlm.nih.gov/pmc/articles/PMC1280835/

Flores, E. N., Duggan, A., Madathany, T., Hogan, A. K., Márquez, F. G., Kumar, G., Seal, R. P., Edwards, R. H., Liberman, M. C., & García-Añoveros, J. (2015). A non-canonical pathway from cochlea to brain signals tissue-damaging noise. Current Biology: CB, 25(5), 606–612. https://doi.org/10.1016/j.cub.2015.01.009

Forsythe, I. D. (2007). A fantasia on Kölliker's organ. Nature, 450(7166), Article 7166. https://doi.org/10.1038/450043a

Fowler, T., Canlon, B., Dolan, D., & Miller, J. M. (1995). The effect of noise trauma following training exposures in the mouse. Hearing Research, 88(1), 1–13. https://doi.org/10.1016/0378-5955(95)00062-9

Franks, N. P., & Lieb, W. R. (1991). Stereospecific Effects of Inhalational General Anesthetic Optical Isomers on Nerve Ion Channels. Science, 254(5030), 427–430. https://doi.org/10.1126/science.1925602

Frenzilli, G., Ryskalin, L., Ferrucci, M., Cantafora, E., Chelazzi, S., Giorgi, F. S., Lenzi, P., Scarcelli, V., Frati, A., Biagioni, F., Gambardella, S., Falleni, A., & Fornai, F. (2017). Loud Noise Exposure Produces DNA, Neurotransmitter and Morphological Damage within Specific Brain Areas. Frontiers in Neuroanatomy, 11. https://www.frontiersin.org/articles/10.3389/fnana.2017.00049

Fuchs, P. A. (2014). A "calcium capacitor" shapes cholinergic inhibition of cochlear hair cells. The Journal of Physiology, 592(16), 3393–3401. https://doi.org/10.1113/jphysiol.2013.267914

Fuchs, P. A., & Lauer, A. M. (2019). Efferent Inhibition of the Cochlea. Cold Spring Harbor Perspectives in Medicine, 9(5), a033530. https://doi.org/10.1101/cshperspect.a033530

Functional subgroups of cochlear inner hair cell ribbon synapses differently modulate their EPSC properties in response to stimulation. (n.d.). Journal of Neurophysiology. https://doi.org/10.1152/jn.00452.2020

Furman, A. C., Kujawa, S. G., & Liberman, M. C. (2013a). Noise-induced cochlear neuropathy is selective for fibers with low spontaneous rates. Journal of Neurophysiology, 110(3), 577–586. https://doi.org/10.1152/jn.00164.2013

Furman, A. C., Kujawa, S. G., & Liberman, M. C. (2013b). Noise-induced cochlear neuropathy is selective for fibers with low spontaneous rates. Journal of Neurophysiology, 110(3), 577–586. https://doi.org/10.1152/jn.00164.2013

Geisler, C. D. (1998). From Sound to Synapse: Physiology of the Mammalian Ear. Oxford University Press.

Geisler, C. D., & Rhode, W. S. (1982). The phases of basilar-membrane vibrations. The Journal of the Acoustical Society of America, 71(5), 1201–1203. https://doi.org/10.1121/1.387768

Grabner, C. P., & Moser, T. (2018). Individual synaptic vesicles mediate stimulated exocytosis from cochlear inner hair cells. Proceedings of the National Academy of Sciences of the United States of America, 115(50), 12811–12816. https://doi.org/10.1073/pnas.1811814115

Grant, L., Yi, E., & Glowatzki, E. (2010). Two Modes of Release Shape the Postsynaptic Response at the Inner Hair Cell Ribbon Synapse. Journal of Neuroscience, 30(12), 4210–4220. https://doi.org/10.1523/JNEUROSCI.4439-09.2010

Graydon, C. W., Cho, S., Li, G.-L., Kachar, B., & Gersdorff, H. von. (2011). Sharp Ca2+ Nanodomains beneath the Ribbon Promote Highly Synchronous Multivesicular Release at Hair Cell Synapses. Journal of Neuroscience, 31(46), 16637–16650. https://doi.org/10.1523/JNEUROSCI.1866-11.2011

Greenberg, S. (1988). Acoustic transduction in the auditory periphery. Journal of Phonetics, 16(1), 3–17. https://doi.org/10.1016/S0095-4470(19)30463-2

Guo, C., & Ma, Y.-Y. (2021). Calcium Permeable-AMPA Receptors and Excitotoxicity in Neurological Disorders. Frontiers in Neural Circuits, 15. https://www.frontiersin.org/articles/10.3389/fncir.2021.711564

Haas, L. (1995). Reprints available directly from the publisher Photocopying permitted by license only. Review of Education, Pedagogy, and Cultural Studies, 17(1), 1–6. https://doi.org/10.1080/1071441950170102

Hackney, C. M., Mahendrasingam, S., Penn, A., & Fettiplace, R. (2005). The concentrations of calcium buffering proteins in mammalian cochlear hair cells. The Journal of Neuroscience: The Official Journal of the Society for Neuroscience, 25(34), 7867–7875. https://doi.org/10.1523/JNEUROSCI.1196-05.2005

Hagan, C. E., Pearce, R. A., Trudell, J. R., & MacIver, M. B. (1998). Concentration measures of volatile anesthetics in the aqueous phase using calcium sensitive electrodes. Journal of Neuroscience Methods, 81(1–2), 177–184. https://doi.org/10.1016/S0165-0270(98)00029-6

Hakuba, N., Koga, K., Gyo, K., Usami, S., & Tanaka, K. (2000). Exacerbation of Noise-Induced Hearing Loss in Mice Lacking the Glutamate Transporter GLAST. Journal of Neuroscience, 20(23), 8750–8753. https://doi.org/10.1523/JNEUROSCI.20-23-08750.2000

Hamernik, R. P., Turrentine, G., Roberto, M., Salvi, R., & Henderson, D. (1984). Anatomical correlates of impulse noise-induced mechanical damage in the cochlea. Hearing Research, 13(3), 229–247. https://doi.org/10.1016/0378-5955(84)90077-7

Han, E., Lee, D. H., Park, S., Rah, Y. C., Park, H.-C., Choi, J. W., & Choi, J. (2022). Noise-induced hearing loss in zebrafish model: Characterization of tonotopy and sex-based differences. Hearing Research, 418, 108485. https://doi.org/10.1016/j.heares.2022.108485

Hao, X., Ou, M., Zhang, D., Zhao, W., Yang, Y., Liu, J., Yang, H., Zhu, T., Li, Y., & Zhou, C. (2020). The Effects of General Anesthetics on Synaptic Transmission. Current Neuropharmacology, 18(10), 936–965. https://doi.org/10.2174/1570159X18666200227125854

Harris, T., Shahidullah, M., Ellingson, J. S., & Covarrubias, M. (2000). General Anesthetic Action at an Internal Protein Site Involving the S4-S5 Cytoplasmic Loop of a Neuronal K+Channel *. Journal of Biological Chemistry, 275(7), 4928–4936. https://doi.org/10.1074/jbc.275.7.4928

Hashimoto, K., Hickman, T. T., Suzuki, J., Ji, L., Kohrman, D. C., Corfas, G., & Liberman, M. C. (2019). Protection from noise-induced cochlear synaptopathy by virally mediated overexpression of NT3. Scientific Reports, 9(1), 15362. https://doi.org/10.1038/s41598-019-51724-6

Heeringa, A. N., Zhang, L., Ashida, G., Beutelmann, R., Steenken, F., & Köppl, C. (2020). Temporal Coding of Single Auditory Nerve Fibers Is Not Degraded in Aging Gerbils. The Journal of Neuroscience, 40(2), 343–354. https://doi.org/10.1523/JNEUROSCI.2784-18.2019

Heinrich, U. R., Maurer, J., & Mann, W. (1999). Ultrastructural evidence for protection of the outer hair cells of the inner ear during intense noise exposure by application of the organic calcium channel blocker diltiazem. ORL; Journal for Oto-Rhino-Laryngology and Its Related Specialties, 61(6), 321–327. https://doi.org/10.1159/000027693

Heinz, M. G., & Young, E. D. (2004). Response Growth With Sound Level in Auditory-Nerve Fibers After Noise-Induced Hearing Loss. Journal of Neurophysiology, 91(2), 784–795. https://doi.org/10.1152/jn.00776.2003

Hemmings, H. C. (2009). Sodium channels and the synaptic mechanisms of inhaled anaesthetics. British Journal of Anaesthesia, 103(1), 61–69. https://doi.org/10.1093/bja/aep144

Herold, K. F., Nau, C., Ouyang, W., & Hemmings, H. C. (2009). Isoflurane Inhibits the Tetrodotoxin-resistant Voltagegated Sodium Channel Nav1.8. Anesthesiology, 111(3), 591–599. https://doi.org/10.1097/ALN.0b013e3181af64d4

Heshmat, A., Sajedi, S., Johnson Chacko, L., Fischer, N., Schrott-Fischer, A., & Rattay, F. (2020). Dendritic Degeneration of Human Auditory Nerve Fibers and Its Impact on the Spiking Pattern Under Regular Conditions and During Cochlear Implant Stimulation. Frontiers in Neuroscience, 14. https://www.frontiersin.org/articles/10.3389/fnins.2020.599868

Hickman, T. T., Hashimoto, K., Liberman, L. D., & Liberman, M. C. (2020). Synaptic migration and reorganization after noise exposure suggests regeneration in a mature mammalian cochlea. Scientific Reports, 10. https://doi.org/10.1038/s41598-020-76553-w

Hofman, P. M., Van Riswick, J. G. A., & Van Opstal, A. J. (1998). Relearning sound localization with new ears. Nature Neuroscience, 1(5), Article 5. https://doi.org/10.1038/1633

Hossain, W. A., Antic, S. D., Yang, Y., Rasband, M. N., & Morest, D. K. (2005). Where Is the Spike Generator of the Cochlear Nerve? Voltage-Gated Sodium Channels in the Mouse Cochlea. The Journal of Neuroscience, 25(29), 6857–6868. https://doi.org/10.1523/JNEUROSCI.0123-05.2005

Hu, B. H., Guo, W., Wang, P. Y., Henderson, D., & Jiang, S. C. (2000). Intense noise-induced apoptosis in hair cells of guinea pig cochleae. Acta Oto-Laryngologica, 120(1), 19–24.

Hu, N., Rutherford, M. A., & Green, S. H. (2020). Protection of cochlear synapses from noise-induced excitotoxic trauma by blockade of Ca2+-permeable AMPA receptors. Proceedings of the National Academy of Sciences of the United States of America, 117(7), 3828–3838. https://doi.org/10.1073/pnas.1914247117

Huang, M., Kantardzhieva, A., Scheffer, D., Liberman, M. C., & Chen, Z.-Y. (2013). Hair cell overexpression of Islet1 reduces age-related and noise-induced hearing loss. The Journal of Neuroscience: The Official Journal of the Society for Neuroscience, 33(38), 15086–15094. https://doi.org/10.1523/JNEUROSCI.1489-13.2013

Hudspeth, A. J., & Corey, D. P. (1977). Sensitivity, polarity, and conductance change in the response of vertebrate hair cells to controlled mechanical stimuli. Proceedings of the National Academy of Sciences of the United States of America, 74(6), 2407–2411. https://doi.org/10.1073/pnas.74.6.2407

Huet, A., Batrel, C., Wang, J., Desmadryl, G., Nouvian, R., Puel, J. L., & Bourien, J. (2019). Sound Coding in the Auditory Nerve: From Single Fiber Activity to Cochlear Mass Potentials in Gerbils. Neuroscience, 407, 83–92. https://doi.org/10.1016/j.neuroscience.2018.10.010

Hunt, D. L., & Castillo, P. E. (2012). Synaptic plasticity of NMDA receptors: Mechanisms and functional implications. Current Opinion in Neurobiology, 22(3), 496–508. https://doi.org/10.1016/j.conb.2012.01.007

Isoflurane, But Not the Nonimmobilizers F6 and F8, Inhibits Rat Spinal Cord Motor Neuron CaV1 Calcium Currents—PMC. (n.d.). Retrieved October 11, 2022, from https://www.ncbi.nlm.nih.gov/pmc/articles/PMC4760920/

Isoflurane modulates activation and inactivation gating of the prokaryotic Na+ channel NaChBac—PMC. (n.d.). Retrieved March 15, 2023, from https://www.ncbi.nlm.nih.gov/pmc/articles/PMC5460948/

Israel, M. R., Tanaka, B. S., Castro, J., Thongyoo, P., Robinson, S. D., Zhao, P., Deuis, J. R., Craik, D. J., Durek, T., Brierley, S. M., Waxman, S. G., Dib-Hajj, S. D., & Vetter, I. (2019). NaV 1.6 regulates excitability of mechanosensitive sensory neurons. The Journal of Physiology, 597(14), 3751–3768. https://doi.org/10.1113/JP278148

Javel, E., & Mott, J. B. (1988). Physiological and psychophysical correlates of temporal processes in hearing. Hearing Research, 34(3), 275–294. https://doi.org/10.1016/0378-5955(88)90008-1

Jean, P., Anttonen, T., Michanski, S., de Diego, A. M. G., Steyer, A. M., Neef, A., Oestreicher, D., Kroll, J., Nardis, C., Pangršič, T., Möbius, W., Ashmore, J., Wichmann, C., & Moser, T. (2020). Macromolecular and electrical coupling between inner hair cells in the rodent cochlea. Nature Communications, 11(1), Article 1. https://doi.org/10.1038/s41467-020-17003-z

Jeffers, P. W. C., Bourien, J., Diuba, A., Puel, J.-L., & Kujawa, S. G. (2021). Noise-Induced Hearing Loss in Gerbil: Round Window Assays of Synapse Loss. Frontiers in Cellular Neuroscience, 15. https://www.frontiersin.org/articles/10.3389/fncel.2021.699978

Jeng, J.-Y., Ceriani, F., Hendry, A., Johnson, S. L., Yen, P., Simmons, D. D., Kros, C. J., & Marcotti, W. (2020). Hair cell maturation is differentially regulated along the tonotopic axis of the mammalian cochlea. The Journal of Physiology, 598(1), 151–170. https://doi.org/10.1113/JP279012

Jensen, J. B., Lysaght, A. C., Liberman, M. C., Qvortrup, K., & Stankovic, K. M. (2015). Immediate and delayed cochlear neuropathy after noise exposure in pubescent mice. PloS One, 10(5), e0125160. https://doi.org/10.1371/journal.pone.0125160

Jia, F., Yue, M., Chandra, D., Homanics, G. E., Goldstein, P. A., & Harrison, N. L. (2008). Isoflurane is a potent modulator of extrasynaptic GABA(A) receptors in the thalamus. The Journal of Pharmacology and Experimental Therapeutics, 324(3), 1127–1135. https://doi.org/10.1124/jpet.107.134569

Johnson, S. L., Eckrich, T., Kuhn, S., Zampini, V., Franz, C., Ranatunga, K. M., Roberts, T. P., Masetto, S., Knipper, M., Kros, C. J., & Marcotti, W. (2011). Position-dependent patterning of spontaneous action potentials in immature cochlear inner hair cells. Nature Neuroscience, 14(6), 711–717. https://doi.org/10.1038/nn.2803

Johnson, S. L., Forge, A., Knipper, M., Münkner, S., & Marcotti, W. (2008). Tonotopic variation in the calcium dependence of neurotransmitter release and vesicle pool replenishment at mammalian auditory ribbon synapses. The Journal of Neuroscience: The Official Journal of the Society for Neuroscience, 28(30), 7670–7678. https://doi.org/10.1523/JNEUROSCI.0785-08.2008

Johnson, S. L., Franz, C., Knipper, M., & Marcotti, W. (2009). Functional maturation of the exocytotic machinery at gerbil hair cell ribbon synapses. The Journal of Physiology, 587(Pt 8), 1715–1726. https://doi.org/10.1113/jphysiol.2009.168542

Johnson, S. L., & Marcotti, W. (2008). Biophysical properties of CaV1.3 calcium channels in gerbil inner hair cells. The Journal of Physiology, 586(4), 1029–1042. https://doi.org/10.1113/jphysiol.2007.145219

Johnsson, L.-G. (1974). Sequence of Degeneration of Corti's Organ and its First-Order Neurons. Annals of Otology, Rhinology & Laryngology, 83(3), 294–303. https://doi.org/10.1177/000348947408300303

Johnsson, L.-G., & Hawkins, J. E. (1972). Sensory and Neural Degeneration with Aging, as Seen in Microdissections of the Human Inner Ear. Annals of Otology, Rhinology & Laryngology, 81(2), 179–193. https://doi.org/10.1177/000348947208100203

Joiner, M. A., & Lee, A. (2015). Voltage-Gated Cav1 Channels in Disorders of Vision and Hearing. Current Molecular Pharmacology, 8(2), 143–148. https://doi.org/10.2174/1874467208666150507104937

Kalluri, R., & Monges-Hernandez, M. (2017). Spatial Gradients in the Size of Inner Hair Cell Ribbons Emerge Before the Onset of Hearing in Rats. JARO: Journal of the Association for Research in Otolaryngology, 18(3), 399–413. https://doi.org/10.1007/s10162-017-0620-1

Kameyama, K., Aono, K., & Kitamura, K. (1999). Isoflurane inhibits neuronal Ca2+ channels through enhancement of current inactivation. British Journal of Anaesthesia, 82(3), 402–411. https://doi.org/10.1093/bja/82.3.402

Keen, E. C., & Hudspeth, A. J. (2006). Transfer characteristics of the hair cell's afferent synapse. Proceedings of the National Academy of Sciences of the United States of America, 103(14), 5537–5542. https://doi.org/10.1073/pnas.0601103103

Keller, S., Polanski, W. H., Enzensperger, C., Reichmann, H., Hermann, A., & Gille, G. (2020). 9-Methyl-β-carboline inhibits monoamine oxidase activity and stimulates the expression of neurotrophic factors by astrocytes. Journal of Neural Transmission, 127(7), 999–1012. https://doi.org/10.1007/s00702-020-02189-9

Kemp, D. T. (2002). Otoacoustic emissions, their origin in cochlear function, and use. British Medical Bulletin, 63, 223–241. https://doi.org/10.1093/bmb/63.1.223

Kerr, A. G., & Byrne, J. E. (1975). Concussive effects of bomb blast on the ear. The Journal of Laryngology and Otology, 89(2), 131–143. https://doi.org/10.1017/s002221510008018x

Khimich, D., Nouvian, R., Pujol, R., tom Dieck, S., Egner, A., Gundelfinger, E. D., & Moser, T. (2005). Hair cell synaptic ribbons are essential for synchronous auditory signalling. Nature, 434(7035), Article 7035. https://doi.org/10.1038/nature03418

Kiang, N. Y., Moxon, E. C., & Levine, R. A. (1970). Auditory-nerve activity in cats with normal and abnormal cochleas. In: Sensorineural hearing loss. Ciba Foundation Symposium, 241–273. https://doi.org/10.1002/9780470719756.ch15

Kim, J. U., Lee, H. J., Kang, H. H., Shin, J. W., Ku, S. W., Ahn, J. H., Kim, Y. J., & Chung, J. W. (2005). Protective Effect of Isoflurane Anesthesia on Noise-Induced Hearing Loss in Mice: The Laryngoscope, 115(11), 1996–1999. https://doi.org/10.1097/01.mlg.0000180173.81034.4d

Kim, K. X., Payne, S., Yang-Hood, A., Li, S.-Z., Davis, B., Carlquist, J., V-Ghaffari, B., Gantz, J. A., Kallogjeri, D., Fitzpatrick, J. A. J., Ohlemiller, K. K., Hirose, K., & Rutherford, M. A. (2019). Vesicular Glutamatergic Transmission in Noise-Induced Loss and Repair of Cochlear Ribbon Synapses. Journal of Neuroscience, 39(23), 4434–4447. https://doi.org/10.1523/JNEUROSCI.2228-18.2019

Kim, K. X., & Rutherford, M. A. (2016). Maturation of NaV and KV Channel Topographies in the Auditory Nerve Spike Initiator before and after Developmental Onset of Hearing Function. The Journal of Neuroscience: The Official Journal of the Society for Neuroscience, 36(7), 2111–2118. https://doi.org/10.1523/JNEUROSCI.3437-15.2016

Kim, W. B., Kang, K.-W., Sharma, K., & Yi, E. (2020). Distribution of Kv3 Subunits in Cochlear Afferent and Efferent Nerve Fibers Implies Distinct Role in Auditory Processing. Experimental Neurobiology, 29(5), 344–355. https://doi.org/10.5607/en20043

Kimbro, J. R., Kelly, P. J., Drummond, J. C., Cole, D. J., & Patel, P. M. (2000). Isoflurane and pentobarbital reduce AMPA toxicity in vivo in the rat cerebral cortex. Anesthesiology, 92(3), 806–812. https://doi.org/10.1097/00000542-200003000-00024

Kk, O., Js, W., & Ll, D. (1999). Early elevation of cochlear reactive oxygen species following noise exposure. Audiology & Neuro-Otology, 4(5). https://doi.org/10.1159/000013846

Klein, A. J., Mills, J. H., & Adkins, W. Y. (1990). Upward spread of masking, hearing loss, and speech recognition in young and elderly listeners. The Journal of the Acoustical Society of America, 87(3), 1266–1271. https://doi.org/10.1121/1.398802

Kobel, M., Le Prell, C. G., Liu, J., Hawks, J. W., & Bao, J. (2017). Noise-induced cochlear synaptopathy: Past findings and future studies. Hearing Research, 349, 148–154. https://doi.org/10.1016/j.heares.2016.12.008

Kong, J.-H., Adelman, J. P., & Fuchs, P. A. (2008). Expression of the SK2 calcium-activated potassium channel is required for cholinergic function in mouse cochlear hair cells. The Journal of Physiology, 586(22), 5471–5485. https://doi.org/10.1113/jphysiol.2008.160077

Kopke, R. D., Weisskopf, P. A., Boone, J. L., Jackson, R. L., Wester, D. C., Hoffer, M. E., Lambert, D. C., Charon, C. C., Ding, D.-L., & McBride, D. (2000). Reduction of noise-induced hearing loss using L-NAC and salicylate in the chinchilla11The views expressed in this article are those of the authors and do not reflect the official policy or position of the Department of the Army, Department of the Navy, Department of Defense, or the United States Government. Hearing Research, 149(1), 138–146. https://doi.org/10.1016/S0378-5955(00)00176-3

Kotani, N., & Akaike, N. (2013). The effects of volatile anesthetics on synaptic and extrasynaptic GABA-induced neurotransmission. Brain Research Bulletin, 93, 69–79. https://doi.org/10.1016/j.brainresbull.2012.08.001

Kubisch, C., Schroeder, B. C., Friedrich, T., Lütjohann, B., El-Amraoui, A., Marlin, S., Petit, C., & Jentsch, T. J. (1999). KCNQ4, a novel potassium channel expressed in sensory outer hair cells, is mutated in dominant deafness. Cell, 96(3), 437–446. https://doi.org/10.1016/s0092-8674(00)80556-5

Kujawa, S. G., & Liberman, M. C. (2006). Acceleration of age-related hearing loss by early noise exposure: Evidence of a misspent youth. The Journal of Neuroscience: The Official Journal of the Society for Neuroscience, 26(7), 2115–2123. https://doi.org/10.1523/JNEUROSCI.4985-05.2006

Kujawa, S. G., & Liberman, M. C. (2009). Adding insult to injury: Cochlear nerve degeneration after "temporary" noise-induced hearing loss. The Journal of Neuroscience: The Official Journal of the Society for Neuroscience, 29(45), 14077–14085. https://doi.org/10.1523/JNEUROSCI.2845-09.2009

Kujawa, S. G., & Liberman, M. C. (2015). Synaptopathy in the noise-exposed and aging cochlea: Primary neural degeneration in acquired sensorineural hearing loss. Hearing Research, 330(Pt B), 191–199. https://doi.org/10.1016/j.heares.2015.02.009

Kujawa, S. G., & Liberman, M. C. (2019). Translating animal models to human therapeutics in noise-induced and age-related hearing loss. Hearing Research, 377, 44–52. https://doi.org/10.1016/j.heares.2019.03.003

Labro, A. J., Priest, M. F., Lacroix, J. J., Snyders, D. J., & Bezanilla, F. (2015). Kv3.1 uses a timely resurgent K+ current to secure action potential repolarization. Nature Communications, 6(1), Article 1. https://doi.org/10.1038/ncomms10173

Le Prell, C. G., Yamashita, D., Minami, S. B., Yamasoba, T., & Miller, J. M. (2007). Mechanisms of Noise-Induced Hearing Loss Indicate Multiple Methods of Prevention. Hearing Research, 226(1–2), 22–43. https://doi.org/10.1016/j.heares.2006.10.006

Lee, S.-Y., Han, J. J., Lee, S.-Y., Jung, G., Min, H. J., Song, J.-J., & Koo, J.-W. (2020). Outcomes of Peptide Vaccine GV1001 Treatment in a Murine Model of Acute Noise-Induced Hearing Loss. Antioxidants (Basel, Switzerland), 9(2). https://doi.org/10.3390/antiox9020112

Lesica, N. A. (2018). Why do hearing aids fail to restore normal auditory perception? Trends in Neurosciences, 41(4), 174–185. https://doi.org/10.1016/j.tins.2018.01.008

Levic, S. (2022). SK Current, Expressed During the Development and Regeneration of Chick Hair Cells, Contributes to the Patterning of Spontaneous Action Potentials. Frontiers in Cellular Neuroscience, 15. https://www.frontiersin.org/articles/10.3389/fncel.2021.766264

Li, J., Zheng, S., & Zuo, Z. (2002). Isoflurane decreases AMPA-induced dark cell degeneration and edematous damage of Purkinje neurons in the rat cerebellar slices. Brain Research, 958(2), 399–404. https://doi.org/10.1016/s0006-8993(02)03700-9

Liberman, L. D., Wang, H., & Liberman, M. C. (2011). Opposing gradients of ribbon size and AMPA receptor expression underlie sensitivity differences among cochlear-nerve/hair-cell synapses. The Journal of Neuroscience: The Official Journal of the Society for Neuroscience, 31(3), 801–808. https://doi.org/10.1523/JNEUROSCI.3389-10.2011

Liberman, M. C. (1982). Single-Neuron Labeling in the Cat Auditory Nerve. Science, 216(4551), 1239–1241. https://doi.org/10.1126/science.7079757

Liberman, M. C. (2015). HIDDEN HEARING LOSS. Scientific American, 313(2), 48–53. https://doi.org/10.1038/scientificamerican0815-48

Liberman, M. C. (2016). Noise-Induced Hearing Loss: Permanent Versus Temporary Threshold Shifts and the Effects of Hair Cell Versus Neuronal Degeneration. Advances in Experimental Medicine and Biology, 875, 1–7. https://doi.org/10.1007/978-1-4939-2981-8_1

Liberman, M. C. (2017). Noise-induced and age-related hearing loss: New perspectives and potential therapies. F1000Research, 6, 927. https://doi.org/10.12688/f1000research.11310.1

Liberman, M. C., & Beil, D. G. (1979). Hair cell condition and auditory nerve response in normal and noise-damaged cochleas. Acta Oto-Laryngologica, 88(3–4), 161–176. https://doi.org/10.3109/00016487909137156

Liberman, M. C., & Dodds, L. W. (1984). Single-neuron labeling and chronic cochlear pathology. III. Stereocilia damage and alterations of threshold tuning curves. Hearing Research, 16(1), 55–74. https://doi.org/10.1016/0378-5955(84)90025-x

Liberman, M. C., Epstein, M. J., Cleveland, S. S., Wang, H., & Maison, S. F. (2016). Toward a Differential Diagnosis of Hidden Hearing Loss in Humans. PloS One, 11(9), e0162726. https://doi.org/10.1371/journal.pone.0162726

Liberman, M. C., & Kiang, N. Y. (1978). Acoustic trauma in cats. Cochlear pathology and auditory-nerve activity. Acta Oto-Laryngologica. Supplementum, 358, 1–63.

Liberman, M. C., & Kujawa, S. G. (2017). Cochlear synaptopathy in acquired sensorineural hearing loss: Manifestations and mechanisms. Hearing Research, 349, 138–147. https://doi.org/10.1016/j.heares.2017.01.003

Liberman, M. C., Liberman, L. D., & Maison, S. F. (2015). Chronic Conductive Hearing Loss Leads to Cochlear Degeneration. PloS One, 10(11), e0142341. https://doi.org/10.1371/journal.pone.0142341

Lin, H. W., Furman, A. C., Kujawa, S. G., & Liberman, M. C. (2011). Primary neural degeneration in the Guinea pig cochlea after reversible noise-induced threshold shift. Journal of the Association for Research in Otolaryngology: JARO, 12(5), 605–616. https://doi.org/10.1007/s10162-011-0277-0

Lingle, C. J., Martinez-Espinosa, P. L., Yang-Hood, A., Boero, L. E., Payne, S., Persic, D., V-Ghaffari, B., Xiao, M., Zhou, Y., Xia, X.-M., Pyott, S. J., & Rutherford, M. A. (2019). LRRC52 regulates BK channel function and localization in mouse cochlear inner hair cells. Proceedings of the National Academy of Sciences of the United States of America, 116(37), 18397–18403. https://doi.org/10.1073/pnas.1907065116

Liu, H., Lu, J., Wang, Z., Song, L., Wang, X., Li, G.-L., & Wu, H. (2019). Functional alteration of ribbon synapses in inner hair cells by noise exposure causing hidden hearing loss. Neuroscience Letters, 707, 134268. https://doi.org/10.1016/j.neulet.2019.05.022

Liu, H., Peng, H., Wang, L., Xu, P., Wang, Z., Liu, H., & Wu, H. (2020). Differences in Calcium Clearance at Inner Hair Cell Active Zones May Underlie the Difference in Susceptibility to Noise-Induced Cochlea Synaptopathy of C57BL/6J and CBA/CaJ Mice. Frontiers in Cell and Developmental Biology, 8, 635201. https://doi.org/10.3389/fcell.2020.635201

Lobarinas, E., Salvi, R., & Ding, D. (2013). Insensitivity of the Audiogram to Carboplatin Induced Inner hair cell loss in Chinchillas. Hearing Research, 0, 113–120. https://doi.org/10.1016/j.heares.2013.03.012

Locher, H., de Groot, J. C. M. J., van Iperen, L., Huisman, M. A., Frijns, J. H. M., & Chuva de Sousa Lopes, S. M. (2015). Development of the stria vascularis and potassium regulation in the human fetal cochlea: Insights into hereditary sensorineural hearing loss. Developmental Neurobiology, 75(11), 1219–1240. https://doi.org/10.1002/dneu.22279

L-type voltage-gated calcium channel agonists improve hearing loss and modify ribbon synapse morphology in the zebrafish model of Usher Syndrome Type 1 | bioRxiv. (n.d.). Retrieved February 7, 2023, from https://www.biorxiv.org/content/10.1101/2019.12.16.878231v2.full

Ma, R., Nc, R., A, R., Ss, N., & L, R. (1997). Basilar-membrane responses to tones at the base of the chinchilla cochlea. The Journal of the Acoustical Society of America, 101(4). https://doi.org/10.1121/1.418265

MacIver, M. B. (2014). Anesthetic Agent-Specific Effects on Synaptic Inhibition. Anesthesia and Analgesia, 119(3), 558–569. https://doi.org/10.1213/ANE.0000000000000321

MacIver, M. B., Mikulec, A. A., Amagasu, S. M., & Monroe, F. A. (1996). Volatile anesthetics depress glutamate transmission via presynaptic actions. Anesthesiology, 85(4), 823–834. https://doi.org/10.1097/00000542-199610000-00018

Maison, S. F., Liu, X.-P., Vetter, D. E., Eatock, R. A., Nathanson, N. M., Wess, J., & Liberman, M. C. (2010). Muscarinic signaling in the cochlea: Presynaptic and postsynaptic effects on efferent feedback and afferent excitability. The Journal of Neuroscience: The Official Journal of the Society for Neuroscience, 30(19), 6751–6762. https://doi.org/10.1523/JNEUROSCI.5080-09.2010

Maison, S. F., Rosahl, T. W., Homanics, G. E., & Liberman, M. C. (2006). Functional Role of GABAergic Innervation of the Cochlea: Phenotypic Analysis of Mice Lacking GABAA Receptor Subunits α1, α2, α5, α6, β2, β3, or δ. The Journal of Neuroscience, 26(40), 10315–10326. https://doi.org/10.1523/JNEUROSCI.2395-06.2006

Maison, S. F., Usubuchi, H., & Liberman, M. C. (2013). Efferent feedback minimizes cochlear neuropathy from moderate noise exposure. The Journal of Neuroscience: The Official Journal of the Society for Neuroscience, 33(13), 5542–5552. https://doi.org/10.1523/JNEUROSCI.5027-12.2013

Makary, C. A., Shin, J., Kujawa, S. G., Liberman, M. C., & Merchant, S. N. (2011). Age-related primary cochlear neuronal degeneration in human temporal bones. Journal of the Association for Research in Otolaryngology: JARO, 12(6), 711–717. https://doi.org/10.1007/s10162-011-0283-2

Mammano, F., & Ashmore, J. F. (1996). Differential expression of outer hair cell potassium currents in the isolated cochlea of the guinea-pig. The Journal of Physiology, 496 (Pt 3)(Pt 3), 639–646. https://doi.org/10.1113/jphysiol.1996.sp021715

Mammano, F., Bortolozzi, M., Ortolano, S., & Anselmi, F. (2007). Ca2+ Signaling in the Inner Ear. Physiology, 22(2), 131–144. https://doi.org/10.1152/physiol.00040.2006

Mao, H., & Chen, Y. (2021). Noise-Induced Hearing Loss: Updates on Molecular Targets and Potential Interventions. Neural Plasticity, 2021, e4784385. https://doi.org/10.1155/2021/4784385

Marcotti, W., Johnson, S. L., Holley, M. C., & Kros, C. J. (2003). Developmental changes in the expression of potassium currents of embryonic, neonatal and mature mouse inner hair cells. The Journal of Physiology, 548(Pt 2), 383–400. https://doi.org/10.1113/jphysiol.2002.034801

Marcotti, W., Johnson, S. L., & Kros, C. J. (2004a). Effects of intracellular stores and extracellular Ca(2+) on Ca(2+)-activated K(+) currents in mature mouse inner hair cells. The Journal of Physiology, 557(Pt 2), 613–633. https://doi.org/10.1113/jphysiol.2003.060137

Marcotti, W., Johnson, S. L., & Kros, C. J. (2004b). A transiently expressed SK current sustains and modulates action potential activity in immature mouse inner hair cells. The Journal of Physiology, 560(Pt 3), 691–708. https://doi.org/10.1113/jphysiol.2004.072868

Martelletti, E., Ingham, N. J., Houston, O., Pass, J. C., Chen, J., Marcotti, W., & Steel, K. P. (2020). Synaptojanin2 Mutation Causes Progressive High-frequency Hearing Loss in Mice. Frontiers in Cellular Neuroscience, 14, 561857. https://doi.org/10.3389/fncel.2020.561857

McClaskey, C. M., Dias, J. W., Schmiedt, R. A., Dubno, J. R., & Harris, K. C. (2022). Evidence for Loss of Activity in Low-Spontaneous-Rate Auditory Nerve Fibers of Older Adults. Journal of the Association for Research in Otolaryngology: JARO, 23(2), 273–284. https://doi.org/10.1007/s10162-021-00827-x

Mehraei, G., Hickox, A. E., Bharadwaj, H. M., Goldberg, H., Verhulst, S., Liberman, M. C., & Shinn-Cunningham, B. G. (2016). Auditory Brainstem Response Latency in Noise as a Marker of Cochlear Synaptopathy. The Journal of Neuroscience: The Official Journal of the Society for Neuroscience, 36(13), 3755–3764. https://doi.org/10.1523/JNEUROSCI.4460-15.2016

Melcher, J. R., & Kiang, N. Y. (1996). Generators of the brainstem auditory evoked potential in cat. III: Identified cell populations. Hearing Research, 93(1–2), 52–71. https://doi.org/10.1016/0378-5955(95)00200-6

Merchan-Perez, A., & Liberman, M. C. (1996). Ultrastructural differences among afferent synapses on cochlear hair cells: Correlations with spontaneous discharge rate. The Journal of Comparative Neurology, 371(2), 208–221. https://doi.org/10.1002/(SICI)1096-9861(19960722)371:2<208::AID-CNE2>3.0.CO;2-6

Meredith, F. L., & Rennie, K. J. (2021). Dopaminergic Inhibition of Na+ Currents in Vestibular Inner Ear Afferents. Frontiers in Neuroscience, 15, 710321. https://doi.org/10.3389/fnins.2021.710321

Merin, R. G. (1986). Isoflurane and Calcium Channel Blockers. In P. Lawin, H. Van Aken, & C. Puchstein (Eds.), Isoflurane (pp. 67–73). Springer. https://doi.org/10.1007/978-3-642-71230-2_12

Meyer, A. C., Frank, T., Khimich, D., Hoch, G., Riedel, D., Chapochnikov, N. M., Yarin, Y. M., Harke, B., Hell, S. W., Egner, A., & Moser, T. (2009). Tuning of synapse number, structure and function in the cochlea. Nature Neuroscience, 12(4), 444–453. https://doi.org/10.1038/nn.2293

Michanski, S., Smaluch, K., Steyer, A. M., Chakrabarti, R., Setz, C., Oestreicher, D., Fischer, C., Möbius, W., Moser, T., Vogl, C., & Wichmann, C. (2019). Mapping developmental maturation of inner hair cell ribbon synapses in the apical mouse cochlea. Proceedings of the National Academy of Sciences of the United States of America, 116(13), 6415–6424. https://doi.org/10.1073/pnas.1812029116

Miller, R. L., Schilling, J. R., Franck, K. R., & Young, E. D. (1997). Effects of acoustic trauma on the representation of the vowel /ɛ/ in cat auditory nerve fibers. The Journal of the Acoustical Society of America, 101(6), 3602–3616. https://doi.org/10.1121/1.418321

Milon, B., Mitra, S., Song, Y., Margulies, Z., Casserly, R., Drake, V., Mong, J. A., Depireux, D. A., & Hertzano, R. (2018). The impact of biological sex on the response to noise and otoprotective therapies against acoustic injury in mice. Biology of Sex Differences, 9(1), 12. https://doi.org/10.1186/s13293-018-0171-0

Minami, K., Yanagihara, N., Toyohira, Y., Tsutsui, M., Shigematsu, A., Wada, A., & Izumi, F. (1994). Isoflurane inhibits nicotinic acetylcholine receptor-mediated 22Na+ influx and muscarinic receptor-evoked cyclic GMP production in cultured bovine adrenal medullary cells. Naunyn-Schmiedeberg's Archives of Pharmacology, 349(3), 223–229. https://doi.org/10.1007/BF00169287

Mizushima, Y., Fujimoto, C., Kashio, A., Kondo, K., & Yamasoba, T. (2017). Macrophage recruitment, but not interleukin 1 beta activation, enhances noise-induced hearing damage. Biochemical and Biophysical Research Communications, 493(2), 894–900. https://doi.org/10.1016/j.bbrc.2017.09.124

Modification of motor nerve terminal excitability by alkanols and volatile anaesthetics. - PMC. (n.d.). Retrieved March 15, 2023, from https://www.ncbi.nlm.nih.gov/pmc/articles/PMC1917076/

Møller, A. R. (2006). History of Cochlear Implants and Auditory Brainstem Implants. In A. R. Møller (Ed.), Advances in Oto-Rhino-Laryngology (Vol. 64, pp. 1–10). S. Karger AG. https://doi.org/10.1159/000094455

Moser, T., Grabner, C. P., & Schmitz, F. (2020). Sensory Processing at Ribbon Synapses in the Retina and the Cochlea. Physiological Reviews, 100(1), 103–144. https://doi.org/10.1152/physrev.00026.2018

Moser, T., & Strenzke, N. (2015). Synaptic encoding and processing of auditory information in physiology and disease. Hearing Research, 330, 155–156. https://doi.org/10.1016/j.heares.2015.06.015

Müller, M., von Hünerbein, K., Hoidis, S., & Smolders, J. W. T. (2005). A physiological place-frequency map of the cochlea in the CBA/J mouse. Hearing Research, 202(1–2), 63–73. https://doi.org/10.1016/j.heares.2004.08.011

Mulroy, M. J. (1986). Permanent noise-induced damage to stereocilia: A scanning electron microscopic study of the lizard's cochlea. Scanning Electron Microscopy, Pt 4, 1451–1457.

Mulroy, M. J., & Whaley, E. A. (1984). Structural changes in auditory hairs during temporary deafness. Scanning Electron Microscopy, Pt 2, 831–840.

Murphy, C. A., Raz, A., Grady, S. M., & Banks, M. I. (2020). Optogenetic Activation of Afferent Pathways in Brain Slices and Modulation of Responses by Volatile Anesthetics. Journal of Visualized Experiments : JoVE, 161, 10.3791/61333. https://doi.org/10.3791/61333

Mutlu, A., Ocal, F. C. A., Erbek, S., & Ozluoglu, L. (2018). The protective effect of adrenocorticotropic hormone treatment against noise-induced hearing loss. Auris Nasus Larynx, 45(5), 929–935. https://doi.org/10.1016/j.anl.2017.12.006

Nam, J.-H., Peng, A. W., & Ricci, A. J. (2015). Underestimated sensitivity of mammalian cochlear hair cells due to splay between stereociliary columns. Biophysical Journal, 108(11), 2633–2647. https://doi.org/10.1016/j.bpj.2015.04.028

Neef, A., Khimich, D., Pirih, P., Riedel, D., Wolf, F., & Moser, T. (2007). Probing the Mechanism of Exocytosis at the Hair Cell Ribbon Synapse. The Journal of Neuroscience, 27(47), 12933–12944. https://doi.org/10.1523/JNEUROSCI.1996-07.2007

Neher, E., & Sakmann, B. (1976). Single-channel currents recorded from membrane of denervated frog muscle fibres. Nature, 260(5554), Article 5554. https://doi.org/10.1038/260799a0

Neiman, A., Dierkes, K., Lindner, B., Han, L., & Shilnikov, A. (2011). Spontaneous voltage oscillations and response dynamics of a Hodgkin-Huxley type model of sensory hair cells. Journal of Mathematical Neuroscience, 1, 11. https://doi.org/10.1186/2190-8567-1-11

Nevoux, J., Alexandru, M., Bellocq, T., Tanaka, L., Hayashi, Y., Watabe, T., Lahlou, H., Tani, K., & Edge, A. S. B. (2021). An antibody to RGMa promotes regeneration of cochlear synapses after noise exposure. Scientific Reports, 11(1), 2937. https://doi.org/10.1038/s41598-021-81294-5

Nicotera, T. M., Hu, B. H., & Henderson, D. (2003). The Caspase Pathway in Noise-Induced Apoptosis of the Chinchilla Cochlea. JARO: Journal of the Association for Research in Otolaryngology, 4(4), 466–477. https://doi.org/10.1007/s10162-002-3038-2

Nin, F., Hibino, H., Doi, K., Suzuki, T., Hisa, Y., & Kurachi, Y. (2008). The endocochlear potential depends on two K+ diffusion potentials and an electrical barrier in the stria vascularis of the inner ear. Proceedings of the National Academy of Sciences, 105(5), 1751–1756. https://doi.org/10.1073/pnas.0711463105

Noise Exposure Potentiates Exocytosis From Cochlear Inner Hair Cells. (n.d.). Frontiers in Synaptic Neuroscience. https://doi.org/10.3389/fnsyn.2021.740368

Noise Exposure Potentiates Exocytosis From Cochlear Inner Hair Cells—PMC. (n.d.). Retrieved October 29, 2022, from https://www.ncbi.nlm.nih.gov/pmc/articles/PMC8511412/

Oak, M.-H., & Yi, E. (2014). Voltage-gated K(+) channels contributing to temporal precision at the inner hair cell-auditory afferent nerve fiber synapses in the mammalian cochlea. Archives of Pharmacal Research, 37(7), 821–833. https://doi.org/10.1007/s12272-014-0411-8

Ohn, T.-L., Rutherford, M. A., Jing, Z., Jung, S., Duque-Afonso, C. J., Hoch, G., Picher, M. M., Scharinger, A., Strenzke, N., & Moser, T. (2016). Hair cells use active zones with different voltage dependence of Ca2+ influx to decompose sounds into complementary neural codes. Proceedings of the National Academy of Sciences of the United States of America, 113(32), E4716–E4725. https://doi.org/10.1073/pnas.1605737113

Oliver, D., Knipper, M., Derst, C., & Fakler, B. (2003). Resting potential and submembrane calcium concentration of inner hair cells in the isolated mouse cochlea are set by KCNQ-type potassium channels. The Journal of Neuroscience: The Official Journal of the Society for Neuroscience, 23(6), 2141–2149. https://doi.org/10.1523/JNEUROSCI.23-06-02141.2003

Ouyang, W., & Hemmings, H. C. (2005). Depression by Isoflurane of the Action Potential and Underlying Voltage-Gated Ion Currents in Isolated Rat Neurohypophysial Nerve Terminals. Journal of Pharmacology and Experimental Therapeutics, 312(2), 801–808. https://doi.org/10.1124/jpet.104.074609

Ouyang, W., Wang, G., & Hemmings, H. C. (2003). Isoflurane and propofol inhibit voltage-gated sodium channels in isolated rat neurohypophysial nerve terminals. Molecular Pharmacology, 64(2), 373–381. https://doi.org/10.1124/mol.64.2.373

Oxenham, A. J., & Plack, C. J. (1998). Suppression and the upward spread of masking. The Journal of the Acoustical Society of America, 104(6), 3500–3510. https://doi.org/10.1121/1.423933

Pak, J. H., Kim, Y., Yi, J., & Chung, J. W. (2020). Antioxidant Therapy against Oxidative Damage of the Inner Ear: Protection and Preconditioning. Antioxidants, 9(11), 1076. https://doi.org/10.3390/antiox9111076

Palmer, A. R., & Russell, I. J. (1986). Phase-locking in the cochlear nerve of the guinea-pig and its relation to the receptor potential of inner hair-cells. Hearing Research, 24(1), 1–15. https://doi.org/10.1016/0378-5955(86)90002-x

Pandit, J. J., Huskens, N., O'Donohoe, P. B., Turner, P. J., & Buckler, K. J. (2020). Competitive Interactions between Halothane and Isoflurane at the Carotid Body and TASK Channels. Anesthesiology, 133(5), 1046–1059. https://doi.org/10.1097/ALN.0000000000003520

Pangrsic, T., & Vogl, C. (2018). Balancing presynaptic release and endocytic membrane retrieval at hair cell ribbon synapses. FEBS Letters, 592(21), 3633–3650. https://doi.org/10.1002/1873-3468.13258

Parker, A., Parham, K., & Skoe, E. (2022). Noise exposure levels predict blood levels of the inner ear protein prestin. Scientific Reports, 12(1), Article 1. https://doi.org/10.1038/s41598-022-05131-z

Parrin, A., Emptoz, A., Bahloul, A., Petit, C., Ciric, D., Dulon, D., Boutet de Monvel, J., Rothman, J. E., Hardelin, J.-P., Goutman, J. D., Guillon, M., Tertrais, M., Sachse, M., Michalski, N. A., Avan, P., Sutton, R. B., Safieddine, S., Auclair, S. M., Krishnakumar, S. S., & Nouaille, S. (n.d.). Otoferlin acts as a Ca<sup>2+</sup> sensor for vesicle fusion and vesicle pool replenishment at auditory hair cell ribbon synapses. ELife. https://doi.org/10.7554/eLife.31013

Passchier-Vermeer, W. (2005). Hearing loss due to continuous exposure to steady-state broad-band noise. The Journal of the Acoustical Society of America, 56(5), 1585. https://doi.org/10.1121/1.1903482

Patuzzi, R. (1996). Cochlear Micromechanics and Macromechanics. In P. Dallos, A. N. Popper, & R. R. Fay (Eds.), The Cochlea (pp. 186–257). Springer. https://doi.org/10.1007/978-1-4612-0757-3_4

Patuzzi, R. (1998). Exponential onset and recovery of temporary threshold shift after loud sound: Evidence for long-term inactivation of mechano-electrical transduction channels. Hearing Research, 125(1–2), 17–38. https://doi.org/10.1016/s0378-5955(98)00126-9

Peineau, T., Belleudy, S., Pietropaolo, S., Bouleau, Y., & Dulon, D. (2021). Synaptic Release Potentiation at Aging Auditory Ribbon Synapses. Frontiers in Aging Neuroscience, 13. https://www.frontiersin.org/articles/10.3389/fnagi.2021.756449

Perouansky, M., Hemmings, H. C., & Pearce, R. A. (2004). Anesthetic effects on glutamatergic neurotransmission: Lessons learned from a large synapse. Anesthesiology, 100(3), 470–472. https://doi.org/10.1097/00000542-200403000-00003

Pitch Perception and Auditory Stream Segregation: Implications for Hearing Loss and Cochlear Implants—PMC. (n.d.). Retrieved February 6, 2023, from https://www.ncbi.nlm.nih.gov/pmc/articles/PMC2901529/

Plack, C. J., Barker, D., & Prendergast, G. (2014). Perceptual Consequences of "Hidden" Hearing Loss. Trends in Hearing, 18, 2331216514550621. https://doi.org/10.1177/2331216514550621

Polanski, W., Enzensperger, C., Reichmann, H., & Gille, G. (2010). The exceptional properties of 9-methyl-beta-carboline: Stimulation, protection and regeneration of dopaminergic neurons coupled with anti-inflammatory effects. Journal of Neurochemistry, 113(6), 1659–1675. https://doi.org/10.1111/j.1471-4159.2010.06725.x

Puel, J. L., Ruel, J., Gervais d'Aldin, C., & Pujol, R. (1998). Excitotoxicity and repair of cochlear synapses after noise-trauma induced hearing loss. Neuroreport, 9(9), 2109–2114. https://doi.org/10.1097/00001756-199806220-00037

Pujol, R., Lenoir, M., Robertson, D., Eybalin, M., & Johnstone, B. M. (1985). Kainic acid selectively alters auditory dendrites connected with cochlear inner hair cells. Hearing Research, 18(2), 145–151. https://doi.org/10.1016/0378-5955(85)90006-1

Pujol, R., & Puel, J.-L. (1999). Excitotoxicity, Synaptic Repair, and Functional Recovery in the Mammalian Cochlea: A Review of Recent Findings. Annals of the New York Academy of Sciences, 884(1), 249–254. https://doi.org/10.1111/j.1749-6632.1999.tb08646.x

Pyott, S. J., & Duncan, R. K. (2016). BK Channels in the Vertebrate Inner Ear. International Review of Neurobiology, 128, 369–399. https://doi.org/10.1016/bs.irn.2016.03.016

Qiu, X., & Müller, U. (2018). Mechanically Gated Ion Channels in Mammalian Hair Cells. Frontiers in Cellular Neuroscience, 12. https://www.frontiersin.org/articles/10.3389/fncel.2018.00100

Recio, A., Rich, N. C., Narayan, S. S., & Ruggero, M. A. (1998). Basilar-membrane responses to clicks at the base of the chinchilla cochlea. The Journal of the Acoustical Society of America, 103(4), 1972–1989.

Recio-Spinoso, A., Narayan, S. S., & Ruggero, M. A. (2009). Basilar Membrane Responses to Noise at a Basal Site of the Chinchilla Cochlea: Quasi-Linear Filtering. JARO: Journal of the Association for Research in Otolaryngology, 10(4), 471–484. https://doi.org/10.1007/s10162-009-0172-0

Recio-Spinoso, A., Temchin, A. N., van Dijk, P., Fan, Y.-H., & Ruggero, M. A. (2005). Wiener-Kernel Analysis of Responses to Noise of Chinchilla Auditory-Nerve Fibers. Journal of Neurophysiology, 93(6), 3615–3634. https://doi.org/10.1152/jn.00882.2004

Reijntjes, D. O. J., & Pyott, S. J. (2016). The afferent signaling complex: Regulation of type I spiral ganglion neuron responses in the auditory periphery. Hearing Research, 336, 1–16. https://doi.org/10.1016/j.heares.2016.03.011

Rhode, W. S. (1971). Observations of the vibration of the basilar membrane in squirrel monkeys using the Mössbauer technique. The Journal of the Acoustical Society of America, 49(4), Suppl 2:1218+. https://doi.org/10.1121/1.1912485

Robertson, D. (1983). Functional significance of dendritic swelling after loud sounds in the guinea pig cochlea. Hearing Research, 9(3), 263–278. https://doi.org/10.1016/0378-5955(83)90031-x

Robles, L., & Ruggero, M. A. (2001). Mechanics of the Mammalian Cochlea. Physiological Reviews, 81(3), 1305–1352.

Rodrigues, J. C., Bachi, A. L. L., Silva, G. A. V., Rossi, M., do Amaral, J. B., Lezirovitz, K., & de Brito, R. (2020). New Insights on the Effect of TNF Alpha Blockade by Gene Silencing in Noise-Induced Hearing Loss. International Journal of Molecular Sciences, 21(8). https://doi.org/10.3390/ijms21082692

Rohmann, K. N., Wersinger, E., Braude, J. P., Pyott, S. J., & Fuchs, P. A. (2015). Activation of BK and SK channels by efferent synapses on outer hair cells in high-frequency regions of the rodent cochlea. The Journal of Neuroscience: The Official Journal of the Society for Neuroscience, 35(5), 1821–1830. https://doi.org/10.1523/JNEUROSCI.2790-14.2015

Rouse, S. L., Matthews, I. R., Li, J., Sherr, E. H., & Chan, D. K. (2020). Integrated stress response inhibition provides sex-dependent protection against noise-induced cochlear synaptopathy. Scientific Reports, 10(1), 18063. https://doi.org/10.1038/s41598-020-75058-w

Ruan, Q., Ao, H., He, J., Chen, Z., Yu, Z., Zhang, R., Wang, J., & Yin, S. (2014). Topographic and quantitative evaluation of gentamicin-induced damage to peripheral innervation of mouse cochleae. NeuroToxicology, 40, 86–96. https://doi.org/10.1016/j.neuro.2013.11.002

Ruebhausen, M. R., Brozoski, T. J., & Bauer, C. A. (2012). A comparison of the effects of isoflurane and ketamine anesthesia on auditory brainstem response (ABR) thresholds in rats. Hearing Research, 287(1–2), 25–29. https://doi.org/10.1016/j.heares.2012.04.005

Ruel, J., Nouvian, R., Gervais d'Aldin, C., Pujol, R., Eybalin, M., & Puel, J. L. (2001). Dopamine inhibition of auditory nerve activity in the adult mammalian cochlea. The European Journal of Neuroscience, 14(6), 977–986. https://doi.org/10.1046/j.0953-816x.2001.01721.x

Ruel, J., Wang, J., Rebillard, G., Eybalin, M., Lloyd, R., Pujol, R., & Puel, J.-L. (2007). Physiology, pharmacology and plasticity at the inner hair cell synaptic complex. Hearing Research, 227(1–2), 19–27. https://doi.org/10.1016/j.heares.2006.08.017

Ruggero, M. A., & Rich, N. C. (1983). Chinchilla auditory-nerve responses to low-frequency tones. The Journal of the Acoustical Society of America, 73(6), 2096–2108. https://doi.org/10.1121/1.389577

Russell, I., & Kossl, M. (1992). Modulation of hair cell voltage responses to tones by low-frequency biasing of the basilar membrane in the guinea pig cochlea. The Journal of Neuroscience, 12(5), 1587–1601. https://doi.org/10.1523/JNEUROSCI.12-05-01587.1992

Rutherford, M. A., von Gersdorff, H., & Goutman, J. D. (2021). Encoding sound in the cochlea: From receptor potential to afferent discharge. The Journal of Physiology, 599(10), 2527–2557. https://doi.org/10.1113/JP279189

Rutherford, M., & Pangršič, T. (2012). Molecular anatomy and physiology of exocytosis in sensory hair cells. Cell Calcium, 52, 327–337. https://doi.org/10.1016/j.ceca.2012.05.008

rutherford mark, AMPA receptors—Google Search. (n.d.). Retrieved March 16, 2023, from https://www.google.com/search?q=rutherford+mark%2C+AMPA+receptors&oq=rutherford+mark%2C+AMPA+receptors&aqs=chrome..69i57j33i160.16048j0j4&sourceid=chrome&ie=UTF-8

Rzadzinska, A. K., Schneider, M. E., Davies, C., Riordan, G. P., & Kachar, B. (2004). An actin molecular treadmill and myosins maintain stereocilia functional architecture and self-renewal. The Journal of Cell Biology, 164(6), 887–897. https://doi.org/10.1083/jcb.200310055

Salimpour, Y., & Abolhassani, M. D. (2006). Auditory wavelet transform based on auditory wavelet families. Conference Proceedings: ... Annual International Conference of the IEEE Engineering in Medicine and Biology Society. IEEE Engineering in Medicine and Biology Society. Annual Conference, 2006, 1731–1734. https://doi.org/10.1109/IEMBS.2006.260717

Santarelli, R., Arslan, E., Carraro, L., Conti, G., Capello, M., & Plourde, G. (2003). Effects of isoflurane on the auditory brainstem responses and middle latency responses of rats. Acta Oto-Laryngologica, 123(2), 176–181. https://doi.org/10.1080/0036554021000028108

Santarelli, R., del Castillo, I., Rodríguez-Ballesteros, M., Scimemi, P., Cama, E., Arslan, E., & Starr, A. (2009). Abnormal Cochlear Potentials from Deaf Patients with Mutations in the Otoferlin Gene. JARO: Journal of the Association for Research in Otolaryngology, 10(4), 545–556. https://doi.org/10.1007/s10162-009-0181-z

Sattler, R., & Tymianski, M. (2000). Molecular mechanisms of calcium-dependent excitotoxicity. Journal of Molecular Medicine, 78(1), 3–13. https://doi.org/10.1007/s001090000077

Schaette, R., & McAlpine, D. (2011). Tinnitus with a Normal Audiogram: Physiological Evidence for Hidden Hearing Loss and Computational Model. Journal of Neuroscience, 31(38), 13452–13457. https://doi.org/10.1523/JNEUROSCI.2156-11.2011

Scheller, M., Bufler, J., Schneck, H., Kochs, E., & Franke, C. (1997). Isoflurane and sevoflurane interact with the nicotinic acetylcholine receptor channels in micromolar concentrations. Anesthesiology, 86(1), 118–127. https://doi.org/10.1097/00000542-199701000-00016

Schmiedt, R. A., Mills, J. H., & Boettcher, F. A. (1996). Age-related loss of activity of auditory-nerve fibers. Journal of Neurophysiology, 76(4), 2799–2803. https://doi.org/10.1152/jn.1996.76.4.2799

Schnupp, J., Nelken, I., & King, A. (2011). Auditory Neuroscience: Making Sense of Sound. MIT Press.

Schuknecht, H. F., & Woellner, R. C. (1955). An Experimental and Clinical Study of Deafness from Lesions of the Cochlear Nerve. The Journal of Laryngology & Otology, 69(2), 75–97. https://doi.org/10.1017/S0022215100050465

Seal, R. P., Akil, O., Yi, E., Weber, C. M., Grant, L., Yoo, J., Clause, A., Kandler, K., Noebels, J. L., Glowatzki, E., Lustig, L. R., & Edwards, R. H. (2008). Sensorineural Deafness and Seizures in Mice Lacking Vesicular Glutamate Transporter 3. Neuron, 57(2), 263–275. https://doi.org/10.1016/j.neuron.2007.11.032

Sebe, J. Y., Cho, S., Sheets, L., Rutherford, M. A., von Gersdorff, H., & Raible, D. W. (2017). Ca2+-Permeable AMPARs Mediate Glutamatergic Transmission and Excitotoxic Damage at the Hair Cell Ribbon Synapse. The Journal of Neuroscience: The Official Journal of the Society for Neuroscience, 37(25), 6162–6175. https://doi.org/10.1523/JNEUROSCI.3644-16.2017

Seist, R., Tong, M., Landegger, L. D., Vasilijic, S., Hyakusoku, H., Katsumi, S., McKenna, C. E., Edge, A. S. B., & Stankovic, K. M. (2020). Regeneration of Cochlear Synapses by Systemic Administration of a Bisphosphonate. Frontiers in Molecular Neuroscience, 13, 87. https://doi.org/10.3389/fnmol.2020.00087

Sensory transduction and frequency selectivity in the basal turn of the guinea-pig cochlea. (1992). Philosophical Transactions of the Royal Society of London. Series B: Biological Sciences, 336(1278), 317–324. https://doi.org/10.1098/rstb.1992.0064

Sergeyenko, Y., Lall, K., Liberman, M. C., & Kujawa, S. G. (2013). Age-related cochlear synaptopathy: An early-onset contributor to auditory functional decline. The Journal of Neuroscience: The Official Journal of the Society for Neuroscience, 33(34), 13686–13694. https://doi.org/10.1523/JNEUROSCI.1783-13.2013

Sewell, W. F. (1984). The effects of furosemide on the endocochlear potential and auditory-nerve fiber tuning curves in cats. Hearing Research, 14(3), 305–314. https://doi.org/10.1016/0378-5955(84)90057-1

Sha, S.-H., & Schacht, J. (2017). Emerging therapeutic interventions against noise-induced hearing loss. Expert Opinion on Investigational Drugs, 26(1), 85–96. https://doi.org/10.1080/13543784.2017.1269171

Sheppard, A. M., Zhao, D.-L., & Salvi, R. (2018). Isoflurane anesthesia suppresses distortion product otoacoustic emissions in rats. Journal of Otology, 13(2), 59–64. https://doi.org/10.1016/j.joto.2018.03.002

Shi, L., Chang, Y., Li, X., Aiken, S., Liu, L., & Wang, J. (2016). Cochlear Synaptopathy and Noise-Induced Hidden Hearing Loss. Neural Plasticity, 2016, 6143164. https://doi.org/10.1155/2016/6143164

Shi, L., Liu, L., He, T., Guo, X., Yu, Z., Yin, S., & Wang, J. (2013). Ribbon Synapse Plasticity in the Cochleae of Guinea Pigs after Noise-Induced Silent Damage. PLOS ONE, 8(12), e81566. https://doi.org/10.1371/journal.pone.0081566

Shiraishi, M., & Harris, R. A. (2004). Effects of Alcohols and Anesthetics on Recombinant Voltage-Gated Na+ Channels. Journal of Pharmacology and Experimental Therapeutics, 309(3), 987–994. https://doi.org/10.1124/jpet.103.064063

Shrestha, B. R., Chia, C., Wu, L., Kujawa, S. G., Liberman, M. C., & Goodrich, L. V. (n.d.). Sensory Neuron Diversity in the Inner Ear Is Shaped by Activity. Cell. https://doi.org/10.1016/j.cell.2018.07.007

Shuster, B., Casserly, R., Lipford, E., Olszewski, R., Milon, B., Viechweg, S., Davidson, K., Enoch, J., McMurray, M., Rutherford, M. A., Ohlemiller, K. K., Hoa, M., Depireux, D. A., Mong, J. A., & Hertzano, R. (2021). Estradiol Protects against Noise-Induced Hearing Loss and Modulates Auditory Physiology in Female Mice. International Journal of Molecular Sciences, 22(22), Article 22. https://doi.org/10.3390/ijms222212208

Signoret, C., & Rudner, M. (2019). Hearing Impairment and Perceived Clarity of Predictable Speech. Ear and Hearing, 40(5), 1140. https://doi.org/10.1097/AUD.0000000000000689

Sly, D. J., Campbell, L., Uschakov, A., Saief, S. T., Lam, M., & O'Leary, S. J. (2016). Applying Neurotrophins to the Round Window Rescues Auditory Function and Reduces Inner Hair Cell Synaptopathy After Noise-induced Hearing Loss. Otology & Neurotology, 37(9), 1223–1230. https://doi.org/10.1097/MAO.0000000000001191

Smith, K. E., Browne, L., Selwood, D. L., McAlpine, D., & Jagger, D. J. (2015). Phosphoinositide Modulation of Heteromeric Kv1 Channels Adjusts Output of Spiral Ganglion Neurons from Hearing Mice. The Journal of Neuroscience, 35(32), 11221–11232. https://doi.org/10.1523/JNEUROSCI.0496-15.2015

Song, Q., Shen, P., Li, X., Shi, L., Liu, L., Wang, J., Yu, Z., Stephen, K., Aiken, S., Yin, S., & Wang, J. (2016). Coding deficits in hidden hearing loss induced by noise: The nature and impacts. Scientific Reports, 6(1), Article 1. https://doi.org/10.1038/srep25200

Speigel, I. A., Patel, K., & Hemmings, H. C. (2022). Distinct effects of volatile and intravenous anaesthetics on presynaptic calcium dynamics in mouse hippocampal GABAergic neurones. British Journal of Anaesthesia, 128(6), 1019–1028. https://doi.org/10.1016/j.bja.2022.01.014

Spoendlin, H. (1971). Primary structural changes in the organ of Corti after acoustic overstimulation. Acta Oto-Laryngologica, 71(2), 166–176. https://doi.org/10.3109/00016487109125346

Squire, L., Berg, D., Bloom, F. E., Lac, S. du, Ghosh, A., & Spitzer, N. C. (2013). Fundamental Neuroscience. Academic Press.

Stronks, H. C., Aarts, M. C. J., & Klis, S. F. L. (2010). Effects of isoflurane on auditory evoked potentials in the cochlea and brainstem of guinea pigs. Hearing Research, 260(1–2), 20–29. https://doi.org/10.1016/j.heares.2009.10.015

Study, R. E. (1994). Isoflurane inhibits multiple voltage-gated calcium currents in hippocampal pyramidal neurons. Anesthesiology, 81(1), 104–116. https://doi.org/10.1097/00000542-199407000-00016

Sun, H., Hashino, E., Ding, D. L., & Salvi, R. J. (2001). Reversible and irreversible damage to cochlear afferent neurons by kainic acid excitotoxicity. The Journal of Comparative Neurology, 430(2), 172–181. https://doi.org/10.1002/1096-9861(20010205)430:2<172::aid-cne1023>3.0.co;2-w

Suthakar, K., & Liberman, M. C. (2021). Auditory-nerve responses in mice with noise-induced cochlear synaptopathy. Journal of Neurophysiology, 126(6), 2027–2038. https://doi.org/10.1152/jn.00342.2021
Suthakar, K., & Liberman, M. C. (2022). Noise Masking in Cochlear Synaptopathy: Auditory Brainstem Response vs. Auditory Nerve Response in Mouse. Journal of Neurophysiology, 127(6), 1574–1585. https://doi.org/10.1152/jn.00402.2021

Suzuki, J., Corfas, G., & Liberman, M. C. (2016). Round-window delivery of neurotrophin 3 regenerates cochlear synapses after acoustic overexposure. Scientific Reports, 6, 24907. https://doi.org/10.1038/srep24907

Syka, J., Melichar, I., & Úlehlová, L. (1981). Longitudinal distribution of cochlear potentials and the K+ concentration in the endolymph after acoustic trauma. Hearing Research, 4(3), 287–298. https://doi.org/10.1016/0378-5955(81)90013-7

Takeda, Sh., Mannström, P., Dash-Wagh, S., Yoshida, T., & Ulfendahl, M. (2017). Effects of Aging and Noise Exposure on Auditory Brainstem Responses and Number of Presynaptic Ribbons in Inner Hair Cells of C57BL/6J Mice. Neurophysiology, 49(5), 316–326. https://doi.org/10.1007/s11062-018-9691-9

Tan, J., Rüttiger, L., Panford-Walsh, R., Singer, W., Schulze, H., Kilian, S. B., Hadjab, S., Zimmermann, U., Köpschall, I., Rohbock, K., & Knipper, M. (2007). Tinnitus behavior and hearing function correlate with the reciprocal expression patterns of BDNF and Arg3.1/arc in auditory neurons following acoustic trauma. Neuroscience, 145(2), 715–726. https://doi.org/10.1016/j.neuroscience.2006.11.067

Tang, X., Zhu, X., Ding, B., Walton, J. P., Frisina, R. D., & Su, J. (2014). Age-related Hearing Loss: GABA, Nicotinic Acetylcholine and NMDA Receptor Expression Changes in Spiral Ganglion Neurons of the Mouse. Neuroscience, 259, 184–193. https://doi.org/10.1016/j.neuroscience.2013.11.058

Teas, D. C., & Kiang, N. Y. (1964). EVOKED RESPONSES FROM THE AUDITORY CERTEX. Experimental Neurology, 10, 91–119. https://doi.org/10.1016/0014-4886(64)90088-3

Temchin, A. N., Rich, N. C., & Ruggero, M. A. (2008a). Threshold tuning curves of chinchilla auditory nerve fibers. II. Dependence on spontaneous activity and relation to cochlear nonlinearity. Journal of Neurophysiology, 100(5), 2899–2906. https://doi.org/10.1152/jn.90639.2008

Temchin, A. N., Rich, N. C., & Ruggero, M. A. (2008b). Threshold Tuning Curves of Chinchilla Auditory-Nerve Fibers. I. Dependence on Characteristic Frequency and Relation to the Magnitudes of Cochlear Vibrations. Journal of Neurophysiology, 100(5), 2889–2898. https://doi.org/10.1152/jn.90637.2008

Topf, N., Jenkins, A., Baron, N., & Harrison, N. L. (2003). Effects of isoflurane on gamma-aminobutyric acid type A receptors activated by full and partial agonists. Anesthesiology, 98(2), 306–311. https://doi.org/10.1097/00000542-200302000-00007

Trautwein, P., Hofstetter, P., Wang, J., Salvi, R., & Nostrant, A. (1996). Selective inner hair cell loss does not alter distortion product otoacoustic emissions. Hearing Research, 96(1–2), 71–82. https://doi.org/10.1016/0378-5955(96)00040-8

Tserga, E., Damberg, P., Canlon, B., & Cederroth, C. R. (2021). Auditory synaptopathy in mice lacking the glutamate transporter GLAST and its impact on brain activity. Progress in Brain Research, 262, 245–261. https://doi.org/10.1016/bs.pbr.2020.04.004

Valenzuela, C. V., Lee, C., Mispagel, A., Bhattacharyya, A., Lefler, S. M., Payne, S., Goodman, S. S., Ortmann, A. J., Buchman, C. A., Rutherford, M. A., & Lichtenhan, J. T. (2020). Is cochlear synapse loss an origin of low-frequency hearing loss associated with endolymphatic hydrops? Hearing Research, 398, 108099. https://doi.org/10.1016/j.heares.2020.108099

Valero, M. D., Burton, J. A., Hauser, S. N., Hackett, T. A., Ramachandran, R., & Liberman, M. C. (2017). Noise-induced cochlear synaptopathy in rhesus monkeys (Macaca mulatta). Hearing Research, 353, 213–223. https://doi.org/10.1016/j.heares.2017.07.003

Viana, L. M., O'Malley, J. T., Burgess, B. J., Jones, D. D., Oliveira, C. A. C. P., Santos, F., Merchant, S. N., Liberman, L. D., & Liberman, M. C. (2015). Cochlear neuropathy in human presbycusis: Confocal analysis of hidden hearing loss in post-mortem tissue. Hearing Research, 327, 78–88. https://doi.org/10.1016/j.heares.2015.04.014

Villavisanis, D. F., Berson, E. R., Lauer, A. M., Cosetti, M. K., & Schrode, K. M. (2020). Sex-Based Differences in Hearing Loss: Perspectives from Non-Clinical Research to Clinical Outcomes. Otology & Neurotology : Official Publication of the American Otological Society, American Neurotology Society [and] European Academy of Otology and Neurotology, 41(3), 290–298. https://doi.org/10.1097/MAO.0000000000002507

Walia, A., Lee, C., Hartsock, J., Goodman, S. S., Dolle, R., Salt, A. N., Lichtenhan, J. T., & Rutherford, M. A. (2021). Reducing Auditory Nerve Excitability by Acute Antagonism of Ca2+-Permeable AMPA Receptors. Frontiers in Synaptic Neuroscience, 13, 34. https://doi.org/10.3389/fnsyn.2021.680621

Wan, G., & Corfas, G. (2017). Transient auditory nerve demyelination as a new mechanism for hidden hearing loss. Nature Communications, 8, 14487. https://doi.org/10.1038/ncomms14487

Wan, G., Gómez-Casati, M. E., Gigliello, A. R., Liberman, M. C., & Corfas, G. (2014). Neurotrophin-3 regulates ribbon synapse density in the cochlea and induces synapse regeneration after acoustic trauma. ELife, 3, e03564. https://doi.org/10.7554/eLife.03564

Wang, H., Yin, S., Yu, Z., Huang, Y., & Wang, J. (2011). Dynamic changes in hair cell stereocilia and cochlear transduction after noise exposure. Biochemical and Biophysical Research Communications, 409(4), 616–621. https://doi.org/10.1016/j.bbrc.2011.05.049

Wang, H.-Y., Eguchi, K., Yamashita, T., & Takahashi, T. (2020). Frequency-Dependent Block of Excitatory Neurotransmission by Isoflurane via Dual Presynaptic Mechanisms. Journal of Neuroscience, 40(21), 4103–4115. https://doi.org/10.1523/JNEUROSCI.2946-19.2020

Wang, J., Dong, W., & Chen, J. (1990). Changes in endocochlear potential during anoxia after intense noise exposure. Hearing Research, 44(2), 143–149. https://doi.org/10.1016/0378-5955(90)90076-2

Wang, J., Yin, S., Chen, H., & Shi, L. (2019). Noise-Induced Cochlear Synaptopathy and Ribbon Synapse Regeneration: Repair Process and Therapeutic Target. In H. Li & R. Chai (Eds.), Hearing Loss: Mechanisms, Prevention and Cure (pp. 37–57). Springer. https://doi.org/10.1007/978-981-13-6123-4_3

Wang, Q., Wang, X., Yang, L., Han, K., Huang, Z., & Wu, H. (2021). Sex differences in noise-induced hearing loss: A cross-sectional study in China. Biology of Sex Differences, 12, 24. https://doi.org/10.1186/s13293-021-00369-0

Wang, Y., Hirose, K., & Liberman, M. C. (2002). Dynamics of Noise-Induced Cellular Injury and Repair in the Mouse Cochlea. JARO: Journal of the Association for Research in Otolaryngology, 3(3), 248–268. https://doi.org/10.1007/s101620020028

Wei, M., Wang, W., Liu, Y., Mao, X., Chen, T. S., & Lin, P. (n.d.). Protection of Cochlear Ribbon Synapses and Prevention of Hidden Hearing Loss. Neural Plasticity. https://doi.org/10.1155/2020/8815990

Wei, W., Shi, X., Xiong, W., He, L., Du, Z.-D., Qu, T., Qi, Y., Gong, S.-S., Liu, K., & Ma, X. (2020). RNA-seq Profiling and Co-expression Network Analysis of Long Noncoding RNAs and mRNAs Reveal Novel Pathogenesis of Noise-induced Hidden Hearing Loss. Neuroscience, 434, 120–135. https://doi.org/10.1016/j.neuroscience.2020.03.023

Weisová, P., Dávila, D., Tuffy, L. P., Ward, M. W., Concannon, C. G., & Prehn, J. H. M. (2011). Role of 5'-adenosine monophosphate-activated protein kinase in cell survival and death responses in neurons. Antioxidants & Redox Signaling, 14(10), 1863–1876. https://doi.org/10.1089/ars.2010.3544

Wernicke, C., Hellmann, J., Zieba, B., Kuter, K., Ossowska, K., Frenzel, M., Dencher, N. A., & Rommelspacher, H. (2010). 9-Methyl-beta-carboline has restorative effects in an animal model of Parkinson's disease. Pharmacological Reports: PR, 62(1), 35–53. https://doi.org/10.1016/s1734-1140(10)70241-3

West, J. W., Patton, D. E., Scheuer, T., Wang, Y., Goldin, A. L., & Catterall, W. A. (1992). A cluster of hydrophobic amino acid residues required for fast Na(+)-channel inactivation. Proceedings of the National Academy of Sciences, 89(22), 10910–10914. https://doi.org/10.1073/pnas.89.22.10910

White, I. L., Franks, N. P., & Dickinson, R. (2005). Effects of isoflurane and xenon on Ba2+-currents mediated by N-type calcium channels. British Journal of Anaesthesia, 94(6), 784–790. https://doi.org/10.1093/bja/aei126

Wichmann, C., & Moser, T. (2015). Relating structure and function of inner hair cell ribbon synapses. Cell and Tissue Research, 361(1), 95–114. https://doi.org/10.1007/s00441-014-2102-7

Wise, A. K., Richardson, R., Hardman, J., Clark, G., & O'Leary, S. (2005). Resprouting and survival of guinea pig cochlear neurons in response to the administration of the neurotrophins brain-derived neurotrophic factor and neurotrophin-3. Journal of Comparative Neurology, 487(2), 147–165. https://doi.org/10.1002/cne.20563

Woods, C. B., Spencer, K. A., Jung, S., Worstman, H. M., Ramirez, J.-M., Morgan, P. G., & Sedensky, M. M. (2021). Mitochondrial Function and Anesthetic Sensitivity in the Mouse Spinal Cord. Anesthesiology, 134(6), 901–914. https://doi.org/10.1097/ALN.0000000000003794

Wu, F., Xiong, H., & Sha, S. (2020). Noise-induced loss of sensory hair cells is mediated by ROS/AMPKα pathway. Redox Biology, 29, 101406. https://doi.org/10.1016/j.redox.2019.101406

Wu, J. S., Yi, E., Manca, M., Javaid, H., Lauer, A. M., & Glowatzki, E. (2020). Sound exposure dynamically induces dopamine synthesis in cholinergic LOC efferents for feedback to auditory nerve fibers. ELife, 9, e52419. https://doi.org/10.7554/eLife.52419

Wu, P., O'Malley, J. T., de Gruttola, V., & Liberman, M. C. (2020). Age-Related Hearing Loss Is Dominated by Damage to Inner Ear Sensory Cells, Not the Cellular Battery That Powers Them. The Journal of Neuroscience, 40(33), 6357–6366. https://doi.org/10.1523/JNEUROSCI.0937-20.2020

Wu, P., O'Malley, J. T., de Gruttola, V., & Liberman, M. C. (2021). Primary Neural Degeneration in Noise-Exposed Human Cochleas: Correlations with Outer Hair Cell Loss and Word-Discrimination Scores. The Journal of Neuroscience, JN-RM-3238-20. https://doi.org/10.1523/JNEUROSCI.3238-20.2021

Wu, P. Z., Liberman, L. D., Bennett, K., de Gruttola, V., O'Malley, J. T., & Liberman, M. C. (2019). Primary Neural Degeneration in the Human Cochlea: Evidence for Hidden Hearing Loss in the Aging Ear. Neuroscience, 407, 8–20. https://doi.org/10.1016/j.neuroscience.2018.07.053

Xiao, Z., Ren, P., Chao, Y., Wang, Q., Kuai, J., Lv, M., Chen, L., Gao, C., & Sun, X. (2015). Protective role of isoflurane pretreatment in rats with focal cerebral ischemia and the underlying molecular mechanism. Molecular Medicine Reports, 12(1), 675–683. https://doi.org/10.3892/mmr.2015.3408

Xu, Y., Seto, T., Tang, P., & Firestone, L. (2000). NMR Study of Volatile Anesthetic Binding to Nicotinic Acetylcholine Receptors. Biophysical Journal, 78(2), 746–751. https://doi.org/10.1016/S0006-3495(00)76632-X

Yamane, H., Nakai, Y., Takayama, M., Iguchi, H., Nakagawa, T., & Kojima, A. (1995). Appearance of free radicals in the guinea pig inner ear after noise-induced acoustic trauma. European Archives of Oto-Rhino-Laryngology: Official Journal of the European Federation of Oto-Rhino-Laryngological Societies (EUFOS): Affiliated with the German Society for Oto-Rhino-Laryngology - Head and Neck Surgery, 252(8), 504–508. https://doi.org/10.1007/BF02114761

Yamashita, M., Mori, T., Zhao, X., Nagata, K., Marszalec, W., Yeh, J. Z., & Narahashi, T. (2005). General anesthetic modulation of neuronal nicotinic acetylcholine receptors. International Congress Series, 1283, 243–246. https://doi.org/10.1016/j.ics.2005.07.048

Yang, H., Zhu, Y., Ye, Y., Guan, J., Min, X., & Xiong, H. (2022). Nitric oxide protects against cochlear hair cell damage and noise-induced hearing loss through glucose metabolic reprogramming. Free Radical Biology and Medicine, 179, 229–241. https://doi.org/10.1016/j.freeradbiomed.2021.11.020

Yang, J., & Zorumski, C. F. (1991). Effects of Isoflurane on N-Methyl-D-Aspartate Gated Ion Channels in Cultured Rat Hippocampal Neurons. Annals of the New York Academy of Sciences, 625, 287–289. https://doi.org/10.1111/J.1749-6632.1991.TB33851.X

Yang, Y., Ou, M., Liu, J., Zhao, W., Zhuoma, L., Liang, Y., Zhu, T., Mulkey, D. K., & Zhou, C. (2020). Volatile Anesthetics Activate a Leak Sodium Conductance in Retrotrapezoid Nucleus Neurons to Maintain Breathing during Anesthesia in Mice. Anesthesiology, 133(4), 824–838. https://doi.org/10.1097/ALN.0000000000003493

Yu, W., Zong, S., Du, P., Zhou, P., Li, H., Wang, E., & Xiao, H. (2021). Role of the Stria Vascularis in the Pathogenesis of Sensorineural Hearing Loss: A Narrative Review. Frontiers in Neuroscience, 15. https://www.frontiersin.org/articles/10.3389/fnins.2021.774585

Yuan, H., Wang, X., Hill, K., Chen, J., Lemasters, J., Yang, S.-M., & Sha, S.-H. (2015). Autophagy Attenuates Noise-Induced Hearing Loss by Reducing Oxidative Stress. Antioxidants & Redox Signaling, 22(15), 1308–1324. https://doi.org/10.1089/ars.2014.6004

Zare, S., Nassiri, P., Monazzam, M. R., Pourbakht, A., Azam, K., & Golmohammadi, T. (2016). Evaluation of the effects of occupational noise exposure on serum aldosterone and potassium among industrial workers. Noise & Health, 18(80), 1–6. https://doi.org/10.4103/1463-1741.174358

Zhang, K. D., & Coate, T. M. (2017). Recent advances in the development and function of type II spiral ganglion neurons in the mammalian inner ear. Seminars in Cell & Developmental Biology, 65, 80–87. https://doi.org/10.1016/j.semcdb.2016.09.017

Zhang-Hooks, Y., Agarwal, A., Mishina, M., & Bergles, D. E. (2016). NMDA Receptors Enhance Spontaneous Activity and Promote Neuronal Survival in the Developing Cochlea. Neuron, 89(2), 337–350. https://doi.org/10.1016/j.neuron.2015.12.016

Zhao, H.-B., Zhu, Y., & Liu, L.-M. (2021). Excess extracellular K+ causes inner hair cell ribbon synapse degeneration. Communications Biology, 4(1), 24. https://doi.org/10.1038/s42003-020-01532-w

Zheng, Q. Y., Johnson, K. R., & Erway, L. C. (1999). Assessment of hearing in 80 inbred strains of mice by ABR threshold analyses. Hearing Research, 130(1–2), 94–107. https://doi.org/10.1016/s0378-5955(99)00003-9

Zhou, C., Johnson, K. W., Herold, K. F., & Hemmings, H. C. (2019). Differential Inhibition of Neuronal Sodium Channel Subtypes by the General Anesthetic Isoflurane. Journal of Pharmacology and Experimental Therapeutics, 369(2), 200–211. https://doi.org/10.1124/jpet.118.254938

Zloczower, E., Tsur, N., Hershkovich, S., Fink, N., & Marom, T. (2022). Efficacy of Oral Steroids for Acute Acoustic Trauma. Audiology & Neuro-Otology, 27(4), 312–320. https://doi.org/10.1159/000522051

Zweig, G. (2016). Nonlinear cochlear mechanics. The Journal of the Acoustical Society of America, 139(5), 2561. https://doi.org/10.1121/1.4941249

Zybura, A., Hudmon, A., & Cummins, T. R. (2021). Distinctive Properties and Powerful Neuromodulation of Nav1.6 Sodium Channels Regulates Neuronal Excitability. Cells, 10(7), 1595. https://doi.org/10.3390/cells10071595